Statistical Emulators of Irrigated Crop Yields and Irrigation Water Requirements

Élodie Blanc

Joint Program on the Science and Policy of Global Change
Massachusetts Institute of Technology
77 Massachusetts Ave
Cambridge, MA 02139, USA
Email: eblanc@mit.edu

Abstract

This study provides statistical emulators of global by gridded crop models included in the Inter-Sectoral Impact Model Intercomparison Project Fast Track project to estimate irrigated crop yields and associated irrigation water withdrawals simulated at the grid cell level. An ensemble of crop model simulations is used to build a panel of monthly summer weather variables and corresponding annual yields and irrigation water withdrawals from five gridded crop models. This dataset is then used to estimate crop-specific response functions for each crop model. The average normalized root mean square errors for the response functions range from 3% to 6% for irrigated yields and 2% to 8% for irrigated water withdrawal. Further in- and out-of-sample validation exercises confirm that the statistical emulators are able to replicate the crop models' spatial patterns of irrigated crop yields and irrigation water withdrawals reasonably well, both in levels and in terms of changes overtime, although accuracy varies by model and by region. The emulators estimated in this study therefore provides a reliable and computationally efficient alternative to global gridded crop yield models.

Key words: crop yields; irrigation; crop model; statistical model; water withdrawals; climate change

Acknowledgments

We thank Niven Winchester for helpful comments and suggestions. We appreciatively acknowledge the ISI-MIP modeling groups (listed in Appendix A, Table A1 of this paper) and the ISI-MIP coordination team for their roles in producing, coordinating, and making available the ISI-MIP model output. We gratefully acknowledge the financial support for this work from the U.S. Department of Energy, Office of Science under DE-FG02-94ER61937, and other government, industry, and foundation sponsors of the Joint Program on the Science and Policy of Global Change. For a complete list of sponsors, please visit http://globalchange.mit.edu/sponsors/all.

1. Introduction

The impact of climate change on crops can be assessed using process-based crop models (Boote et al. 2013; Deryng et al. 2014; Parry et al. 1999; Rosenzweig and Parry 1994a, 1994b; White et al. 2011), statistical models (Auffhammer and Schlenker 2014; Blanc and Strobl 2013; Haim, Shechter, and Berliner 2007; Hsiang 2016; Lobell and Field 2007; Schlenker and Roberts 2009) or a combination of both (i.e. a process model with parameters statistically estimated using historical observations) (Roberts et al. 2017). These models can then be included in Integrated assessment models (IAMs) to represent the agricultural sector by considering socio-economic and natural response mechanisms. Calvin and Fisher-Vanden (2017) find that combining statistical or process-based models within IAMs helps predict climate change impacts on crop yields more accurately than on their own. Alternatively, the implementation of statistical emulators—statistical models trained on the outputs of a process-based model to capture the response functions from complex, computationally demanding and sometimes proprietary process-based crop models—in IAMs can help account for feedback loops from the agricultural sector (Ruane et al. 2017) and can help account for modeling uncertainty (Monier et al. 2018).

Statistical emulators have been used by Holzkämper, Calanca, and Fuhrer (2012) and Lobell and Burke (2010) to assess the capacity of statistical models to predict out-of-sample crop yields. Other studies have used emulated response functions to compare statistical and process based models for 'diagnostic purposes' (Lobell and Asseng 2017; Schauberger et al. 2017; Moore, Baldos, and Hertel 2017). Crop yield emulators have also been developed to provide climate change impact assessment tools. Oyebamiji et al. (2015) provides crop yield emulators at the global level for five different crops but only considers one process-based crop model. Blanc and Sultan (2015) consider only maize but for five climate models. The scope of these emulators was expanded to three other crops (Blanc, 2017) and to both climate and crop models (Ostberg et al., 2018). While Oyebamiji et al. (2015) and Ostberg et al. (2018) estimate emulators for irrigated crop yields, they don't consider water requirements for irrigation. However, as water availability may pose serious constraints to irrigation (Blanc et al. 2017; Elliott et al. 2014), water necessary to irrigate those crop is a concern when estimating climate change impact on agriculture. This study proposes to fill this gap by developing statistical emulators of global gridded crop models for irrigated crops yields as well as the associated irrigation water withdrawals.

Building on Blanc and Sultan (2015) and Blanc (2017), the statistical emulators developed in this study are estimated based upon an ensemble of global gridded crop models (GGCM) simulations from the Inter-Sectoral Impact Model Intercomparison Project (ISI-MIP) Fast Track experiment (Rosenzweig et al. 2013; Warszawski et al. 2014). This project was designed to compare GGCMs simulations, all driven by the same bias-corrected climate change projections obtained from the Coupled Model Intercomparison Project, phase 5 (CMIP5) simulations ensemble (Hempel et al. 2013; Taylor, Stouffer, and Meehl 2012). In this study, the statistical emulators focus on irrigated crops and are estimated for maize, rice, soybean and wheat and five different GGCMs to provide an accessible tool for assessing the impact of climate change on irrigated crop yields and irrigation water withdrawals, while accounting for crop modeling uncertainty. In combination with the statistical emulators of rainfed crop yields developed in Blanc (2017), these emulators enhance integrated assessment modeling by facilitating the estimation of the impact of climate change on, separately, rainfed and irrigated crops.

The remainder of this paper presents the data and methods used to statistically estimate the emulators in Section 2 and the results are presented and discussed in Section 3. Validation of the emulators, both in- and out-of-sample are presented in Section 4. Section 5 concludes.

2. Material and methods

2.1. Data

In this analysis, data are sourced from the ISI-MIP Fast Track experiment, an inter-model comparison exercise where different GGCMs were used to simulate annual crop yields and irrigation water withdrawals under the same set of weather and CO_2 concentration inputs taken from the CMIP5 climate simulations.[1] Using these data, a panel dataset of GGCM outputs and atmospheric conditions is constructed for the period 1975-2099.

2.1.1. Weather and CO_2

Weather data at a 0.5×0.5-degree resolution (about 50km^2) used as input into each GGCM are obtained from the CMIP5 climate data simulations. A subset of climate simulations is selected to be representative of the broadest plausible range of future climate change. Three General Circulation Models (GCMs), HadGEM2-ES, NorESM1-M, and GFDL-ESM2M, are selected to be representative of respectively, high, medium and low levels of global warming (Warszawski et al. 2014). Daily bias-corrected weather data generated by these GCMs are provided for the 'historical' period of 1975 to 2005 and the 'future' period of 2006 to 2099. For the 'future' period, only one greenhouse gas Representative Concentration Pathway is considered, RCP 8.5, which is consistent with the highest level of global warming amongst the different RCPs.

[1] The data are available for download at https://www.pik-potsdam.de/research/climate-impacts-and-vulnerabilities/research/rd2-cross-cutting-activities/isi-mip/data-archive/fast-track-data-archive

Based on the daily precipitation, and daily minimum (*Tmin*) and maximum (*Tmax*) temperatures, monthly averages of precipitation (*Pr*) and mean temperature (*Tmean* = (*Tmin* + *Tmax*)/2) are calculated for each summer month. For ease of reference, weather variables for each summer month are denoted by numbers suffixes so that _1, _2, and _3 refer to, respectively, June, July and August in the Northern Hemisphere and December, January and February in the Southern Hemisphere. For each climate scenario considered, the corresponding CO_2 concentrations data are extracted from Riahi, Grübler, and Nakicenovic (2007).[2]

2.1.2. Irrigated crop yields

Simulated annual irrigated crop yields (*YIR*) in metric tons per hectare (t/ha) at a 0.5×0.5-degree resolution are obtained from the ISI-MIP Fast Track experiment for five GGCMs: (1) the Geographic Information System (GIS)-based Environmental Policy Integrated Climate (GEPIC) model (Liu et al. 2007; Williams and Singh 1995); (2) the Lund Potsdam-Jena managed Land (LPJmL) dynamic global vegetation and water balance model (Bondeau et al. 2007; Waha et al. 2012); (3) the Lund-Potsdam-Jena General Ecosystem Simulator (LPJ-GUESS) with managed land model (Bondeau et al. 2007; Linzdeskog et al. 2013; Smith, Prentice, and Sykes 2001); (4) the parallel Decision Support System for Agro-technology Transfer (pDSSAT) model (Elliott et al. 2013; Jones et al. 2003); and (5) the Predicting Ecosystem Goods And Services Using Scenarios (PEGASUS) model (Deryng et al. 2011). Although these GGCMs differ in their representation of crop phenology, leaf area development, root expansion, nutrient assimilation, and yield formation, they all account for the effect of water, heat stress and CO_2 fertilization, and assume no technological change.[3] However, the LPJ-GUESS model simulates potential yields (yield not limited by nutrient or management constraints) whereas the other crop models simulate actual yields. Other differences and GGCM-specific periodic patterns of yield projections are discussed in Blanc and Sultan (2015).

[2] The data are available at http://tntcat.iiasa.ac.at/RcpDb/dsd?Action=htmlpage&page=welcome.
[3] See Rosenzweig et al. (2014) for more details regarding each model's processes. Caveats are discussed at https://www.pik-potsdam.de/research/climate-impacts-and-vulnerabilities/research/rd2-cross-cutting-activities/isi-mip/data-archive/fast-track-data-archive/data-caveats.

2.1.3. Irrigation water withdrawals

Associated with irrigated crop yields projections, GGCMs report irrigation water demand, or potential irrigation water withdrawal (*PIRRWW*), in mm per year at a 0.5×0.5-degree resolution. As the crop models make different assumptions about the efficiency of irrigation, the reported *PIRRWW* is harmonized across all models to obtain estimates of water directly available to the crop assuming no losses during conveyance and application. To impose this harmonization assumption, *PIRRWW* data provided by pDSSAT are multiplied by 0.75 for maize, soy and wheat, and *PIRRWW* data provided by LPJmL are multiplied by grid specific project efficiencies applicable to all crops. [4] All other models assume an irrigation use efficiency of 100%.

2.1.4. Soil orders

To account for soil conditions, soil orders are extracted from the FAO-UNESCO (2005) Soil Map of the World at the 0.5×0.5-degree resolution. It uses the USDA soil taxonomy (Soil Survey Staff 1999)[5] classifying soils on the basis of physical and chemical properties observed in situ (e.g. soil horizons, structure, texture, color) and inferred from environmental conditions (e.g., soil temperature and moisture regimes). Soils are grouped into 12 main soil orders (Gelisols, Histosols, Spodosols, Andisols, Oxisols, Vertisols, Aridisols, Ultisols, Mollisols, ,Inceptisols, and Entisols) as described in Blanc (2017).

2.1.5. Summary statistics

Globally, the sample for each crop-GGCM combination is composed of, on average, 15 million records covering about 44,000 grid cells (see Table 1).[6] Simulations from the PEGASUS and pDSSAT models for rice and pDSSAT model for soybean are not available. For wheat, simulations by the pDSSAT model are only available for the HadGEM2 GCM.

[4] The spatial file containing project efficiencies is available for download at https://www.isimip.org/documents/213/irrigation_project_efficiencies.nc.
[5] Soil order data are available for download at https://www.nrcs.usda.gov/wps/portal/nrcs/detail/soils/use/?cid=nrcs142p2_054013
[6] In the final sample, grid cells for which there are less than 10 output records after data cleaning are omitted.

Table 1. GGCMs summary information

Crop	Model	Records	Grid Cells
Maize	**GEPIC**	16,176,798	44,902
	LPJ-GUESS	15,958,849	43,824
	LPJmL	16,696,167	45,597
	PEGASUS	11,427,653	43,301
	pDSSAT	13,221,217	42,877
Rice	**GEPIC**	16,277,183	45,312
	LPJ-GUESS	15,252,499	43,789
	LPJmL	16,721,941	45,236
Soybean	**GEPIC**	16,197,571	45,211
	LPJ-GUESS	15,538,632	43,422
	LPJmL	16,650,813	45,558
	PEGASUS	8,314,743	39,642
Wheat	**GEPIC**	16,468,355	45,326
	LPJ-GUESS	14,960,416	41,820
	LPJmL	16,859,028	45,724
	PEGASUS	11,839,747	43,387
	pDSSAT	13,484,362	43,073

Summary statistics for irrigated crop yields and irrigation demand are detailed by GGCM and GCM in Table A1 in Appendix A. The global average of irrigated crop yields differs amongst crops with yields ranging from 1.8t/Ha for soybean to 3.5t/ha for maize. Across GGCMs, the largest variation is observed for wheat, which ranges from 1.73t/ha for the PEGASUS model to 4.4t/ha for the LPJ-GUESS model. Regarding irrigation, soybean requires the least water on average (92.5mm/year) and rice the most (114mm/year). Across GCMs, average irrigation water withdrawals are the largest under the NorESM1_M scenario and the lowest under the GFDL_ESM2M scenario. Irrigation requirements vary greatly across models, with the PEGASUS model simulating average irrigation water withdrawals below 40mm/year for all crops, whereas estimates for all other GGCMs (except GEPIC for soybean and LPJ-GUESS for rice) exceed 100mm/year.

Atmospheric CO_2 concentrations, which are the same for all GCM-GGCM combinations, range from 331 to 927 parts per million (ppm) between 1975 and the end of the century. Summary statistics of *Tmean* and *Pr*, and *CO2* averaged over all GGCMs are presented in Table 2. On average, temperatures are the highest in the second month of summer and precipitation is the lowest in the first month of summer. Across GCMs, temperatures are the greatest under the HadGEM2-ES model and the lowest under the GFDL-ESM2M GCM, but no clear pattern of precipitation emerges amongst GCMs. Weather summary statistics at the soil-order level indicate that mid-summer temperatures range between 18˚C in the Spodosols regions (acidic soils developing under coniferous vegetation) to 30˚C in the Vertisols regions (clay-rich soils in climates with distinct dry seasons). Precipitation ranges from less than 1mm/day in the Aridisols regions (prone to salinization and typical to arid regions) to more than 7mm/day in the Oxisols regions (mineral soils found in tropical and subtropical latitudes). More details regarding the weather variables statistics are available in Blanc (2017).

Table 2. Mean values of summer temperature and precipitation by GCM at the global level

Variable	Unit	GFDL_ESM2M	HadGEM2_ES	NorESM1_M
Tmean_1	˚C	21.4	22.8	22.0
Tmean_2	˚C	23.1	24.5	23.9
Tmean_3	˚C	22.4	23.8	22.9
Pr_1	mm/day	3.2	3.0	3.0
Pr_2	mm/day	3.5	3.5	3.5
Pr_3	mm/day	3.5	3.5	3.5

Note: suffixes _1, _2, _3 denote, respectively, June, July and August in the Northern Hemisphere and December January and February in the Southern Hemisphere.

2.2. Methods

The methodology extends the work of Blanc and Sultan (2015) and Blanc (2017). In these studies, rainfed yields (YRF) are estimated for each crop, GGCM and soil type using a parsimonious specification that only includes average summer precipitation and temperature weather variables, CO_2 concentrations, and interactions among these variables. For irrigated crops, the five GGCMs considered in this study assume that irrigation is applied to compensate for the lack of precipitation. Therefore, the preferred specification assumes that precipitation has no impact on crop growth, and yields for each crop and model are specified as a function of temperature and CO_2, and corresponding interaction terms:

$$YIR_{lat,lon,gcm,y} = \alpha + \sum_{i=1}^{3} \theta_i Tmean_{i_{lat,lon,gcm,y}} + \vartheta CO2_{gcm,y} + \sum_{i=1}^{3} \gamma_i Tmean\_i_{lat,lon,gcm,y} * CO2_{gcm,y} + \delta_{lat,lon} + \rho_{lat,lon,gcm,y} \quad (1)$$

where for each year, *y*, *YIR* corresponds to irrigated crop yields simulated by process-based crop models for each grid cell (defined by its longitude, *lon*, and latitude, *lat*) under each climate model, *gcm*; *Pr* and *Tmean* variables correspond to mean precipitation and temperature variables for each summer month *i*. *CO2* is the annual midyear CO_2 concentration level in the atmosphere; δ is a grid cell fixed effect; and ρ an error term. Following Blanc and Sultan (2015), adjustments to the specification are made to account for soil fertility erosion and CO_2 concentration for the pDSSAT and GEPIC models respectively.

Associated with each crop yield, GGCMS also provide annual irrigation water requirements (*PIRRWW*). Consistent with the methodology used to estimate crop yields, water demand for irrigation for each crop and GGCM is estimated as a function of monthly temperature and precipitation and CO_2 concentrations:

$$PIRRWW_{lat,lon,gcm,y} = \alpha + \sum_{i=1}^{3} \beta_i Pr_{i_{lat,lon,gcm,y}} + \sum_{i=1}^{3} \theta_i Tmean_{i_{lat,lon,gcm,y}} + \vartheta CO2_{gcm,y} + \sum_{i=1}^{3} \gamma_i Pr_{i_{lat,lon,gcm,y}} * Tmean_{i_{lat,lon,gcm,y}} + \sum_{i=1}^{3} \gamma_i Pr_{i_{lat,lon,gcm,y}} * CO2_{gcm,y} + \sum_{i=1}^{3} \gamma_i Tmean\_i_{lat,lon,gcm,y} * CO2_{gcm,y} + \delta_{lat,lon} + \rho_{lat,lon,gcm,y} \quad (2)$$

Following Blanc (2017), a fractional polynomial specification is preferred to model non-linearities as it relaxes the symmetry constraint imposed by quadratic terms but allows non-parametric flexibility from multinomial transformations. Additionally, the response functions are estimated separately for each soil order[7] as the effect of weather on crops differs across soil types. This specification is labeled S1fpintsoil.

[7] In this analysis, response functions for the Gelisols soil order are not estimated, as this soil order represents soils permanently frozen.

To consider the effect of alternative specifications on the emulators' performance, additional specifications are considered and comparisons of goodness of fit measures are provided in Appendix A.

3. Results

Based on the methodology presented Section 2, multiple specifications are estimated for both irrigated yields and irrigation demand. Results for irrigated crop yields and irrigation water requirements are presented in Section 3.1 and 3.2 respectively. The power terms used for the fractional polynomial specifications are reported in Appendix B and the regression results are presented in Appendix C. The corresponding estimated values for δ (the grid cell fixed effect) are provided in Appendix D.

3.1. Regression results for irrigated yields

For each crop and GGCM, the S1fpintsoil regression results show that summer temperatures have a significant impact on irrigated yields from all GGCMs and crops. Figure 1 provides an illustration of the average effect of temperature during the second month of summer for each soil sample, while holding covariates at their mean values. The figure shows that fractional polynomial transformation captures the non-linear effect of mid-summer temperature on irrigated crop yields, with in some cases, a negative skewness of the curve representative of a sharp decrease in yields associated with high temperature. Similar to the results in (Blanc 2017a), the average effect of temperature on crop yields differs depending on the soil order sample considered. As for rainfed yields, the yield response to temperature are generally high in fertile Andisols and Mollisols. Additionally, the temperature effect is also very large in Aridisols subsamples for irrigated crops, which are not water-limited. The confidence intervals are relatively small, except in a few cases (e.g. Tmean_2 of maize with LPJmL in the Aridisols subsample) for which the emulator are likely to be less accurate.

Figure 1. Effect of *Tmean_2* on *YIR* by crop and GGCM for the S1fpintsoil specification

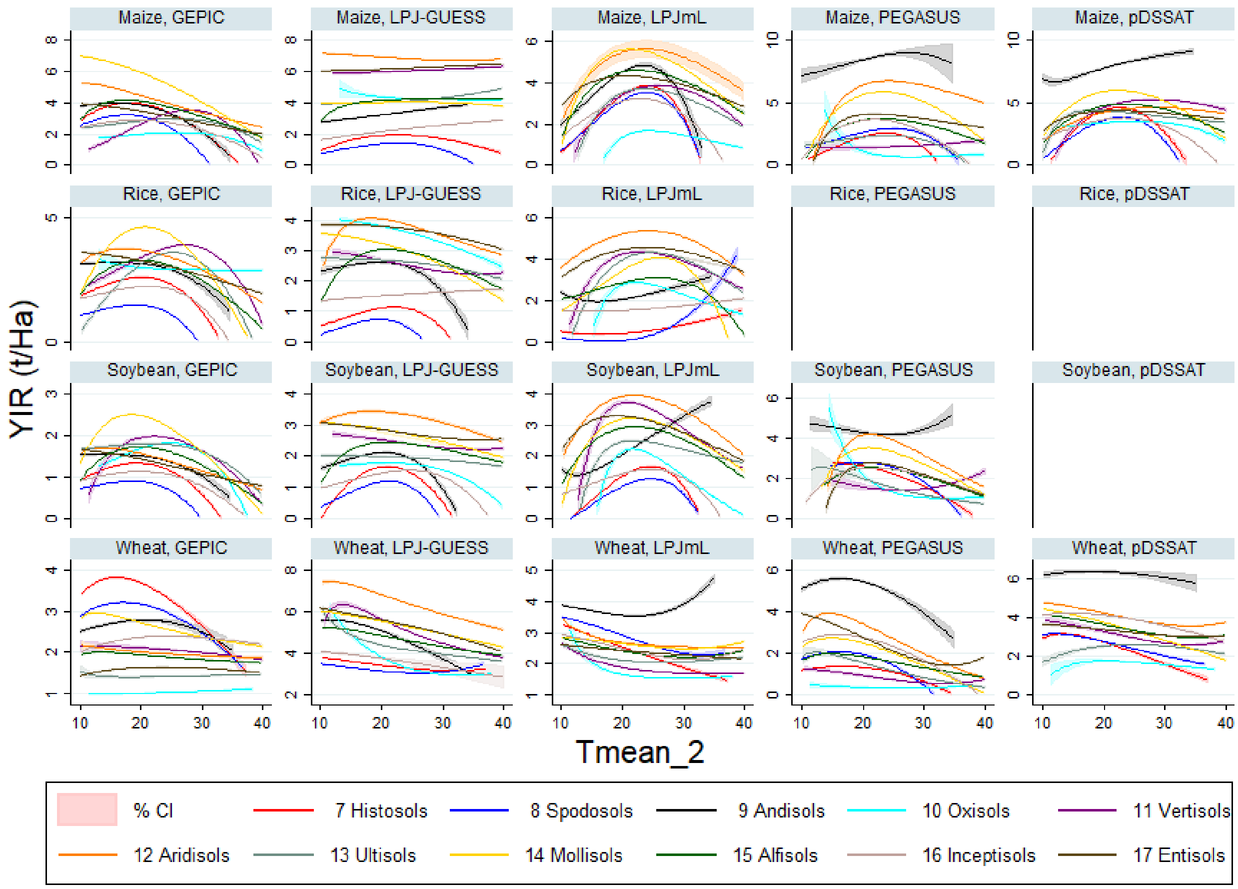

Note: covariates are held at their mean values. The response functions represent the fit across the soil type for which it was estimated.

3.2. Regression results for irrigation water withdrawal

As for irrigated crop yields, the regression results for the S1fpintsoil specification indicate that summer weather have a significant impact on irrigation water withdrawals from all GGCMs and crops. Illustrations of the average effect of temperature and precipitation during the second month of summer while holding covariates at their mean values detailed for each soil sample are provided in Figure 2 and Figure 3. The figures indicate that the average effect of weather on irrigation water withdrawals varies by soil type. For instance, the effect of mid-summer temperature on irrigation water withdrawals presented in Figure 2 is the largest in Aridisols regions, which are characteristic of arid regions. In most cases, temperature increases (with other co-variates held at their mean value) entail an increase in irrigation water withdrawals, which is consistent with an increase in evaporation associated with higher temperatures.

Figure 2. Effect of *Tmean_2* on *PIRRWW* by crop and GGCM for the S1fpintsoil specification

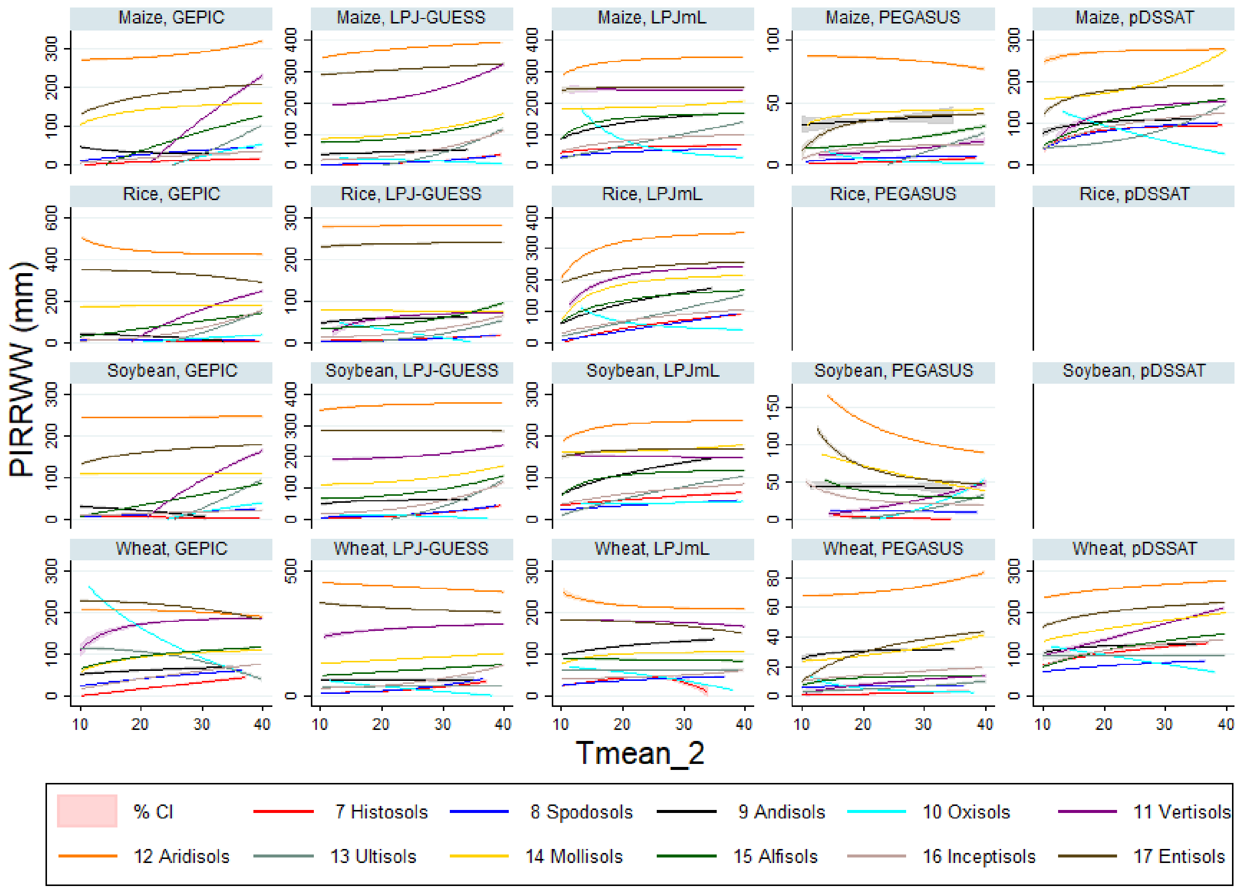

Note: covariates are held at their mean values.

Figure 3 indicates that in most cases, at low level of precipitation, an increase in rainfall is associated with a sharp decline in irrigation water withdrawals, especially in Vertisols subsamples. Alternatively, the effect of precipitation is almost flat for samples such as Aridisols. For most soil regions, however, the effect levels off and is almost null in most cases when precipitation rates exceed 2mm/day. The shape of the response functions is mostly similar across GGCMs for a given crop, although the level of irrigation withdrawal differs greatly.

Figure 3. Effect of *Pr_2* on *PIRWW* by crop and GGCM for the S1fpintsoil specification

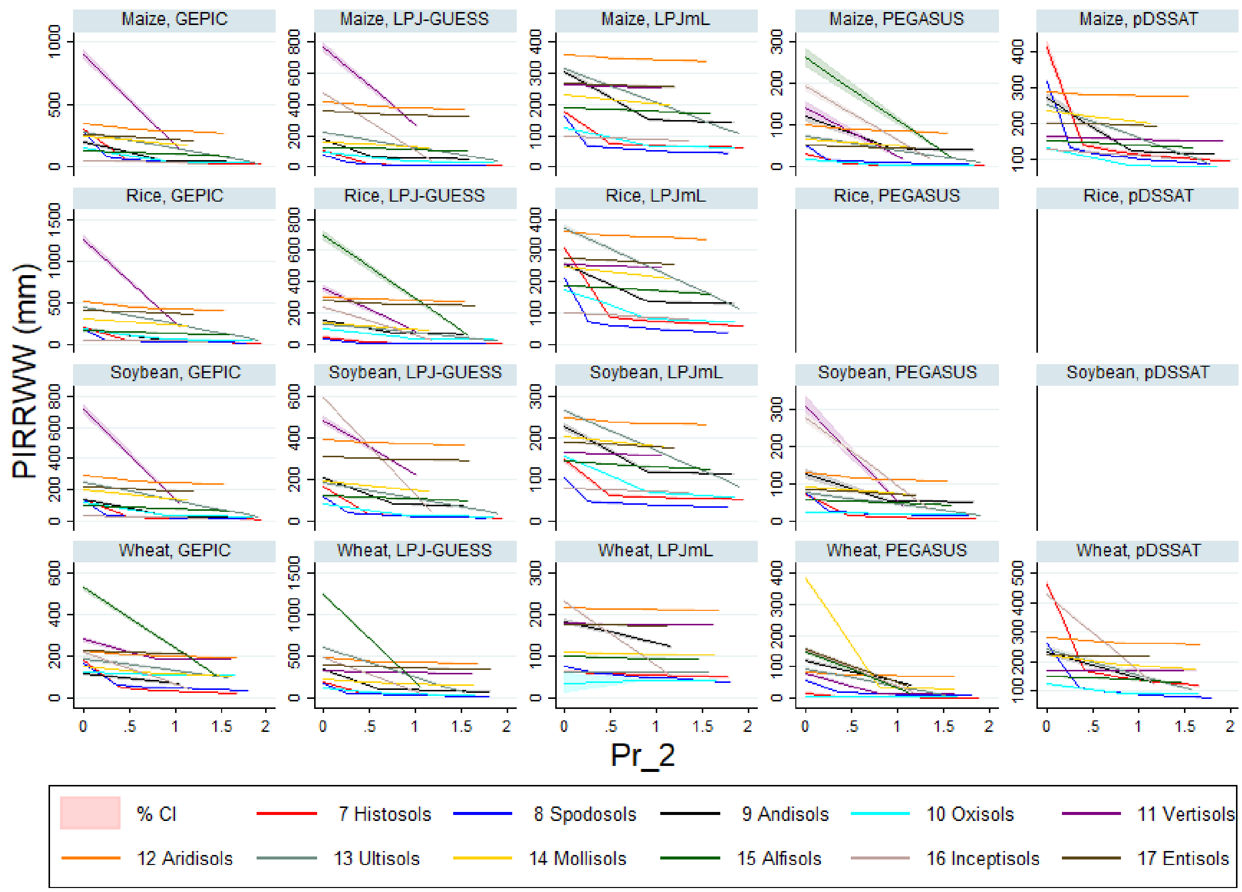

Note: covariates are held at their mean values. Graphs truncated for Pr_2>2mm.

4. Validation

To evaluate the accuracy of the statistical models at reproducing irrigated crop yields and associated irrigation water withdrawals simulated by GGCMs, the emulators' within- and out-of-sample projections are compared with those from GCCMs. Both validation exercises are lead using the preferred specification, S1fpintsoil.

4.1. In-sample validation

4.1.1. Irrigated crop yields

The within-sample validation exercise is performed on the full sample of irrigated yields estimates for each crop, grid cell, year, and climate model. Considering a simple deviance measure, the normalized root mean square error (NRMSE), is calculated by dividing the RMSE by the difference between maximum and minimum yields within each soil sample. Global NRMSE weighted-average values[8] for each, crop and model for *YIR* are presented in Figure 4. The graphs indicate that the average error between predicted and 'actual' irrigated yields range from around 4% to 6% for maize and rice yields, 3% to 6% for soybean yields and 2% to 5% of wheat yields. Across GGCMs, the graph shows that lowest NRMSE are found for the LPJml and LPJ-GUESS models, while GEPIC has the highest NRMSEs for all crops except maize. NRMSE values for *YIR* compared to *YRF* indicate that irrigated rice, soybean and wheat yields are generally slightly harder to emulate than their rainfed counterparts.

Figure 4. Goodness of fit of the yield statistical emulators by crop and independent variable (S1fpintsoil specification)

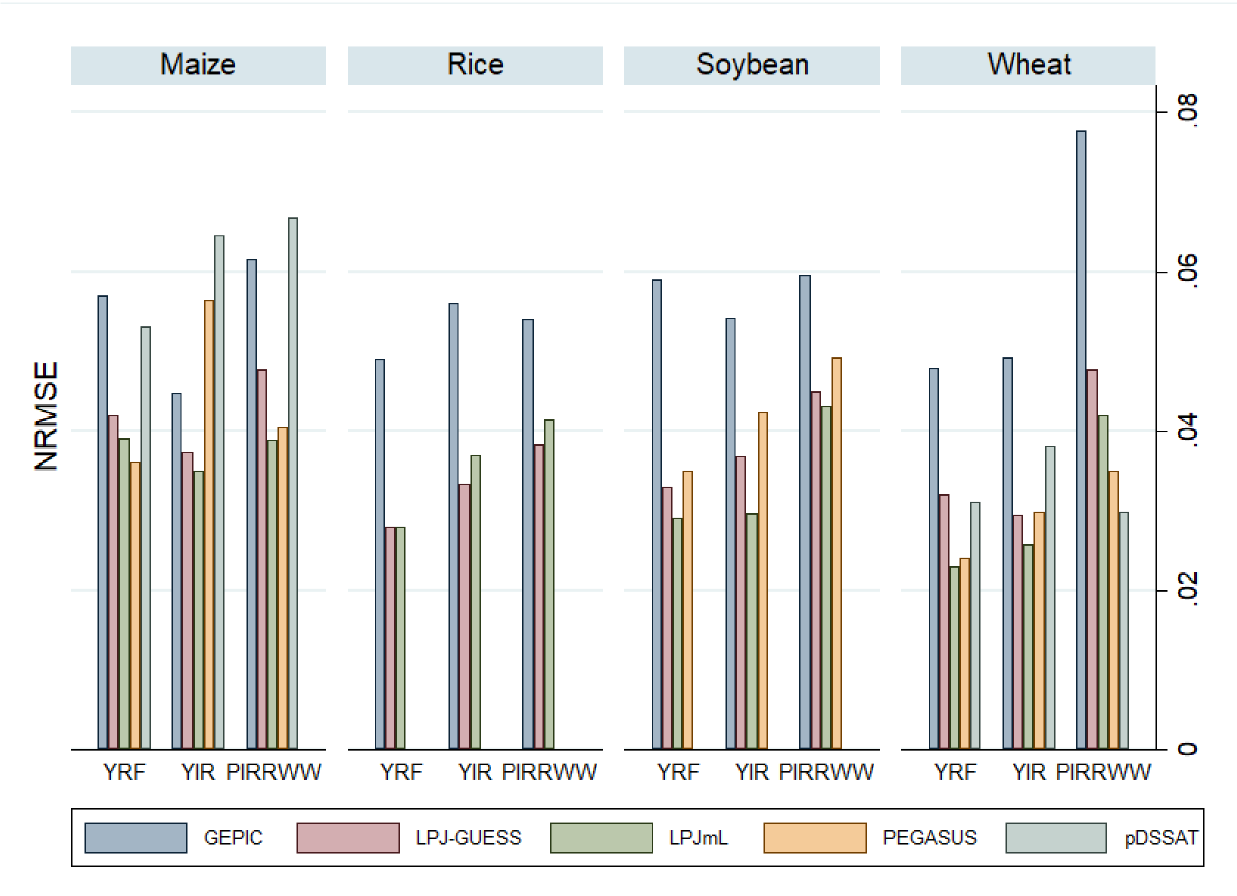

Note: NRMSE values for YRF are source from Blanc (2017).

[8] Global NRMSE averages are weighted by soil sub-sample size.

To evaluate the emulators' prediction accuracy overtime, time series of average irrigated crop yields from GGCMs and statistical emulators are presented in Figure 5. The left-hand graphs present annual irrigated yields for each crop averaged over the three climate models and all grid cells for the whole globe. Similar global averages but weighted by crop-specific irrigated harvested area (sourced from the MIRCA2000 dataset; Portmann, Siebert, and Döll 2010) are presented in the right-hand graphs. The light colored lines represent the GGCMs' projections and the dark colored lines characterize simulations from the emulator (using the S1fpintsoil specification). The graphs show that, while global average yields projections driven by the same climate data differ between GGCMs, predictions from the statistical emulators follow, on average, the same trend as projections from GGCMs, although inter-annual variability is captured with less accuracy. Similar observations apply when considering yields weighted by irrigated areas, except for irrigated yields for maize simulated with the pDSSAT model, rice with the LPJ-GUESS model, and soybean with the PEGASUS model, where greater inter-annual bias between the emulators and the GGCMs are observed at the beginning and at the end of the sample.

Figure 5. Average irrigated crop yields from GGCMs and statistical emulators (S1fpintsoil specification)

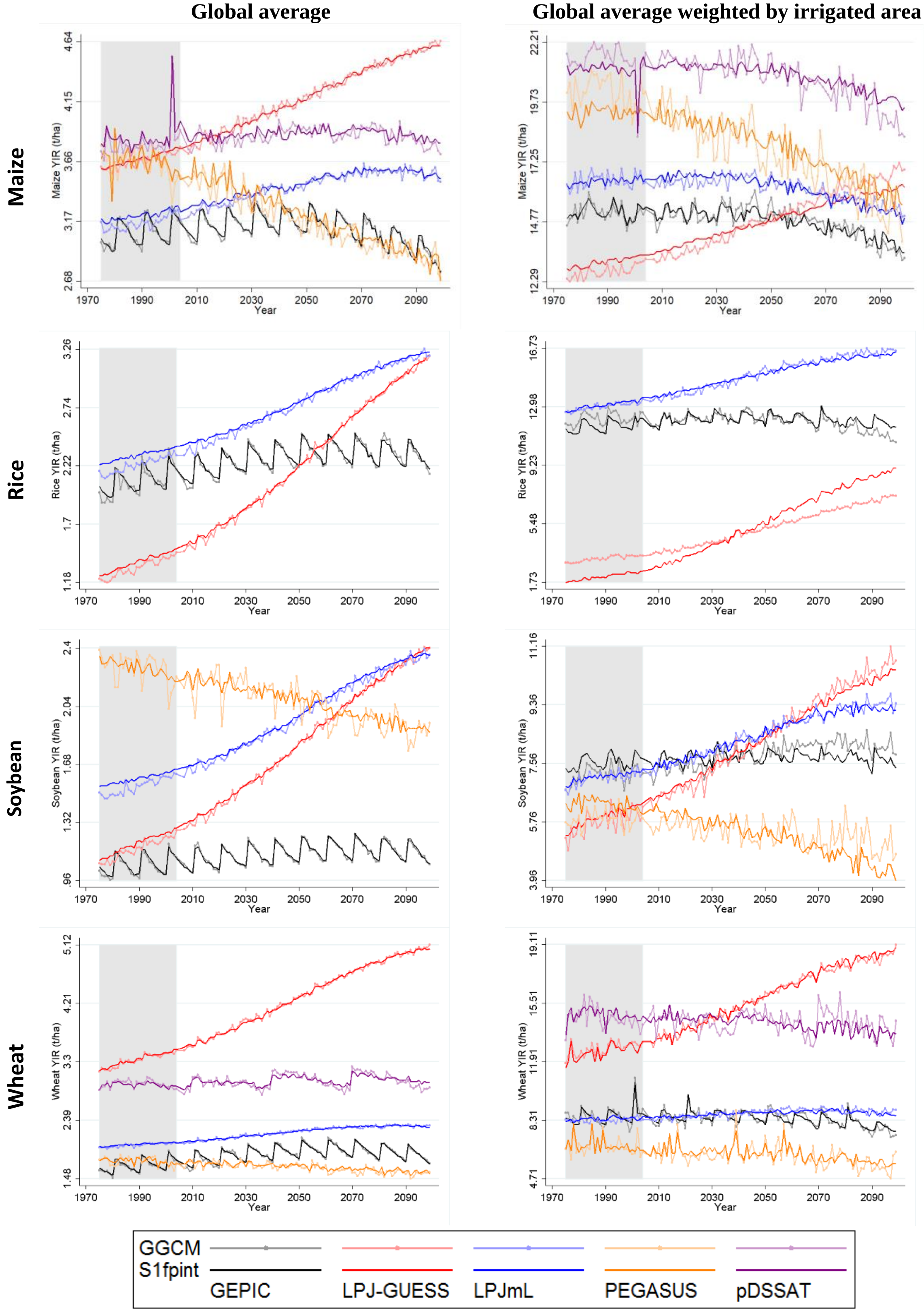

Note: Shaded areas represents the ‘historical’ period.

To assess the degree of spatial agreement between the emulator and the GGCMs, maps presenting climate change impact projections estimated by those models over the 2090s period are provided for each crop at the global level in Appendix G. The maps show that the emulators reproduce the spatial patterns of irrigated crop yields with reasonable accuracy and that the largest differences between model and emulator outputs are largely observed in regions where yields are low. However, as reported in Table 3, wheat yields tend to be overestimated by the emulators for all models, especially LPJ-GUESS, while maize yields errors are more balanced across models.

Table 3. Percentage of global grid cells for which the emulator overestimates *YIR* and *PIRRWW* averaged over 2090–2099 compared to the GGCMs

Crop	Model	*YIR*	*PIRRWW*
Maize	**GEPIC**	44%	45%
	LPJ-GUESS	50%	60%
	LPJmL	51%	40%
	PEGASUS	48%	42%
	pDSSAT	51%	50%
Rice	**GEPIC**	51%	45%
	LPJ-GUESS	48%	65%
	LPJmL	56%	45%
Soybean	**GEPIC**	48%	47%
	LPJ-GUESS	46%	66%
	LPJmL	53%	47%
	PEGASUS	61%	56%
Wheat	**GEPIC**	63%	53%
	LPJ-GUESS	79%	65%
	LPJmL	66%	50%
	PEGASUS	56%	50%
	pDSSAT	63%	54%

To assess the accuracy of the emulators over important areas, similar maps are reproduced focusing on the main growing regions for each crops. Figure 6 to Figure 9 present results for the ‘easiest’ and ‘hardest’ models to emulate, based on NRMSE values for each region, for each crop. Yield projections from both the GGCMs and the emulators averaged over the period 2090-2099 are presented, as well as the simple difference between the two. In addition, to assess the magnitude of emulator prediction errors relative to spread of estimates by different GGCMs, these figures include maps of the error compared to the 'ensemble spread'.[9] Figure 6 show that the pDDSAT emulator tends to overestimate maize yields over the central part of the Corn Belt in the US. The bottom map shows that this overestimation is mostly located in an area where the error is larger than the ensemble spread is small (represented in purple). By contrast, the emulator for the easiest to emulate model in this region for maize, LPJ-GUESS, underestimate irrigated yields and the errors are consistently lower than the ensemble spread.

[9] The ensemble spread is calculated as the standard deviation of YIR across GGCMs over the period 2090–2099. See Appendices H and G for maps of the ensemble error over each producing region and at the global level.

Figure 6. Irrigated maize yields averaged over 2090–2099 for the LPJ-GUESS and pDSSAT models and S1fpintsoil specification over US cornbelt

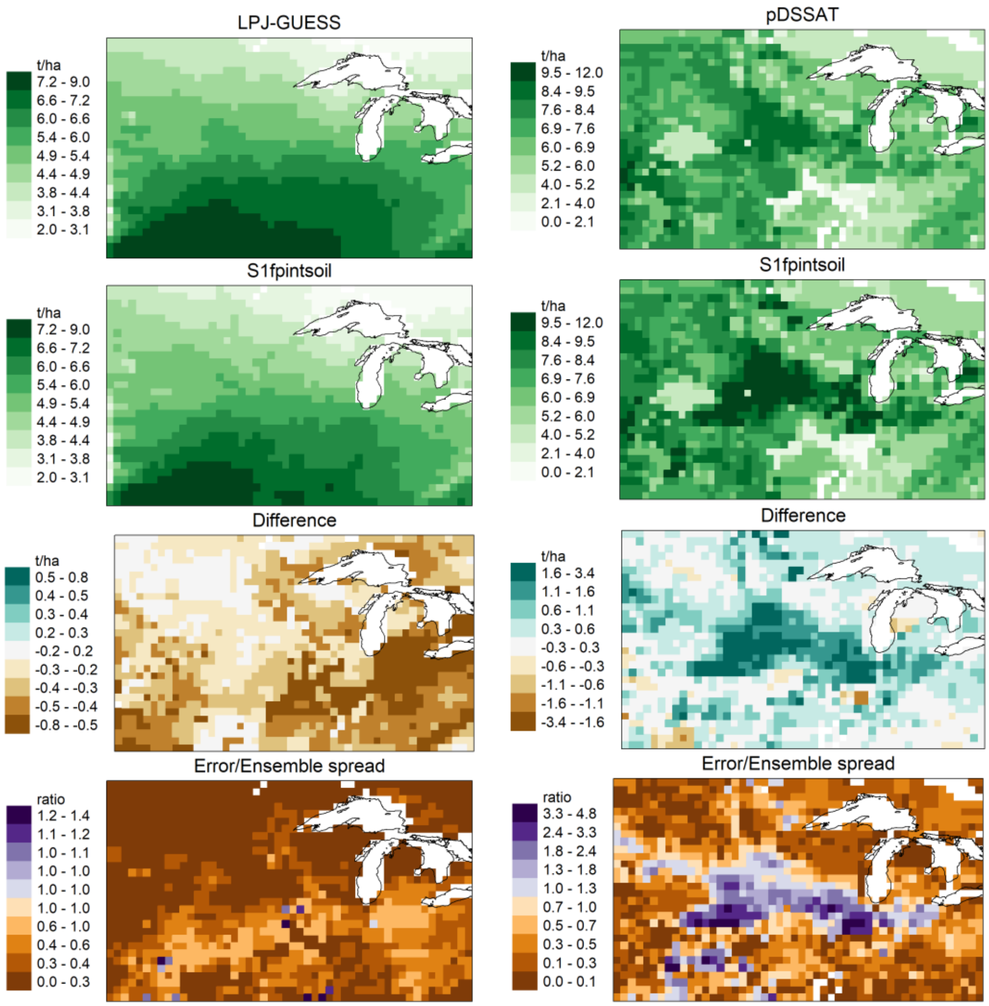

For rice, the emulator for the hardest to emulate model, LPJ-GUESS, overestimates irrigated yields in the north of the South East Asia region, but this area is characterized by a relatively large ensemble spread, and therefore the error introduced by the emulator is smaller than differences in predictions across models. For the GEPIC model, similar conclusions can be drawn, albeit with smaller errors relative to the level of yields projected by the GGCMs.

Figure 7. Irrigated rice yields averaged over 2090–2099 for the GEPIC and LPJ-GUESS and models and S1fpintsoil specification over South East Asia

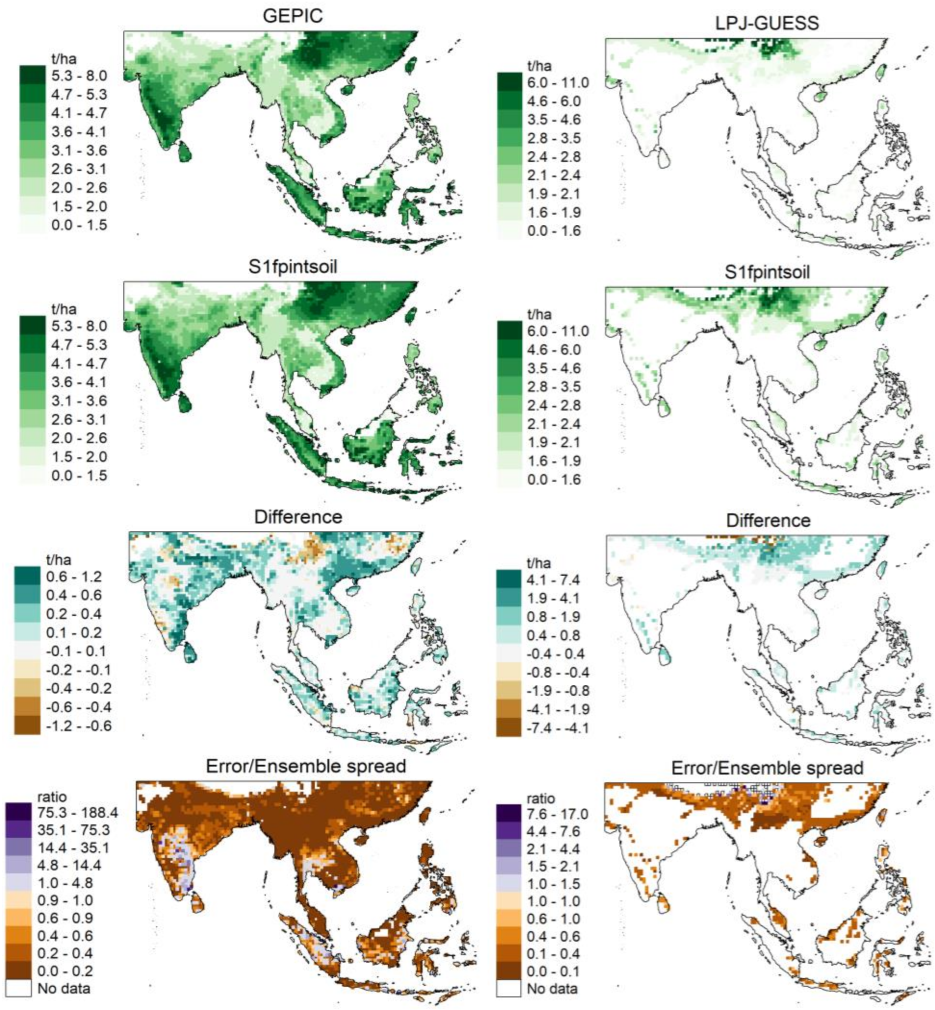

Soybean yields emulated for the GEPIC model are overestimated in the western part of this region, which is characterized by low yields and large ensemble spreads. Alternatively, emulated yields for the LPJmL model are underestimated in this same region, albeit to a relatively smaller degree. Reassuringly, the errors are smaller than the ensemble spread for both models in most grid cells.

Figure 8. Irrigated soybean yields averaged over 2090–2099 for the LPJmL and GEPIC models and S1fpintsoil specification over Brazil

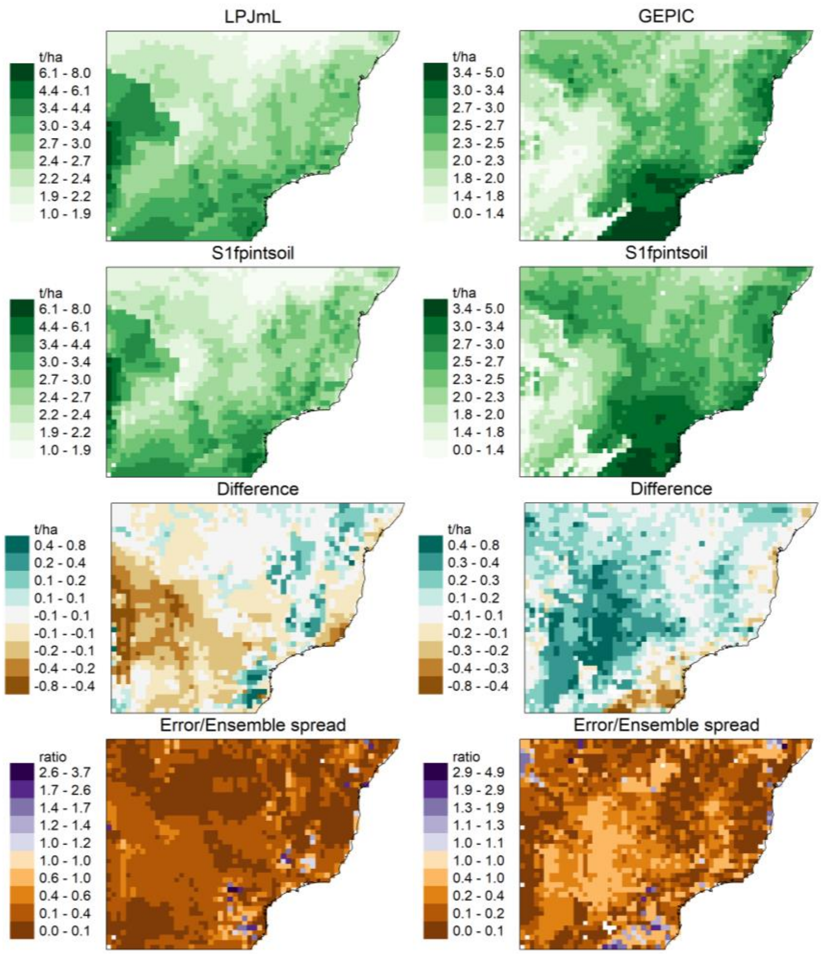

For wheat, the emulator for both LPJmL and PEGASUS models, on average, overestimate yields in France where productivity is relatively high and ensemble spreads are relatively low. However, the errors are relatively smaller for the LPJmL model.

Figure 9. Irrigated wheat yields averaged over 2090–2099 for the LPJmL and PEGASUS models and S1fpintsoil specification over Europe

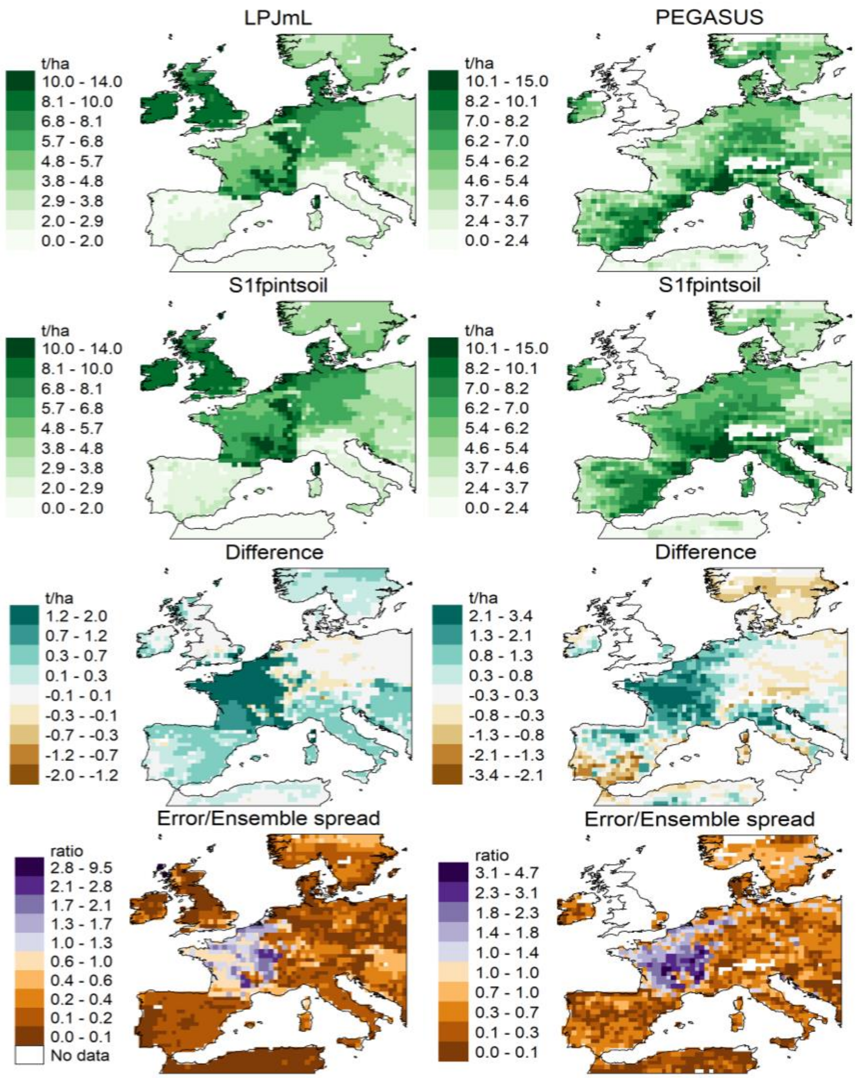

Similar spatial assessment maps considering the change in irrigated crop yields from 2000s to 2090s are provided in Appendix G. Overall, the maps show that GGCMs project increases in irrigated crop yields poleward for most crops by the end of the century. For other regions, the effects depend on the crop and model considered. However, the maps show that, overall, the emulators reproduce reasonably well the spatial patterns of climate change impacts on irrigated crop yields simulated by the GGCMs.

4.1.2. Irrigation water withdrawals

The same within-sample validation exercise as for irrigated crop yields is performed on irrigation water withdrawal estimates for each crop, grid cell, year, and climate model. The NRMSE values for *PIRRWW* presented in Figure 4 indicate that errors for wheat with GEPIC reach almost 8% whiles with pDSSAT they are closer to 2%. NRMSE values for *PIRRWW* are in most cases slightly higher than those for irrigated yields, and indicate that this process is harder to emulate.

Time series of irrigation water withdrawals averaged at the global level and weighted by crop-specific irrigated harvested area are reported in Figure 10. The graphs show that projections from the emulator (in dark colors) follow the same trend as projections from GGCMs (in light colors). As for irrigated crop yields, inter-annual variability is emulated with less precision than the long-run trend. However, divergences are only observed for rice simulated by the LPJ-GUESS model when considering average irrigation water withdrawals weighted by irrigated areas.

Figure 10. Average irrigation water withdrawals from GGCMs and statistical emulators (S1fpintsoil specification)

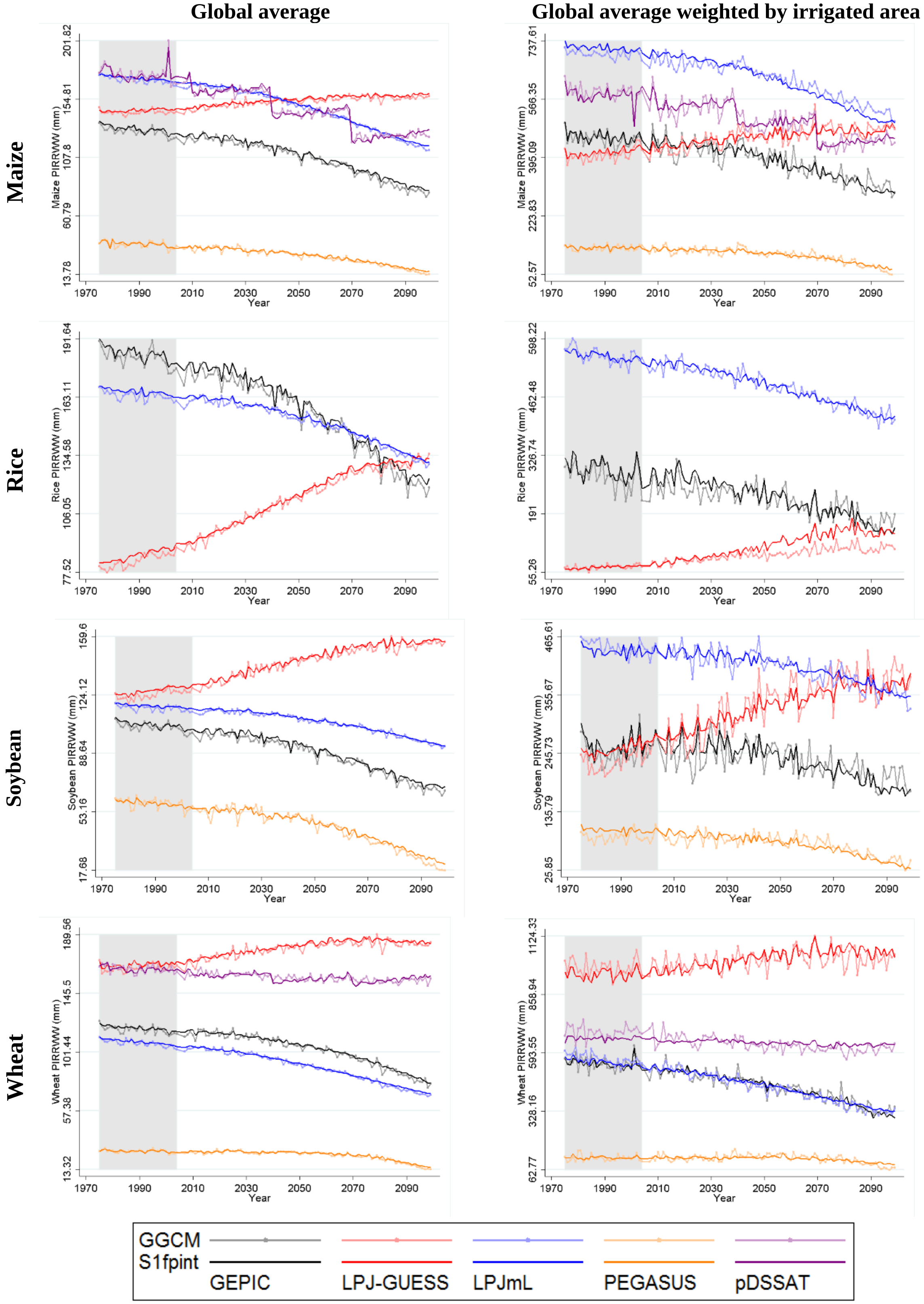

Note: Shaded areas represents the 'historical' period.

To assess the spatial agreement in irrigation water withdrawals estimated by the GGCMs and the statistical emulators for each crop, maps presenting climate change impact projections over the 2090s period are presented in Appendix H for the globe at the grid cell level. These maps show that the emulators are able to reproduce the spatial patterns of irrigation demand over the globe, which differ greatly across models. Table 3 show that the emulators for the LPJ-GUESS model, on average, overestimates irrigation requirements for all crops.

Maps representing major production regions for each crop are presented in Figure 11 for each of the hardest and easiest models to emulate GGCMs, again defined using NRMSE values. The emulator for the LPJmL model underestimates requirements in most regions, but the largest of those errors occur in regions with relatively low water requirements. Reassuringly, the errors are generally lower than the ensemble spread, indicating that the emulator’s performance does not exceed the uncertainty across models. For the PEGASUS model, the emulator overestimates irrigation requirements in the western part of the cornbelt where the level is high, but the errors are lower than the ensemble spread in all grid cells in the region.

Figure 11. Irrigation water withdrawals for maize averaged over 2090–2099 for the LPJmL and PEGASUS models and S1fpintsoil specification over the US cornbelt

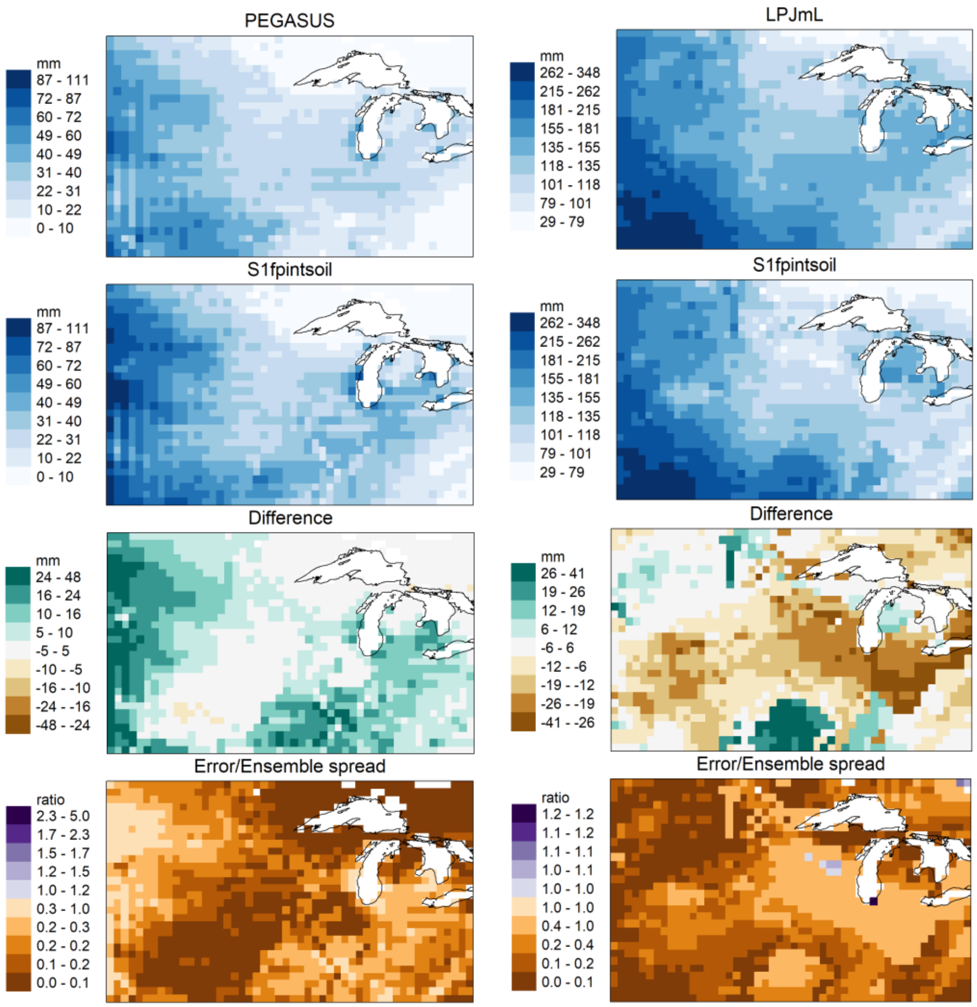

For rice, the emulator for the hardest to emulate model, LPJ-GUESS, overestimates requirements over India on average, but the ratio of error over the ensemble spread is low in all grid cells. Similar conclusions can be drawn for the emulator for the GEPIC model, although there is more agreement among models in this region (i.e., lower ensemble spreads).

Figure 12. Irrigation water withdrawals for wheat averaged over 2090–2099 for the GEPIC and LPJ-GUESS models and S1fpintsoil specification over South East Asia

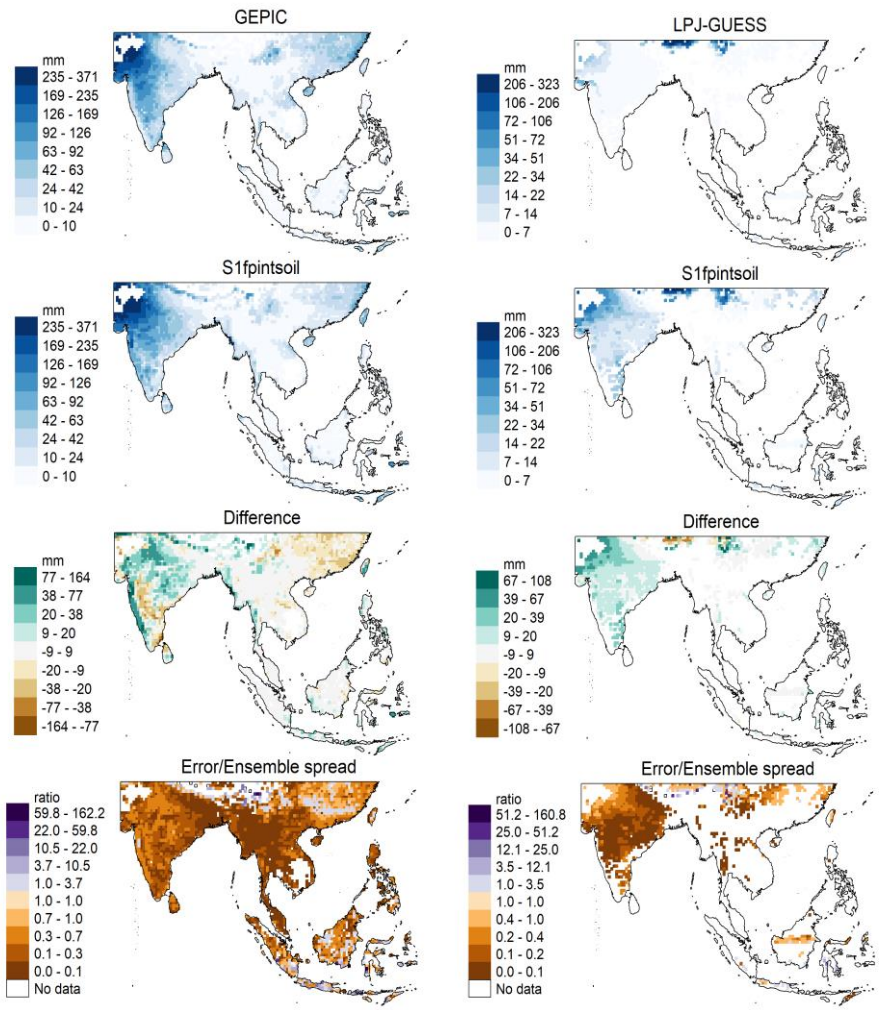

For Soybean in Brazil, emulators for both the GEPIC and LPJmL models underestimates irrigation requirements in the north east where irrigation requirements are high. However, for this region, the emulator prediction errors are low relative to the ensemble spreads for both models.

Figure 13. Irrigation water withdrawals for soybean averaged over 2090–2099 for the GEPIC and LPJ-GUESS models and S1fpintsoil specification over Brazil

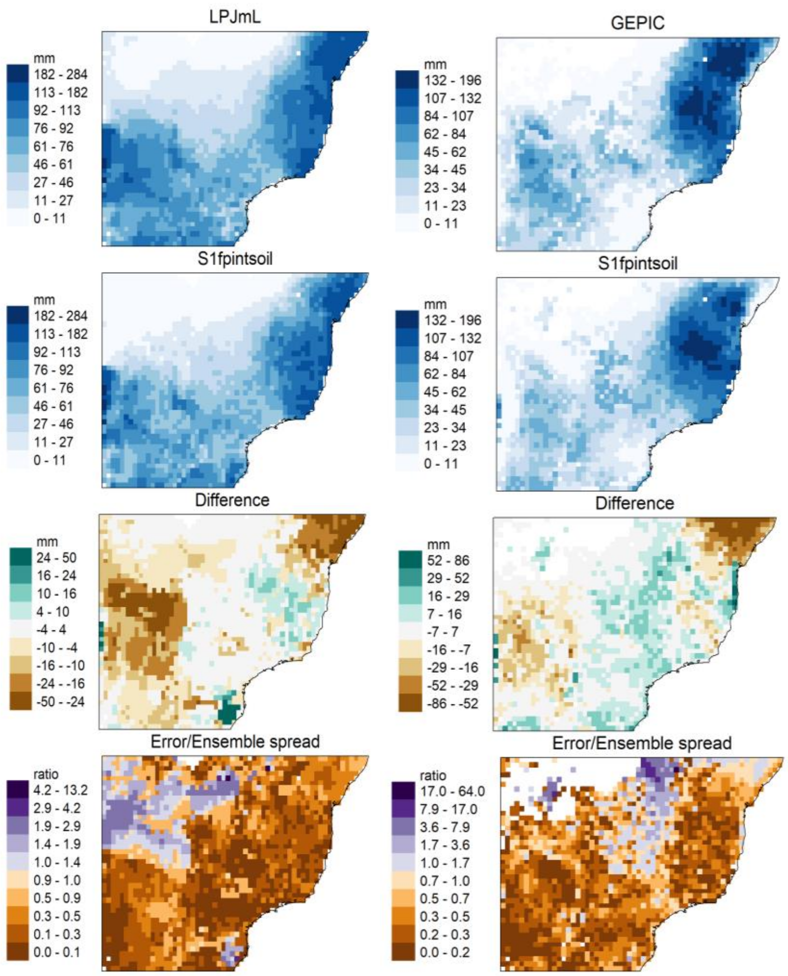

In Europe, the emulator for the PEGASUS model overestimates wheat irrigation requirements in most grid cells in this region. Over the northern part of France and Germany, errors are larger than the ensemble spread. For the LPJ-GUESS model, the emulator underestimates irrigation water withdrawals over France and northern Spain, but the prediction errors are smaller than the ensemble spread. For both models, predictions from the emulators are reasonably accurate in areas where little irrigation is required.

Figure 14. Irrigation water withdrawals for wheat averaged over 2090–2099 for the LPJ-GUESS and PEGASUS models and S1fpintsoil specification over Europe

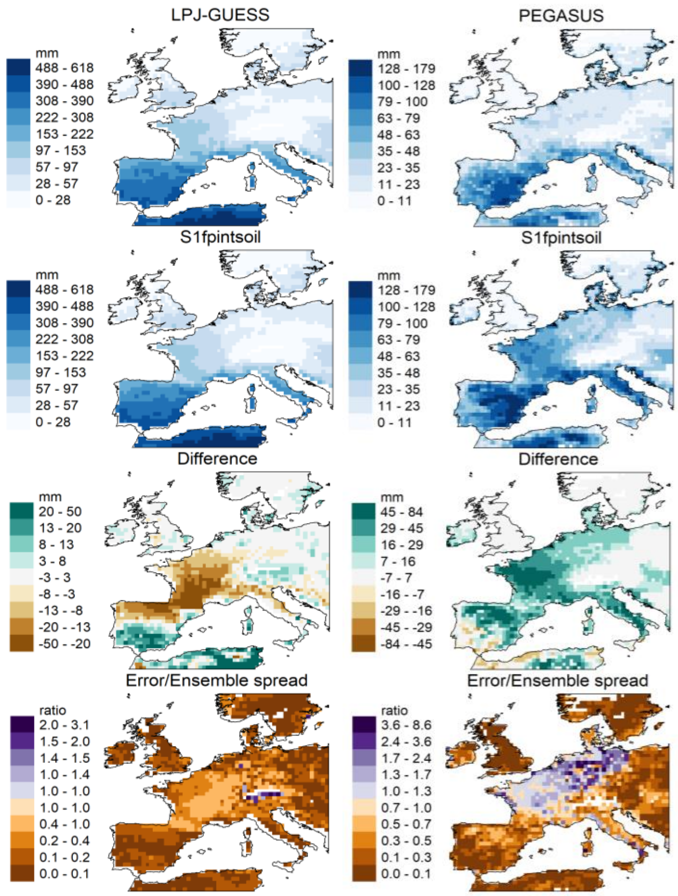

Maps representing spatial agreement in terms of changes from 2000s to 2090s for major production regions are presented in Appendix H. The maps show that large decreases in irrigation demand are expected by most GGCMs. Estimated changes from the 2000s to the 2090sare reproduced reasonably well by most emulators.

4.2. Out-of-sample validation

The out-of-sample validation exercise consists of comparing predictions from emulators that are re-estimated using (sub-) sample that excludes weather variables from one climate model, to outputs from GGCMs under the excluded climate model sub-sample. This exercise is performed for both irrigated yields and irrigation water withdrawal.

4.2.1. Irrigated crop yields

For irrigated crop yields, the NRMSE statistics calculated for each sub-sample are reported in Table 4 and compared to the NRMSEs from the full sample estimation presented in Section 3. Unsurprisingly, the prediction errors from the out-of-sample exercise are larger than those from the in-sample estimations. The differences between the NRMSEs averaged over all leave-one-out samples and the in-sample NRMSEs are however relatively small, with differences ranging between 0.002 and 0.009. The errors are generally the smallest for the estimates with the NorESM1-M climate model excluded from the estimation sample.

Table 4. NRMSE statistics for the leave-one-GCM-out validation (S1fpintsoil specification) compared to the full sample

Crop	Model	Climate model predictions excluded from the sub-sample			Overall	Full sample
		GFDL-ESM2M	HadGEM2-ES	NorESM1-M		
Maize	GEPIC	0.051	0.057	0.048	0.052	0.045
	LPJ-GUESS	0.049	0.045	0.042	0.045	0.037
	LPJmL	0.045	0.040	0.040	0.042	0.035
	pDSSAT	0.076	0.071	0.074	0.074	0.065
	PEGASUS	0.057	0.061	0.055	0.058	0.056
Rice	GEPIC	0.065	0.068	0.059	0.064	0.056
	LPJ-GUESS	0.044	0.038	0.038	0.040	0.033
	LPJmL	0.043	0.042	0.037	0.041	0.037
Soybean	GEPIC	0.066	0.066	0.054	0.062	0.054
	LPJ-GUESS	0.049	0.046	0.041	0.045	0.037
	LPJmL	0.035	0.034	0.031	0.033	0.030
	PEGASUS	0.048	0.052	0.043	0.048	0.042
Wheat	GEPIC	0.054	0.057	0.052	0.055	0.049
	LPJ-GUESS	0.039	0.037	0.036	0.038	0.029
	LPJmL	0.033	0.032	0.029	0.032	0.026
	pDSSAT	0.643	0.669	0.570	0.627	0.572
	PEGASUS	0.033	0.037	0.031	0.034	0.030

Time series of irrigated crops yields weighted by irrigated area harvested for each crop, GGCM and leave-one-GCM-out combination are presented in Figure 15. The graphs show that, as for the in-sample validation, the emulators are able to reproduce the out-of-sample trend in crop yields of most GGCMs. However, in some cases, the emulator and GGCM outputs differ depending on the climate sample excluded. For instance, for maize yields with the GEPIC model, the graphs indicate that, in the case where data from the HadGEM2-ES model is excluded from the training dataset, the emulated irrigated maize crop yields are overestimated while they are underestimated in the case where the NorESM1-M model is excluded. In such cases, the use of the largest sample of plausible climate change is essential to estimate the response functions.

Figure 15. Average irrigated crop yield projections from GGCMs and statistical models (S1fpintsoil specification) weighted by irrigated area harvested in the leave-one-GCM-out validation exercise

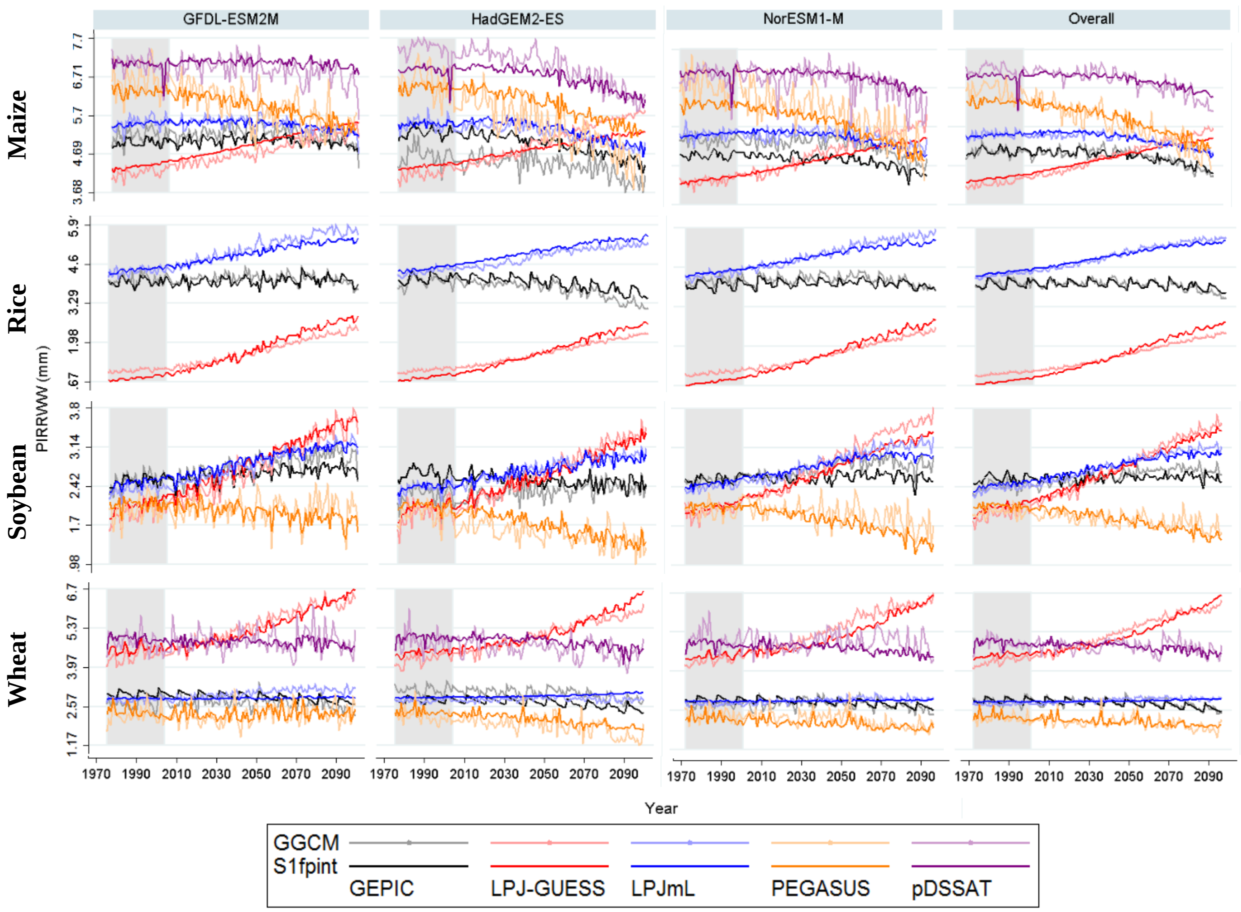

4.2.2. Irrigation water withdrawals

As for irrigated crop yields, the NRMSE statistics calculated for irrigation water withdrawal for each excluded sample (see Table 5) show that the prediction errors from the out-of-sample exercise are slightly larger than those from the in-sample estimations. As for irrigated yields, the errors are generally the smallest under the excluded NorESM1-M climate model.

Table 5. NRMSE statistics for the leave-one-GCM-out validation (S1fpintsoil specification) compared to the full sample

Crop	Model	Climate model predictions excluded from the sub-sample			Overall	Full sample
		GFDL -ESM2M	HadGEM2-ES	NorESM1-M		
Maize	**GEPIC**	0.070	0.081	0.078	0.076	0.061
	LPJ-GUESS	0.059	0.058	0.052	0.056	0.048
	LPJmL	0.049	0.045	0.042	0.045	0.039
	pDSSAT	0.084	0.074	0.074	0.077	0.067
	PEGASUS	0.044	0.047	0.040	0.044	0.040
Rice	**GEPIC**	0.061	0.071	0.063	0.065	0.054
	LPJ-GUESS	0.048	0.049	0.043	0.047	0.038
	LPJmL	0.054	0.048	0.045	0.049	0.041
Soybean	**GEPIC**	0.068	0.075	0.068	0.070	0.060
	LPJ-GUESS	0.055	0.061	0.051	0.056	0.045
	LPJmL	0.055	0.049	0.048	0.051	0.043
	PEGASUS	0.056	0.057	0.049	0.054	0.049
Wheat	**GEPIC**	0.096	0.103	0.094	0.098	0.078
	LPJ-GUESS	0.060	0.059	0.052	0.057	0.048
	LPJmL	0.053	0.053	0.050	0.052	0.042
	pDSSAT	0.055	0.045	0.050	0.050	0.030
	PEGASUS	0.043	0.043	0.036	0.041	0.035

Time series of average irrigation water withdrawals weighted by irrigated area harvested are presented in Figure 16 for each crop, GGCM and leave-one-GCM-out combination. The graphs show that out-of-sample irrigation water withdrawals are generally overestimated by the emulators in cases where projections from GGCMs are the smallest and underestimated where projections are the largest.

Figure 16. Average irrigation water withdrawal projections from GGCMs and statistical models (S1fpintsoil specification) weighted by irrigated area harvested in the leave-one-GCM-out validation exercise

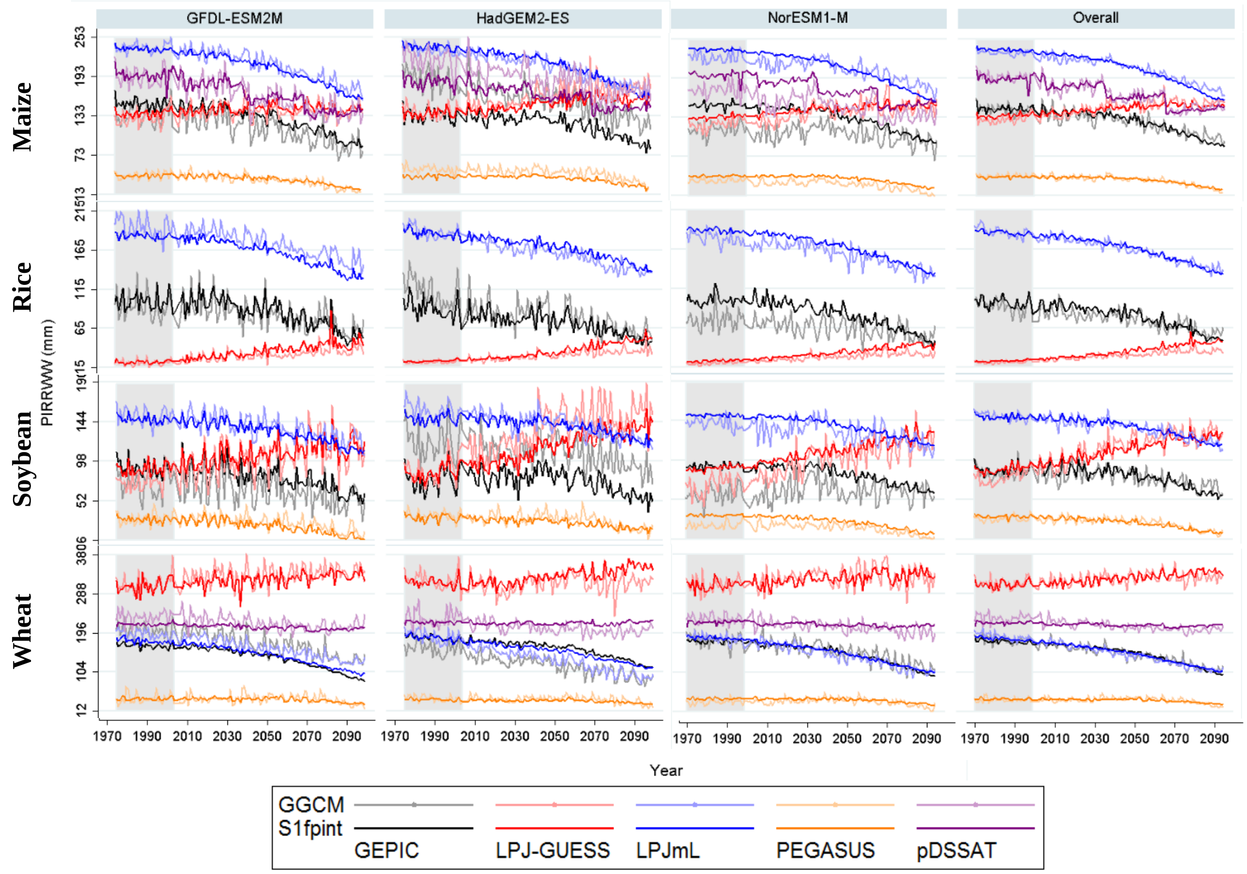

5. Conclusion

Based on the methodology developed in Blanc and Sultan (2015) and Blanc (2017), this analysis develops statistical emulators of global gridded crop models for irrigated crops yields and associated water withdrawals. The emulators for maize, rice, soybean and wheat are estimated using data from an ensemble of simulations from five GGCMs as part of the ISI-MIP Fast Track intercomparison exercise. Crop-specific response functions for each GGCM are estimated at the grid-cell level for both irrigated crop yields and irrigation water withdrawals.

To evaluate the statistical emulators' ability to reproduce irrigated crop yields and associated irrigation water withdrawals estimated by crop models, both in-and out-of-sample validation exercises are conducted.

These exercises show that, in most cases, outputs from the statistical emulators follow the same trend as projections from GGCMs. Inter-annual yield variability is captured with less accuracy but spatial analyses reveal that, overall, the emulators tend to capture the spatial patterns of climate change impacts on irrigated crop yields and irrigation water withdrawals reasonably accurately. Similar spatial agreements are observed when considering the changes in outputs between the beginning and end of the 21st century, despite some disagreements regarding the strength of the impacts in different regions depending on the GGCM considered. When using the emulators for regional assessments of climate change impacts, caution should therefore be exercised when selecting an ensemble of emulators that best capture the impact projected by the underlying GGCMs.

Out-of-sample validation exercises also show a general agreement between the estimates from the emulators and the GGCMs. However, as expected, prediction accuracy is lowered when excluding output responses to weather variables outside the range of values found in the estimation sample. Estimating the statistical emulator using the largest sample available, which is designed to encompass the largest range of plausible changes in climate over the century, is essential.

The statistical emulators estimated in this study offer an accessible and reliable tool to estimate climate change impacts on irrigated crop yields and associated irrigation water withdrawals under alternative plausible user-defined scenarios. However, as previously noted in Blanc (2017), the emulator is better suited to assess long-term climate change impacts rather than inter-annual yield and irrigation withdrawal variations. It is also important to note that, as no GGCMS is considered more accurate than another at projecting future crop yields, predictions from multiple models should be considered. In this regard, the emulators developed in this study provide a computationally efficient way to consider modeling uncertainty in climate change impact assessments for several crops.

The emulators estimated in this study are easily applicable using user-defined scenarios using the variable transformation and regression coefficients provided in Appendices B, C and D. For the emulators for rainfed crop yields developed by Blanc (2017), a tool was developed in Blanc (2017b) to increase the accessibility of the emulators.. Employing the tool, users could access estimated changes in rainfed crop yields at the grid-cell level by entering user-defined climate variables in an easy-to-use interface. A similar tool will be developed for the irrigated crop yield and irrigation water withdrawal emulators developed this study.

6. References

Auffhammer, Maximilian, and Wolfram Schlenker. 2014. "Empirical Studies on Agricultural Impacts and Adaptation." *Energy Economics* 46 (November). North-Holland:555–61. https://doi.org/10.1016/J.ENECO.2014.09.010.

Blanc, Élodie. 2017a. "Statistical Emulators of Irrigated Crop Yields and Irrigation Requirements from Global Gridded Crop Models," in preparation.

———. 2017b. "Statistical Emulators of Maize, Rice, Soybean and Wheat Yields from Global Gridded Crop Models." *Agricultural and Forest Meteorology* 236:145–61. https://doi.org/10.1016/j.agrformet.2016.12.022.

———. 2017c. "Aggregation of Gridded Emulated Rainfed Crop Yield Projections at the National or Regional Level." *Journal of Global Economic Analysis* 2 (2):112–27. https://doi.org/10.21642/JGEA.020203AF.

Blanc, Élodie, Justin Caron, Charles Fant, and Erwan Monier. 2017. "Climate Change Impact on Water Resources and Irrigated Crop Yields in the US." *Earth's Future* forthcomin:in press.

Blanc, Élodie, and Eric Strobl. 2013. "The Impact of Climate Change on Cropland Productivity: Evidence from Satellite Based Products at the River Basin Scale in Africa." *Climatic Change* 117 (4):873–90. https://doi.org/10.1007/s10584-012-0604-4.

Blanc, Élodie, and Benjamin Sultan. 2015. "Emulating Maize Yields from Global Gridded Crop Models Using Statistical Estimates." *Agricultural and Forest Meteorology* 214–215:134–47. https://doi.org/http://dx.doi.org/10.1016/j.agrformet.2015.08.256.

Bondeau, Alberte, Pascalle C. Smith, Sonke Sönke Zaehle, Sibyll Schaphoff, Wolfgang Lucht, Wolfgang Cramer, Dieter Gerten, et al. 2007. "Modelling the Role of Agriculture for the 20th Century Global Terrestrial Carbon Balance." *Global Change Biology* 13 (3). Blackwell Publishing Ltd:679–706. https://doi.org/10.1111/j.1365-2486.2006.01305.x.

Boote, Kenneth J., James W. Jones, Jeffrey W. White, Senthold Asseng, and Jon I. Lizaso. 2013. "Putting Mechanisms into Crop Production Models." *Plant, Cell & Environment* 36 (9). Wiley/Blackwell (10.1111):1658–72. https://doi.org/10.1111/pce.12119.

Calvin, Katherine, and Karen Fisher-Vanden. 2017. "Quantifying the Indirect Impacts of Climate on Agriculture: An Inter-Method Comparison." *Environmental Research Letters* 12 (11). IOP Publishing:115004. https://doi.org/10.1088/1748-9326/aa843c.

Deryng, Delphine, Declan Conway, Navin Ramankutty, Jeff Price, and Rachel Warren. 2014. "Global Crop Yield Response to Extreme Heat Stress under Multiple Climate Change Futures." *Environmental Research Letters* 9 (3):34011. http://stacks.iop.org/1748-9326/9/i=3/a=034011.

Deryng, Delphine, W. J. Sacks, C. C. Barford, and Navin Ramankutty. 2011. "Simulating the Effects of Climate and Agricultural Management Practices on Global Crop Yield." *Global Biogeochemical Cycles* 25 (2):n/a-n/a. https://doi.org/10.1029/2009GB003765.

Elliott, Joshua, Delphine Deryng, Christoph Müller, Katja Frieler, Markus Konzmann, Dieter Gerten, Michael Glotter, et al. 2014. "Constraints and Potentials of Future Irrigation Water Availability on Agricultural Production under Climate Change." *Proceedings of the National Academy of Sciences* 111 (9). National Academy of Sciences:3239–44.

https://doi.org/10.1073/pnas.1222474110.

Elliott, Joshua, Michael Glotter, N Best, D Kelly, M Wilde, and I Foster. 2013. “The Parallel System for Integrating Impact Models and Sectors (PSIMS).” In *Conference on Extreme Science and Engineering Discovery Environment: Gateway to Discovery (XSEDE ’13)*, 21:1–8. Association for Computing Machinery.

FAO-UNESCO. 2005. “ Soil Map of the World, Digitized by ESRI.” Washington D.C.: USDA-NRCS, Soil Science Division, World Soil Resources.

Haim, David, Mordechai Shechter, and Pedro Berliner. 2007. “Assessing the Impact of Climate Change on Representative Field Crops in Israeli Agriculture: A Case Study of Wheat and Cotton.” *Climatic Change*.

Hempel, S, K Frieler, Lila Warszawski, J Schewe, and F Piontek. 2013. “A Trend-Preserving Bias Correction – the ISI-MIP Approach.” *Earth System Dynamics* 4 (2):219–36.

Holzkämper, A, P. Calanca, and J Fuhrer. 2012. “Statistical Crop Models: Predicting the Effects of Temperature and Precipitation Changes.” *Climate Research* 51 (1):11–21. https://doi.org/10.3354/cr01057.

Hsiang, Solomon. 2016. “Climate Econometrics.” *Annual Review of Resource Economics* 8 (1). Annual Reviews :43–75. https://doi.org/10.1146/annurev-resource-100815-095343.

Jones, J, G Hoogenboom, C Porter, Kenneth J. Boote, W Batchelor, L Hunt, and J Ritchie. 2003. “The DSSAT Cropping System Model.” *European Journal of Agronomy* 18 (3–4):235–65.

Lindeskog, M, A Arneth, Alberte Bondeau, Katharina Waha, J Seaquist, S Olin, and B Smith. 2013. “Implications of Accounting for Land Use in Simulations of Ecosystem Services and Carbon Cycling in Africa.” *Earth System Dynamics Discussions* 4:235–78.

Liu, Junguo, Jimmy R Williams, Alexander J B Zehnder, and Hong Yang. 2007. “GEPIC – Modelling Wheat Yield and Crop Water Productivity with High Resolution on a Global Scale.” *Agricultural Systems* 94 (2):478–93. https://doi.org/http://dx.doi.org/10.1016/j.agsy.2006.11.019.

Lobell, David B, and Senthold Asseng. 2017. “Comparing Estimates of Climate Change Impacts from Process-Based and Statistical Crop Models.” *Environmental Research Letters* 12 (1):15001. http://stacks.iop.org/1748-9326/12/i=1/a=015001.

Lobell, David B, and Marshall B Burke. 2010. “On the Use of Statistical Models to Predict Crop Yield Responses to Climate Change.” *Agricultural and Forest Meteorology* 150 (11):1443–52. https://doi.org/http://dx.doi.org/10.1016/j.agrformet.2010.07.008.

Lobell, David, and Christopher Field. 2007. “Global Scale Climate-Crop Yield Relationships and the Impacts of Recent Warming.” *Environmental Research Letters* 2 (1):1–7.

Monier, Erwan, Sergey Paltsev, Andrei P. Sokolov, Y.-H. Henry Chen, Xiang Gao, Qudsia Ejaz, Evan Couzo, et al. 2018. “Toward a Consistent Modeling Framework to Assess Multi-Sectoral Climate Impacts.” *Nature Communications* 9 (1):660. https://doi.org/10.1038/s41467-018-02984-9.

Moore, Frances C, Uris Lantz C Baldos, and Thomas Hertel. 2017. “Economic Impacts of Climate Change on Agriculture: A Comparison of Process-Based and Statistical Yield Models.” *Environmental Research Letters* 12 (6):65008. http://stacks.iop.org/1748-

9326/12/i=6/a=065008.

Ostberg, S., J. Schewe, K. Childers, and K. Frieler. 2018. "Changes in Crop Yields and Their Variability at Different Levels of Global Warming." *Earth System Dynamics Discussions* 9:479–96. https://doi.org/https://doi.org/10.5194/esd-2017-69.

Oyebamiji, Oluwole K, Neil R Edwards, Philip B Holden, Paul H Garthwaite, Sibyll Schaphoff, and Dieter Gerten. 2015. "Emulating Global Climate Change Impacts on Crop Yields." *Statistical Modelling* In Press.

Parry, Martin L., G Fischer, M Livermore, Cynthia Rosenzweig, and A Iglesias. 1999. "Climate Change and World Food Security: A New Assessment." *Global Environmental Change* 9:551–67.

Portmann, F T, S Siebert, and P Döll. 2010. "MIRCA2000 - Global Monthly Irrigated and Rainfed Crop Areas around the Year 2000: A New High-Resolution Data Set for Agricultural and Hydrological Modeling." *Global Biogeochemical Cycles* 24.

Riahi, Keywan, Arnulf Grübler, and Nebojsa Nakicenovic. 2007. "Scenarios of Long-Term Socio-Economic and Environmental Development under Climate Stabilization." *Technological Forecasting and Social Change* 74 (7):887–935. https://doi.org/http://dx.doi.org/10.1016/j.techfore.2006.05.026.

Roberts, Michael J, Noah O Braun, Thomas R Sinclair, David B Lobell, and Wolfram Schlenker. 2017. "Comparing and Combining Process-Based Crop Models and Statistical Models with Some Implications for Climate Change." *Environmental Research Letters* 12 (9). IOP Publishing:095010. https://doi.org/10.1088/1748-9326/aa7f33.

Rosenzweig, Cynthia, Joshua Elliott, Delphine Deryng, Alex C Ruane, Christoph Müller, Almut Arneth, Kenneth J. Boote, et al. 2014. "Assessing Agricultural Risks of Climate Change in the 21st Century in a Global Gridded Crop Model Intercomparison." *Proceedings of the National Academy of Sciences* 111 (9):3268–73. https://doi.org/10.1073/pnas.1222463110.

Rosenzweig, Cynthia, J W Jones, J L Hatfield, A C Ruane, Kenneth J. Boote, P Thorburn, John M Antle, et al. 2013. "The Agricultural Model Intercomparison and Improvement Project (AgMIP): Protocols and Pilot Studies." *Agricultural and Forest Meteorology* 170 (0):166–82. https://doi.org/http://dx.doi.org/10.1016/j.agrformet.2012.09.011.

Rosenzweig, Cynthia, and Martin L. Parry. 1994a. "Potential Impacts of Climate Change on World Food Supply." *Nature* 367:133–38. https://doi.org/10.1038/367133a0.

———. 1994b. "Potential Impact of Climate Change on World Food Supply." *Nature* 367 (6459). Nature Publishing Group:133–38. https://doi.org/10.1038/367133a0.

Ruane, Alex C, Cynthia Rosenzweig, Senthold Asseng, Kenneth J. Boote, Joshua Elliott, Frank Ewert, James W Jones, et al. 2017. "An AgMIP Framework for Improved Agricultural Representation in Integrated Assessment Models." *Environmental Research Letters* 12 (12):125003. http://stacks.iop.org/1748-9326/12/i=12/a=125003.

Schauberger, Bernhard, Sotirios Archontoulis, Almut Arneth, Juraj Balkovic, Philippe Ciais, Delphine Deryng, Joshua Elliott, et al. 2017. "Consistent Negative Response of US Crops to High Temperatures in Observations and Crop Models." *Nature Communications* 8 (January). The Author(s):13931. http://dx.doi.org/10.1038/ncomms13931.

Schlenker, Wolfram, and Michael J Roberts. 2009. "Nonlinear Temperature Effects Indicate

Severe Damages to U.S. Crop Yields under Climate Change.” *Proceedings of the National Academy of Sciences of the United States of America* 106 (37). National Academy of Sciences:15594–98. https://doi.org/10.1073/pnas.0906865106.

Smith, Benjamin, I Colin Prentice, and Martin T Sykes. 2001. “Representation of Vegetation Dynamics in the Modelling of Terrestrial Ecosystems: Comparing Two Contrasting Approaches within European Climate Space.” *Global Ecology and Biogeography* 10 (6). Blackwell Science Ltd:621–37. https://doi.org/10.1046/j.1466-822X.2001.t01-1-00256.x.

Soil Survey Staff. 1999. *Soil Taxonomy: A Basic System of Soil Classification for Making and Interpreting Soil Surveys.* 2nd editio. Natural Resources Conservation Service, U.S. Department of Agriculture Handbook 436.

Taylor, Karl E., Ronald J. Stouffer, and Gerald A. Meehl. 2012. “An Overview of CMIP5 and the Experiment Design.” *Bulletin of the American Meteorological Society* 93 (4):485. https://doi.org/10.1175/BAMS-D-11-00094.1.

Waha, Katharina, L G J van Bussel, C Müller, and Alberte Bondeau. 2012. “Climate-Driven Simulation of Global Crop Sowing Dates.” *Global Ecology and Biogeography* 21 (2). Blackwell Publishing Ltd:247–59. https://doi.org/10.1111/j.1466-8238.2011.00678.x.

Warszawski, Lila, Katja Frieler, Veronika Huber, Franziska Piontek, Olivia Serdeczny, and Jacob Schewe. 2014. “The Inter-Sectoral Impact Model Intercomparison Project (ISI-MIP): Project Framework.” *Proceedings of the National Academy of Sciences* 111 (9):3228–32. https://doi.org/10.1073/pnas.1312330110.

White, Jeffrey W., Gerrit Hoogenboom, Bruce A. Kimball, and Gerard W. Wall. 2011. “Methodologies for Simulating Impacts of Climate Change on Crop Production.” *Field Crops Research* 124 (3). Elsevier:357–68. https://doi.org/10.1016/J.FCR.2011.07.001.

Williams, Jimmy R, and V. P. Singh. 1995. “Chapter 25. The EPIC.” In *Computer Models of Watershed Hydrology*, 909–1000. Littleton, CO: Water Resources Publications.

7. Appendices

Appendix A. **MATERIAL AND METHODS**

Table A1. Modeling group information

Model	Institution	Modelers' names
GEPIC	EAWAG (Switzerland)	Christian Folberth
LPJ-GUESS	Institutionen för naturgeografi och ekosystemvetenskap (INES), Lunds Universitet (Sweden)	Thomas Pugh, Stephan Olin
LPJmL	PIK (Germany)	Christoph Muller
PEGASUS	Tyndall Centre, University of East Anglia (UK)	Delphine Deryng
pDSSAT	University of Chicago (USA)	Joshua Elliott

Figure A1. Global soil regions based on the FAO-UNESCO Soil Map of the World using the USDA soil taxonomy

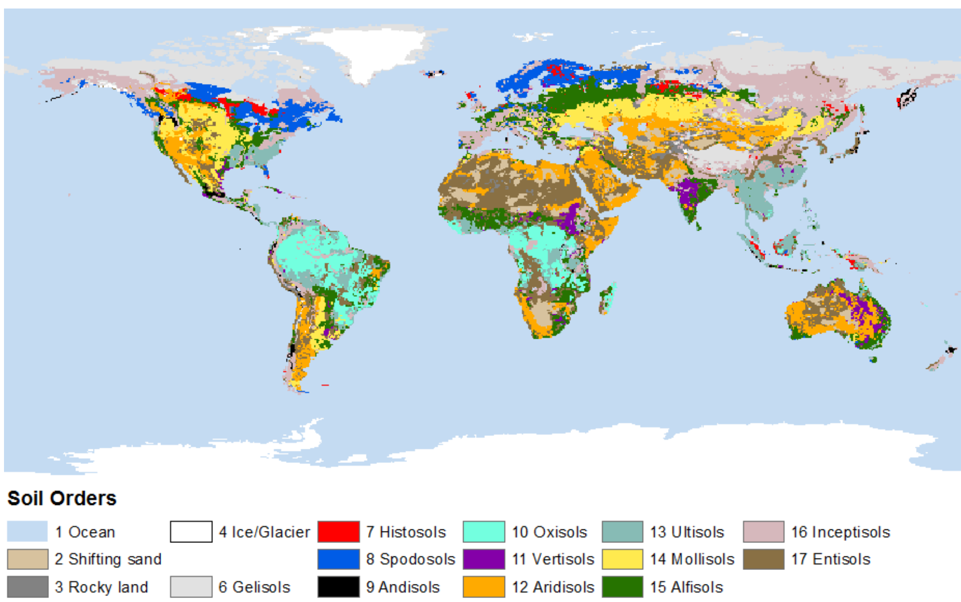

Table A1. Summary statistics by GGCM and GCM

Crop	GGCM	Irrigated crop yields (t/Ha), *YIR*									Irrigation water withdrawals (mm), *PIRRWW*								
		GFDL_ESM2M			HadGEM2_ES			NorESM1_M			GFDL_ESM2M			HadGEM2_ES			NorESM1_M		
		Mean	Min	Max	Mean	Min	Max	Mean	Min	Max	Mean	Min	Max	Mean	Min	Max	Mean	Min	Max
Maize	GEPIC	3.22	0.00	14.74	3.07	0.00	13.01	3.27	0.00	13.24	106.38	0.00	1068.00	109.37	0.00	935.10	90.65	0.00	914.30
	LPJ-GUESS	3.71	0.00	15.27	3.95	0.00	12.30	3.91	0.00	12.91	129.90	0.00	762.05	136.42	0.00	766.58	125.11	0.00	752.18
	LPJmL	3.17	0.00	26.81	3.38	0.00	30.40	3.30	0.00	26.66	156.16	0.00	1114.07	152.64	0.00	1119.02	150.24	0.00	1125.14
	PEGASUS	3.00	0.00	35.00	3.24	0.00	35.00	3.29	0.00	34.99	26.31	0.00	800.67	29.53	0.00	829.34	23.07	0.00	792.11
	pDSSAT	3.81	0.00	24.09	4.39	0.00	24.10	4.17	0.00	24.11	138.51	0.00	1000.50	150.69	0.00	1018.50	125.62	0.00	1055.25
Rice	GEPIC	2.74	0.00	13.25	2.60	0.00	12.06	2.81	0.00	12.16	143.09	0.00	1734.60	144.94	0.00	1630.20	122.79	0.00	1582.60
	LPJ-GUESS	2.13	0.00	20.69	2.19	0.00	22.84	2.29	0.00	20.83	85.43	0.00	1129.64	85.64	0.00	1059.34	81.13	0.00	1046.81
	LPJmL	2.63	0.00	23.08	2.68	0.00	23.36	2.69	0.00	23.74	150.54	0.00	962.42	149.43	0.00	993.82	145.71	0.00	970.27
Soybean	GEPIC	1.38	0.00	5.89	1.33	0.00	6.06	1.41	0.00	6.30	84.63	0.00	996.90	83.99	0.00	889.00	71.35	0.00	910.40
	LPJ-GUESS	1.75	0.00	12.14	1.82	0.00	11.66	1.89	0.00	12.25	121.51	0.00	968.59	126.60	0.00	1335.53	119.44	0.00	1306.70
	LPJmL	1.99	0.00	19.47	2.06	0.00	19.66	2.08	0.00	20.73	112.38	0.00	779.93	111.59	0.00	763.87	108.79	0.00	786.50
	PEGASUS	1.98	0.00	22.21	2.17	0.00	23.74	2.21	0.00	22.52	39.40	0.00	713.44	44.12	0.00	801.95	35.06	0.00	707.18
Wheat	GEPIC	2.18	0.00	10.06	2.18	0.00	9.60	2.24	0.00	9.73	117.64	0.00	721.80	107.13	0.00	639.50	103.61	0.00	612.10
	LPJ-GUESS	4.36	0.00	24.12	4.35	0.00	22.69	4.53	0.00	22.28	155.47	0.00	1059.80	159.79	0.00	1048.93	151.65	0.00	1052.28
	LPJmL	2.47	0.00	16.63	2.39	0.00	16.14	2.48	0.00	15.15	105.25	0.00	1047.35	99.09	0.00	979.18	103.79	0.00	951.06
	PEGASUS	1.72	0.00	34.76	1.67	0.00	34.79	1.80	0.00	34.98	20.87	0.00	712.25	23.93	0.00	722.45	18.89	0.00	718.73
	pDSSAT	3.01	0.00	32.72	3.09	0.00	34.83	3.13	0.00	34.54	138.40	0.00	2693.25	149.91	0.00	2797.50	141.12	0.00	2823.00

Alternative specifications

For irrigated crops, the five GGCMs considered in this study assume that irrigation is applied to compensate for the lack of precipitation. More specifically, for the GEPIC model, *"full irrigation was set as a complete elimination of water stress of crops"* (Rosenzweig et al. 2014). In the four other models, however, irrigation is triggered when soil moisture is insufficient. More specifically, For the LPJ-GUESS and LPJmL models, *"additional water is provided as soon as the water content of the upper soil layer is insufficient"* (Bondeau et al. 2007). The PEGASUS model ensures *"that soil is sufficiently moist to avoid water stress in irrigated land"* (Deryng et al. 2011). The pDSSAT model, "*Determines daily irrigation, based on read-in values or automatic applications based on soil water depletion"* (Jones et al. 2003). For these models, water stress may not necessarily be completely eliminated by full irrigation (Rosenzweig et al. 2014).

To assess the effect of precipitation that may not have been completely eliminated by irrigation, a second specification (S2fpintsoil) including precipitation is specified as:

$$YIR_{lat,lon,gcm,y} = \alpha + \sum_{i=1}^{3} \beta_i Pr_{i_{lat,lon,gcm,y}} + \sum_{i=1}^{3} \theta_i Tmean_{i_{lat,lon,gcm,y}} + \vartheta CO2_{gcm,y} +$$
$$\sum_{i=1}^{3} \gamma_i Pr_{i_{lat,lon,gcm,y}} * Tmean_{i_{lat,lon,gcm,y}} + \sum_{i=1}^{3} \varepsilon_i Pr_{i_{lat,lon,gcm,y}} * CO2_{gcm,y} +$$
$$\sum_{i=1}^{3} \kappa_i Tmean\_i_{lat,lon,gcm,y} * CO2_{gcm,y} + \delta_{lat,lon} + \rho_{lat,lon,gcm,y} \quad (3)$$

For annual irrigation water requirements (*PIRRWW*), a second specification (S2fpintsoil) considers evapotranspiration (*ETo*) instead of temperature to account for the effect of summer weather on irrigation requirements:

$$PIRRWW_{lat,lon,gcm,y} = \alpha + \sum_{i=1}^{3} \beta_i Pr_{i_{lat,lon,gcm,y}} + \sum_{i=1}^{3} \theta_i ETo_{i_{lat,lon,gcm,y}} + \vartheta CO2_{gcm,y} +$$
$$\sum_{i=1}^{3} \gamma_i Pr_{i_{lat,lon,gcm,y}} * ETo_{i_{lat,lon,gcm,y}} + \sum_{i=1}^{3} \gamma_i Pr_{i_{lat,lon,gcm,y}} * CO2_{gcm,y} +$$
$$\sum_{i=1}^{3} \gamma_i Tmean\_i_{lat,lon,gcm,y} * CO2_{gcm,y} + \delta_{lat,lon} + \rho_{lat,lon,gcm,y} \quad (5)$$

The specifications used to estimate *YIR* and *PIRRWW* are summarized in Table A2.

Table A2. Specification description

Dependent variable	Specification	Variables and non-linear transformations
YIR	S1fpintsoil	*Tmean_p1, Tmean_p2, CO2_p1, CO2_p2*
	S2fpintsoil	*Pr_p1, Pr_p2, Tmean_p1, Tmean_p2, CO2_p1, CO2_p2*
PIRRWW	S1fpintsoil	*Pr, Tmean_p1, Tmean_p2, CO2_p1, CO2_p2*
	S2fpintsoil	*Pr, ETo _p1, ETo _p2, CO2_p1, CO2_p2*

Note: the suffixes _p1 and _p2 denote the fractional polynomial power terms; All specifications include interaction terms between *Tmean, Pr* and CO2 and are estimated at the soil order level.

For each crop and GGCM, regressions for irrigated yields are estimated for each specification S1 and S2 considering the fractional polynomial transformations at the soil order subsample level (S1fpintsoil and S2fpintsoil). As presented in Figure A2, the normalized root mean square error (NRMSE), which is calculated by dividing the RMSE by the difference between maximum and minimum yields, indicates that only slightly lower NRMSEs are found for the S2 specification compared to S1 across most crops and GGCMs. To favor simplicity, the most parsimonious S1 specification assuming that irrigation eliminates water stress (i.e. excluding the effect of precipitation) is thereafter preferred.

Figure A2. Goodness of fit of the irrigated yield statistical emulators by crop and GGCM (S1fpintsoil and S2fpintsoil specifications)

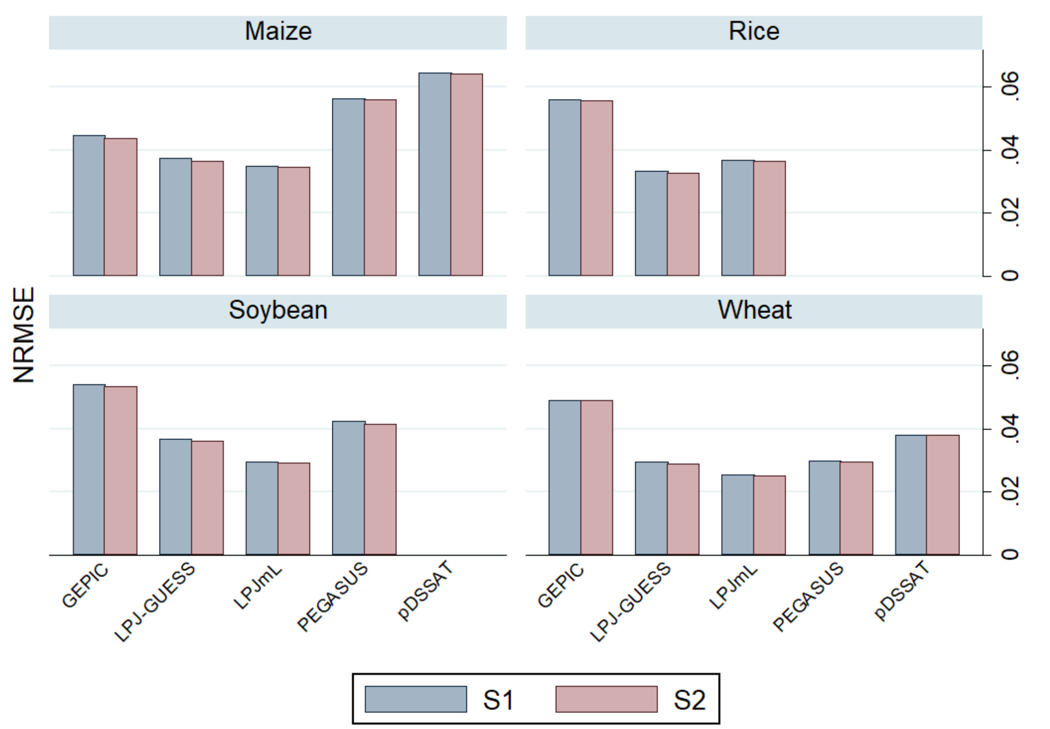

As for crop yields, regressions for irrigation water withdrawal are estimated for each crop and GGCM at the soil order subsample level considering both specifications S1 and S2 with fractional polynomial transformations (S1fpintsoil and S2fpintsoil). The NRMSE presented in Figure A3, shows that across all crops and models, the NRMSE for the S1 specification is found to be slightly lower or equal to the S2 specification. The S1 specification is thereafter preferred.

Figure A3. Goodness of fit of the irrigation water withdrawal statistical emulators by crop and GGCM (S1fpintsoil and S2fpintsoil specifications)

Appendix B. **FRACTIONAL POLYNOMIAL TRANSFORMATION**

See Excel file *Appendix_B_Variable_transformations.xslx* attached composed of the following table:

Table B1. Variable formulas for fractional polynomial transformation used in specification S1fpintsoil for *YIR*

Table B2. Variable formulas for fractional polynomial transformation used in specification S1fpintsoil for *PIRWW*

Appendix C. **REGRESSION RESULTS FOR *YIR* (S1FPINTSOIL SPECIFICATION)**

See Excel file *Appendix_C_regression_results_YIR.xls* attached composed of the following tables:

Table C1. Regression results for maize *YIR* at the soil order level (specification S1fpintsoil)

Table C2. Regression results for rice *YIR* at the soil order level (specification S1fpintsoil)

Table C3. Regression results for soybean *YIR* at the soil order level (specification S1fpintsoil)

Table C4. Regression results for wheat *YIR* at the soil order level (specification S1fpintsoil)

Appendix D. **REGRESSION RESULTS FOR *PIRRWW* (S1FPINTSOIL SPECIFICATION)**

See Excel file *Appendix_D_regression_results_PIRRWW.xls* attached composed of the following tables:

Table D1. Regression results for maize *PIRRWW* at the soil order level (specification S1fpintsoil)

Table D2. Regression results for rice *PIRRWW* at the soil order level (specification S1fpintsoil)

Table D3. Regression results for soybean *PIRRWW* at the soil order level (specification S1fpintsoil)

Table D4. Regression results for wheat *PIRRWW* at the soil order level (specification S1fpintsoil)

Appendix E. **FIXED EFFECTS (Δ) FOR *YIR* (S1FPINTSOIL SPECIFICATION)**

See Excel file *Appendix_E_Grid_cells_FE_yir.xls* attached composed of the following tables:

Table E1. Grid cell fixed effect (δ) by GGCM for maize

Table E2. Grid cell fixed effect (δ) by GGCM for rice

Table E3. Grid cell fixed effect (δ) by GGCM for soybean

Table E4. Grid cell fixed effect (δ) by GGCM for wheat

Appendix F. **FIXED EFFECTS (Δ) FOR *PIRRWW* (S1FPINTSOIL SPECIFICATION)**

See Excel file *Appendix_F_Grid_cells_FE_pirrww.xls* attached composed of the following tables:

Table F1. Grid cell fixed effect (δ) by GGCM for maize

Table F2. Grid cell fixed effect (δ) by GGCM for rice

Table F3. Grid cell fixed effect (δ) by GGCM for soybean

Table F4. Grid cell fixed effect (δ) by GGCM for wheat

Appendix G. **IN-SAMPLE VALIDATION FOR *YIR* (S1FPINTSOIL SPECIFICATION)**

Figure G1. Irrigated maize yields averaged over 2090–2099 for the GEPIC model and S1fpintsoil specification

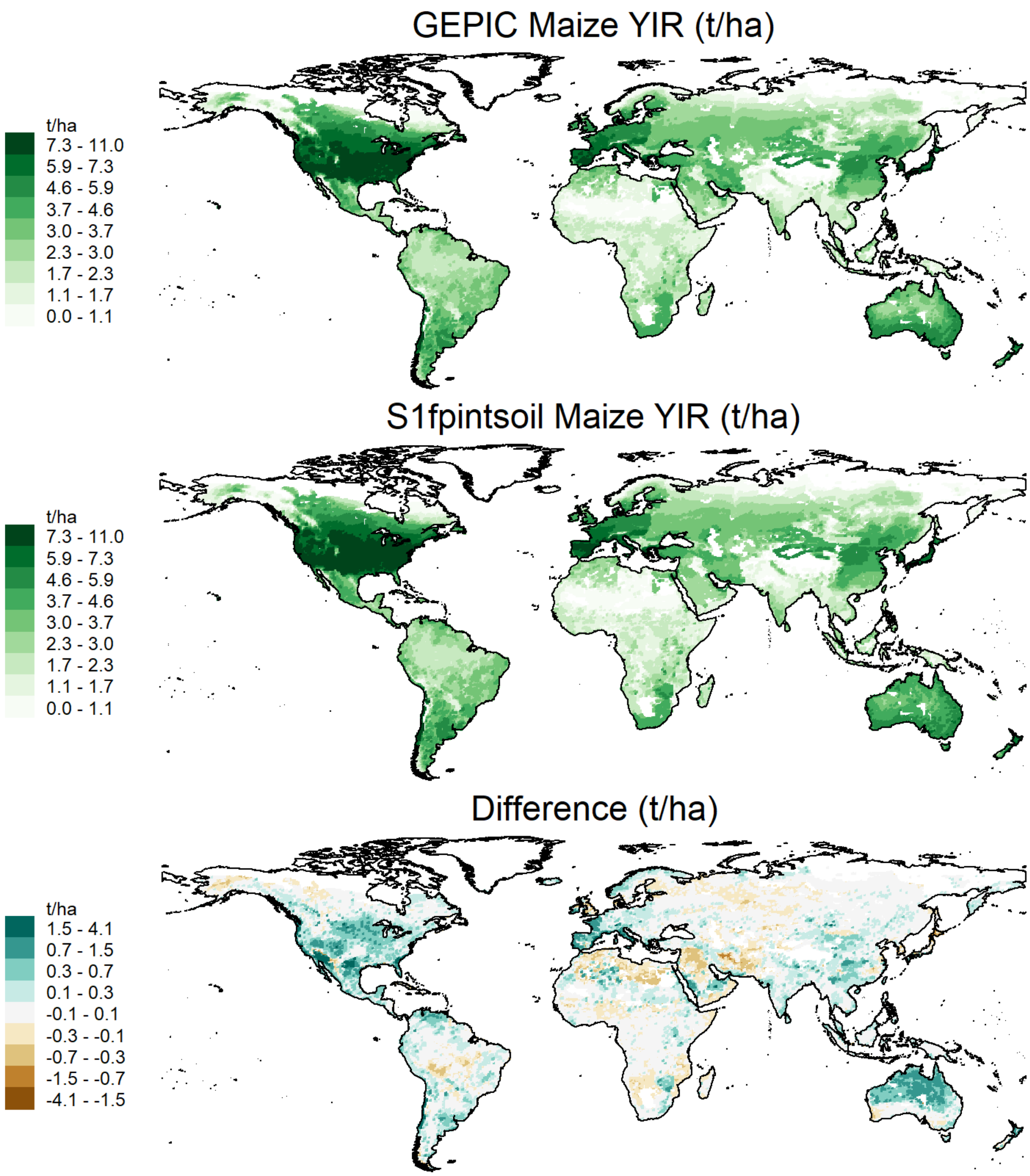

Figure G2. Irrigated maize yields averaged over 2090–2099 for the LPJ-GUESS model and S1fpintsoil specification

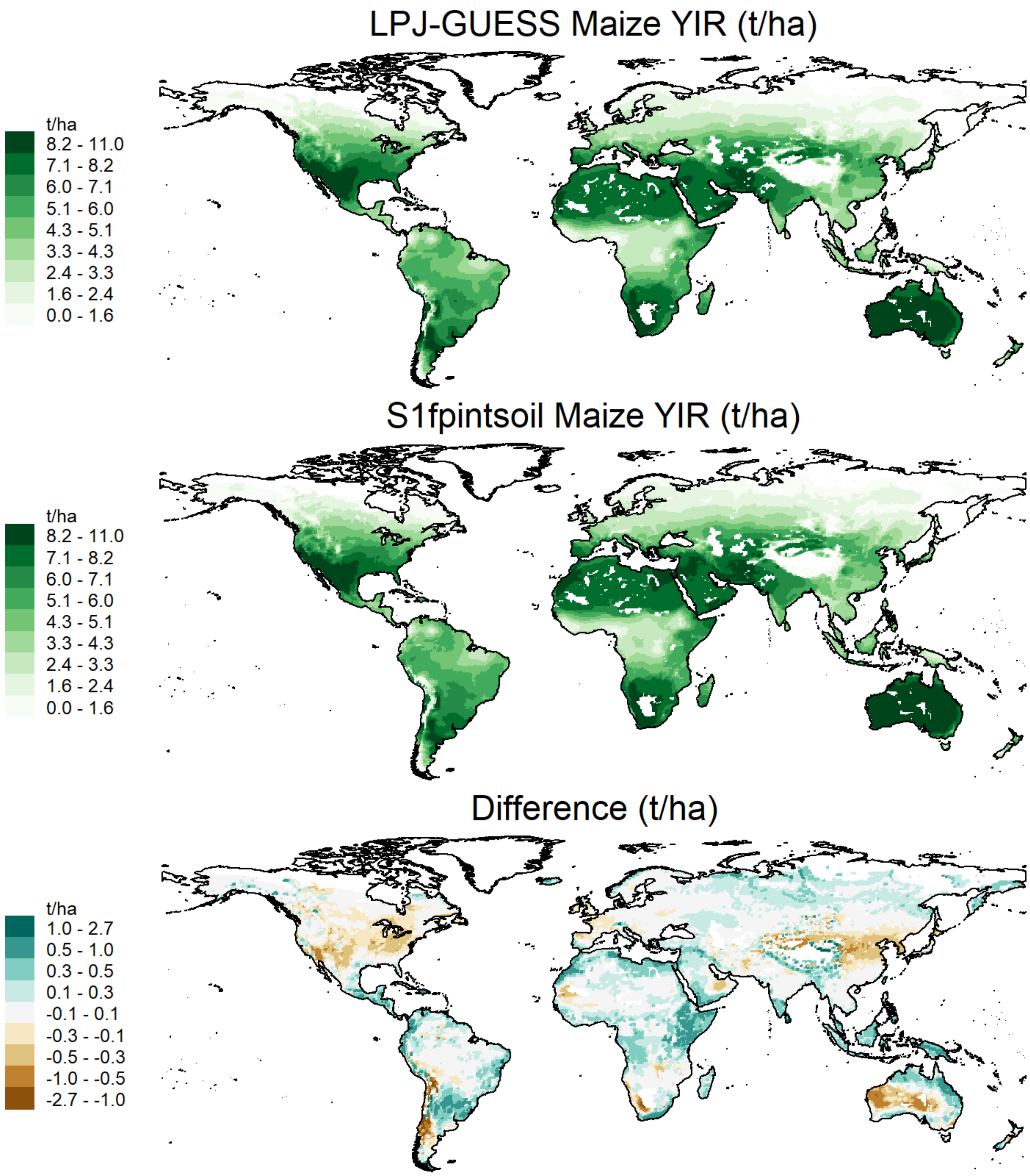

Figure G3. Irrigated maize yields averaged over 2090–2099 for the LPJmL model and S1fpintsoil specification

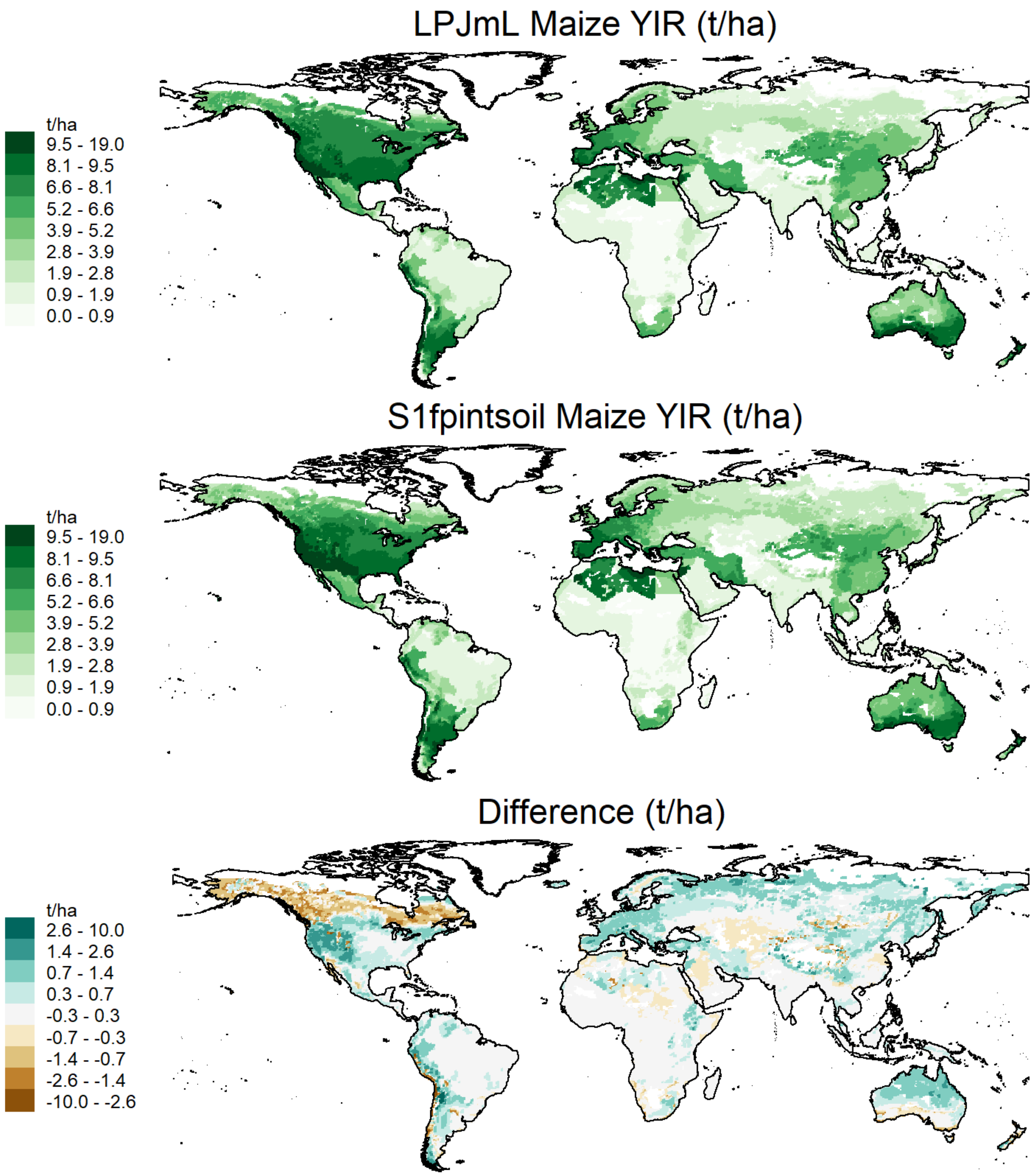

Figure G4. Irrigated maize yields averaged over 2090–2099 for the pDSSAT model and S1fpintsoil specification

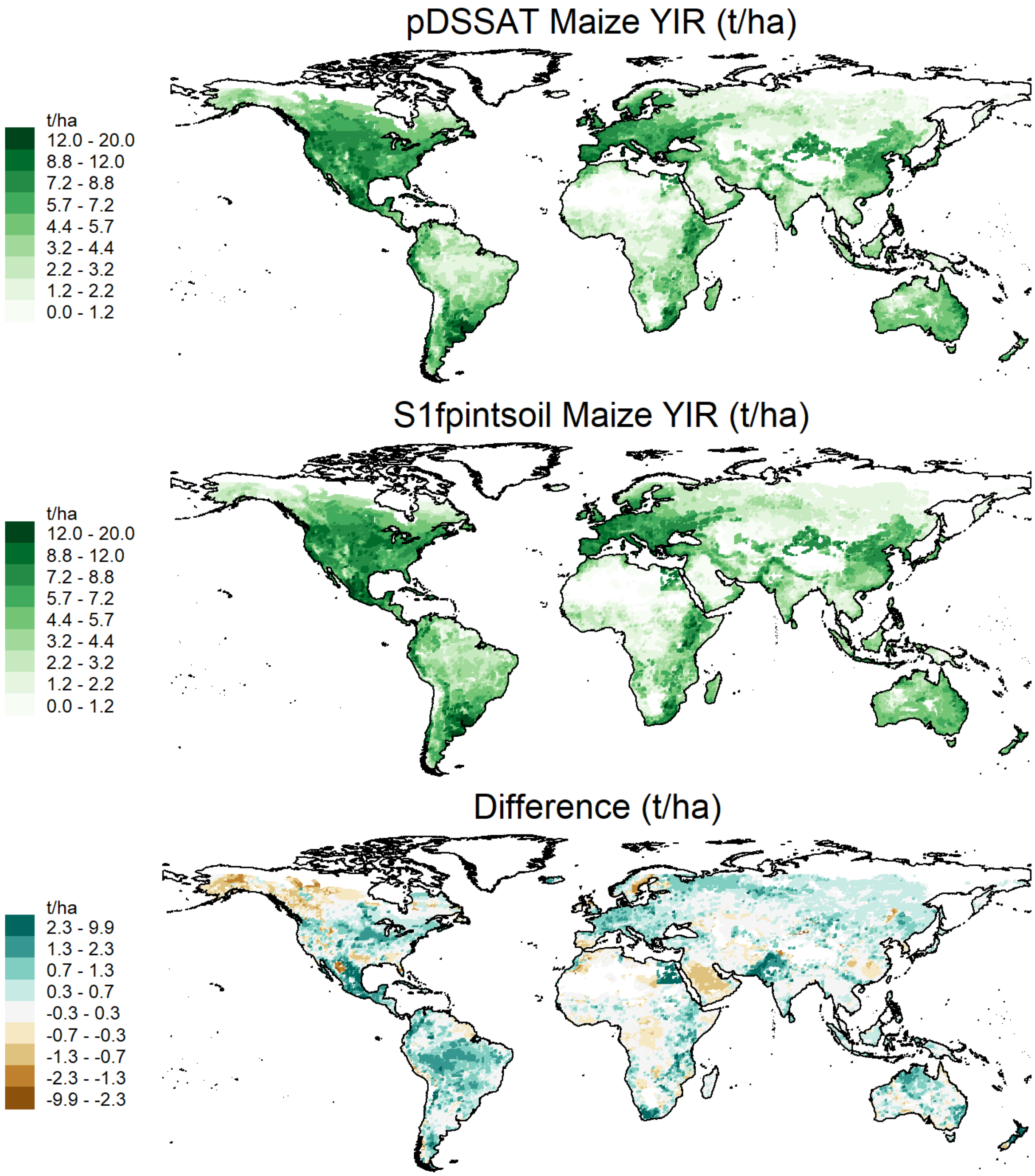

Figure G5. Irrigated maize yields averaged over 2090–2099 for the PEGASUS model and S1fpintsoil specification

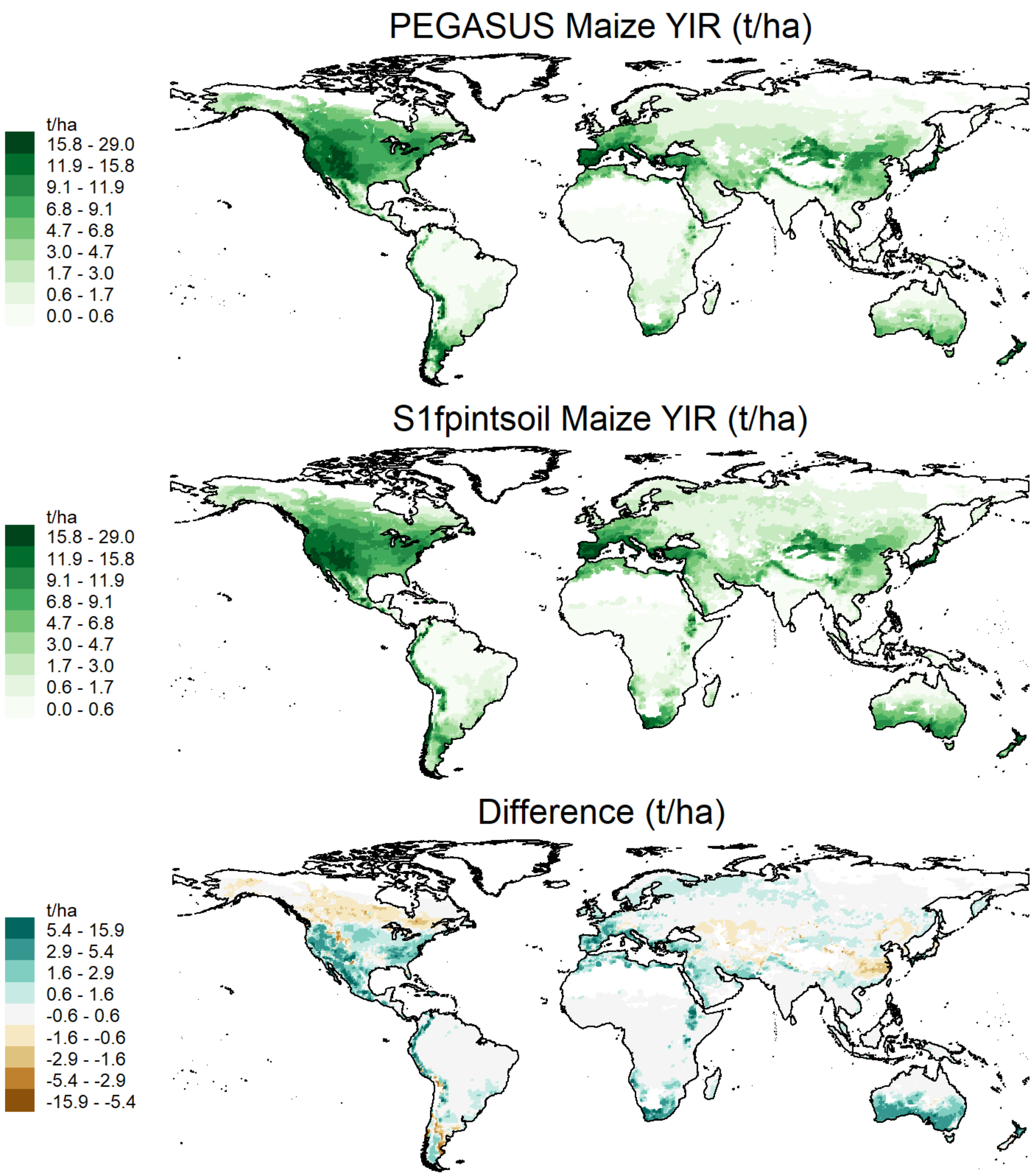

Figure G6. Irrigated rice yields averaged over 2090–2099 for the GEPIC model and S1fpintsoil specification

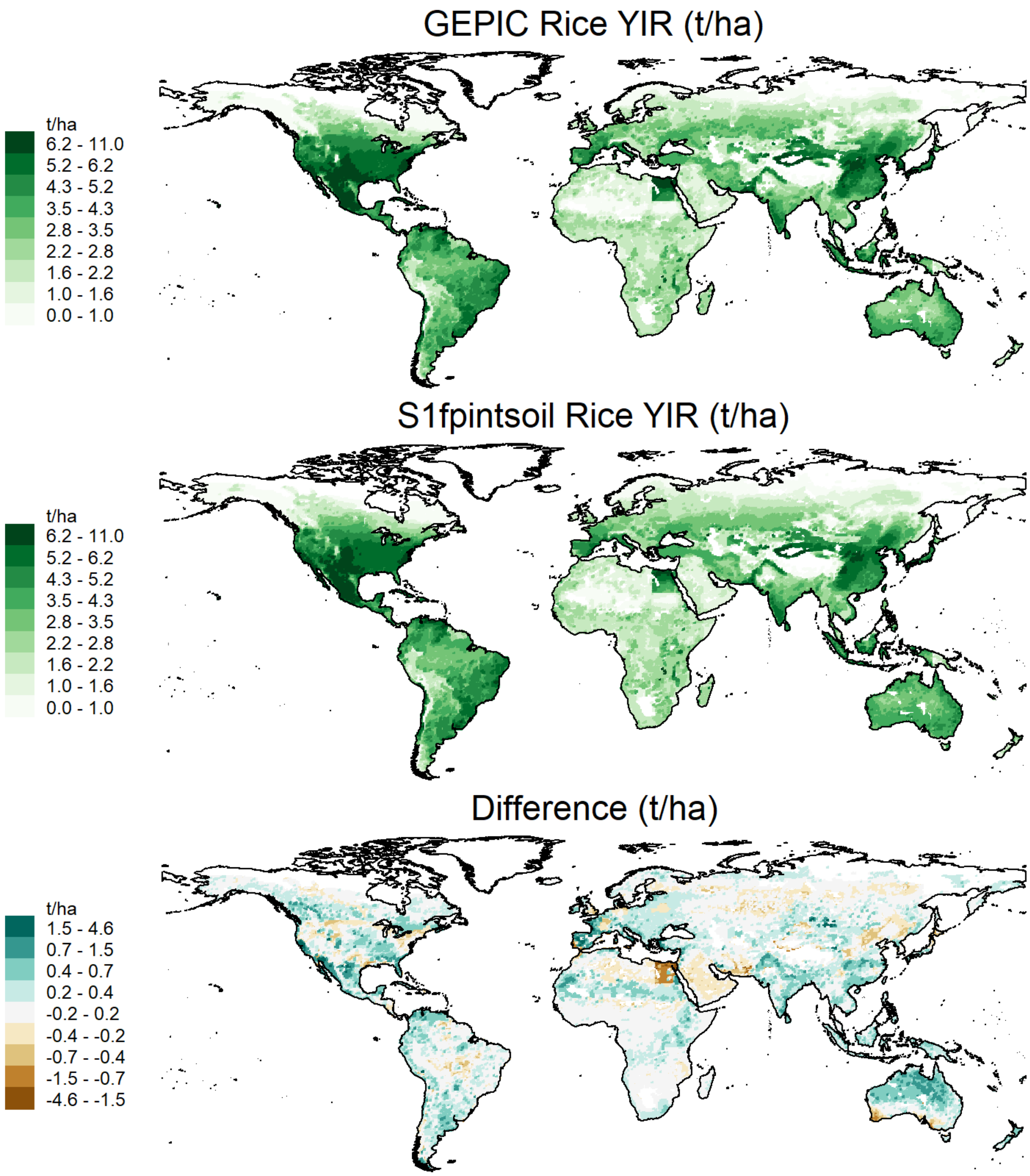

Figure G7. Irrigated rice yields averaged over 2090–2099 for the LPJ-GUESS model and S1fpintsoil specification

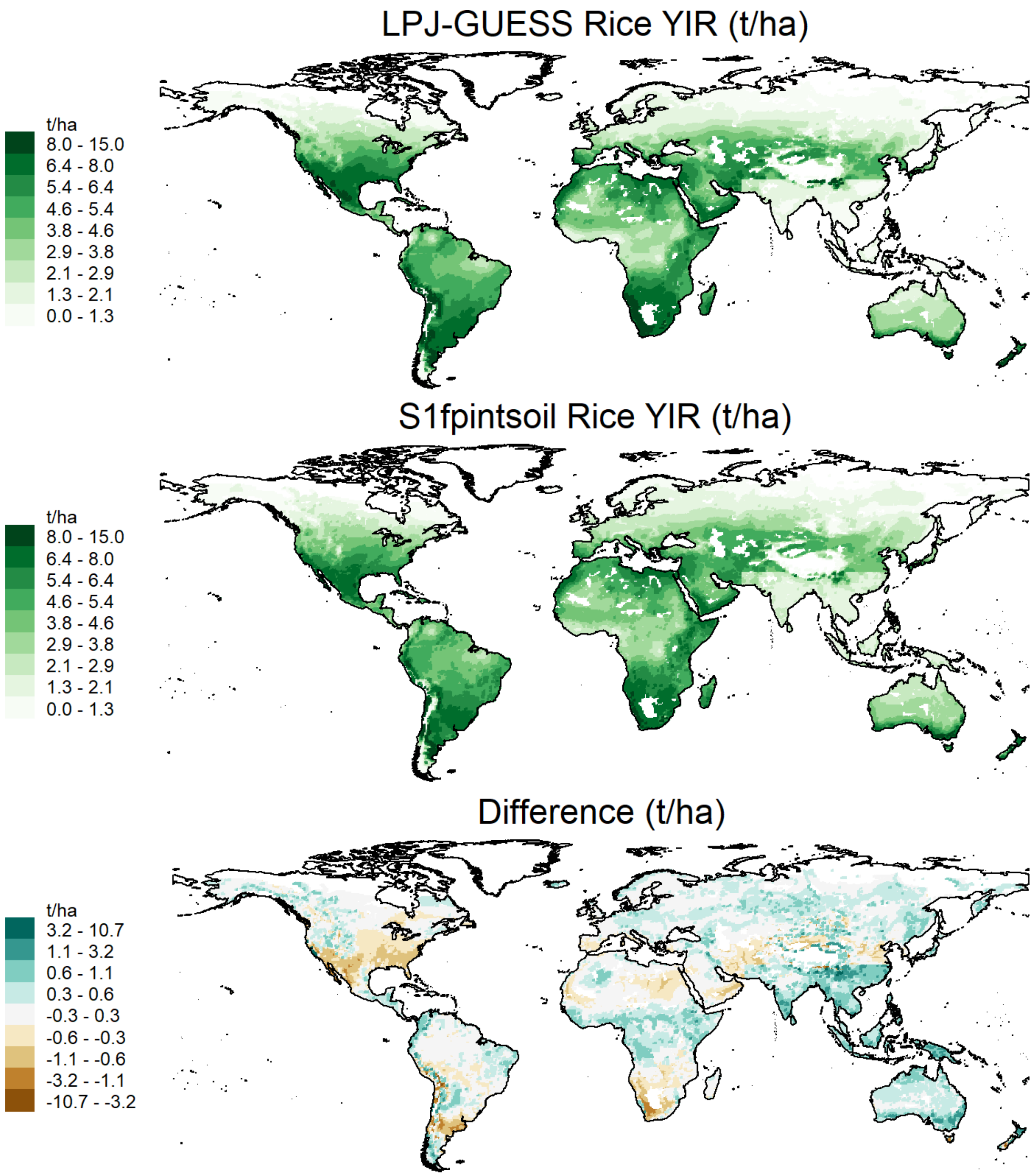

Figure G8. Irrigated rice yields averaged over 2090–2099 for the LPJmL model and S1fpintsoil specification

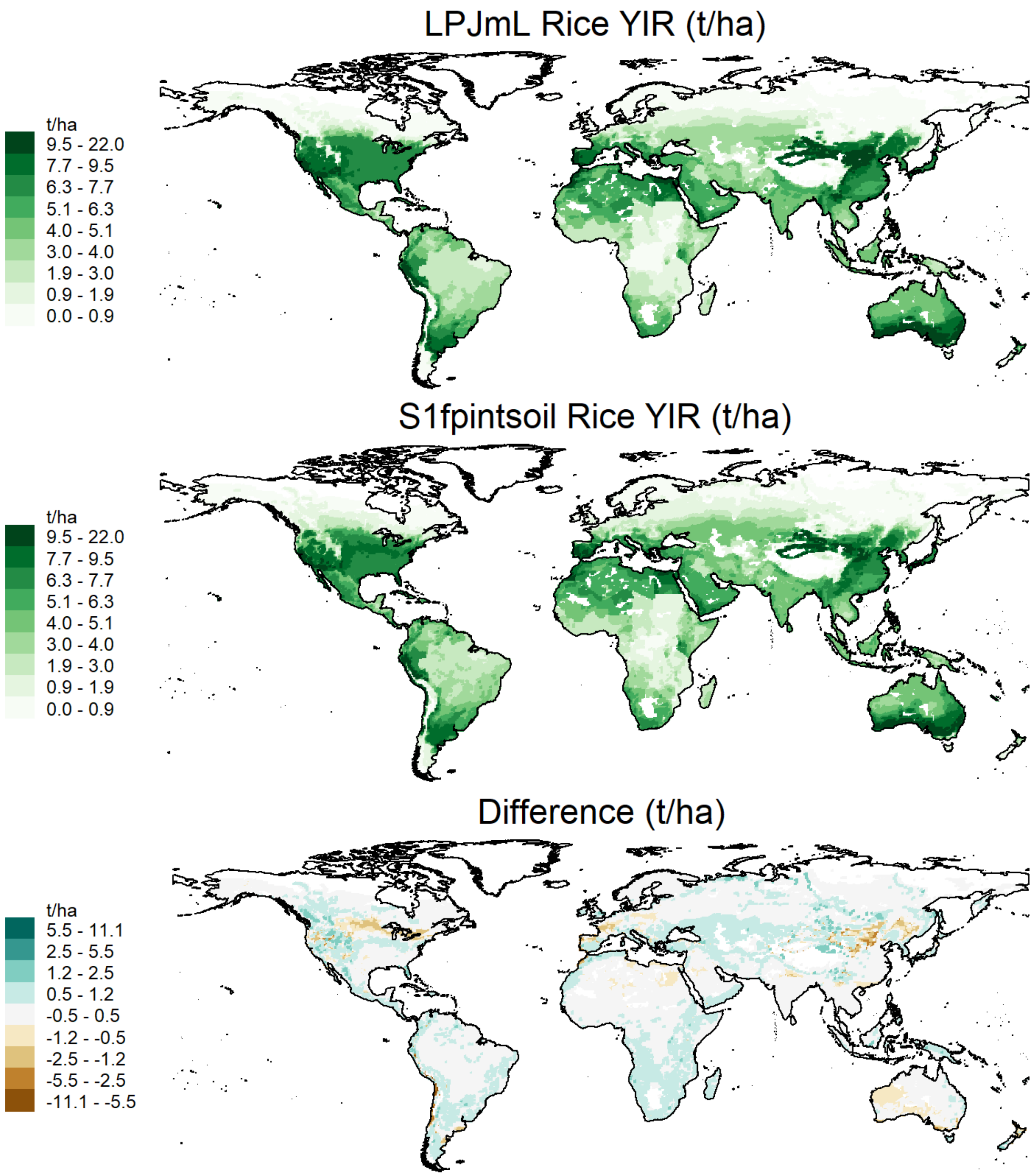

Figure G9. Irrigated soybean yields averaged over 2090–2099 for the GEPIC model and S1fpintsoil specification

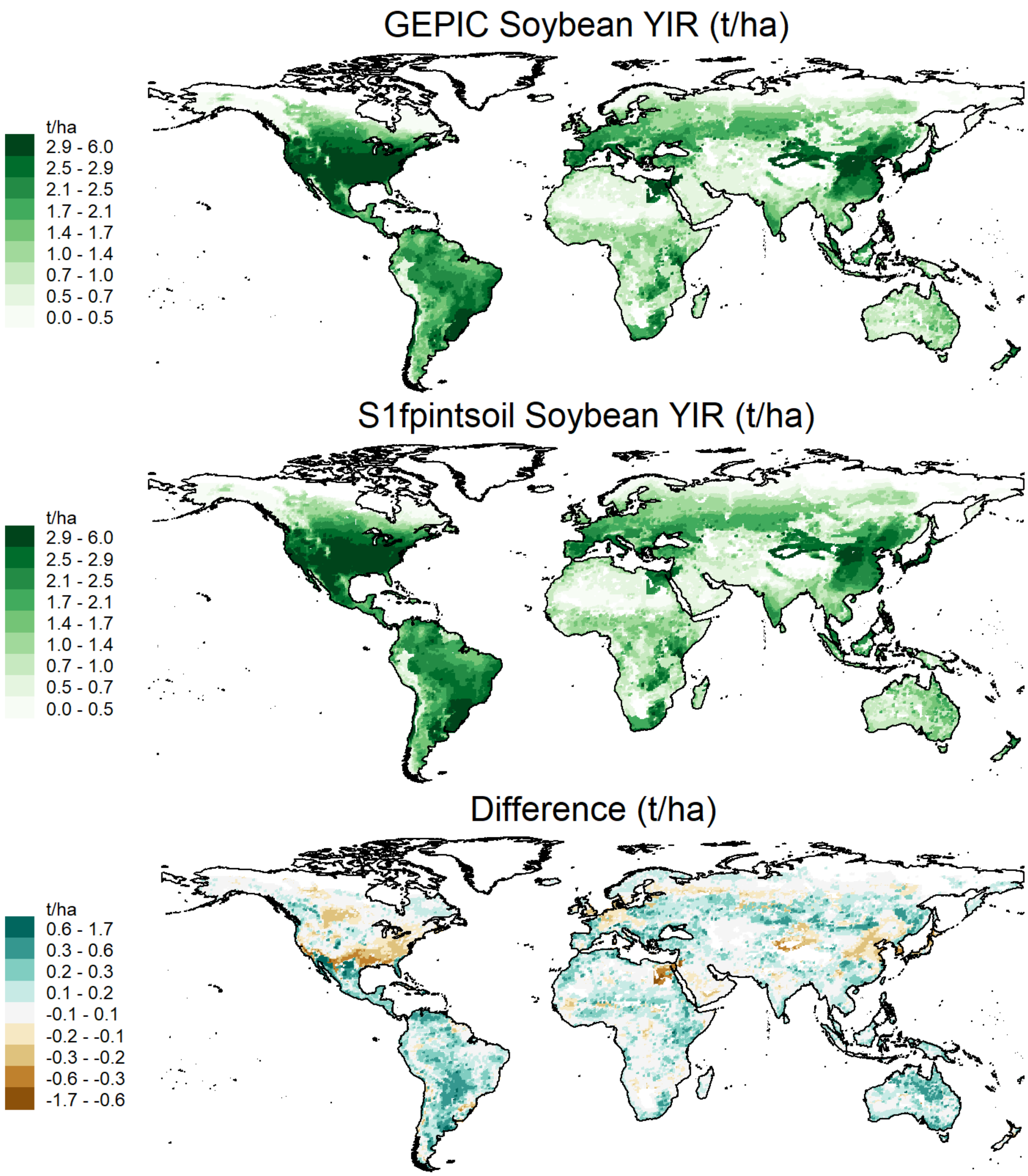

Figure G10. Irrigated soybean yields averaged over 2090–2099 for the LPJ-GUESS model and S1fpintsoil specification

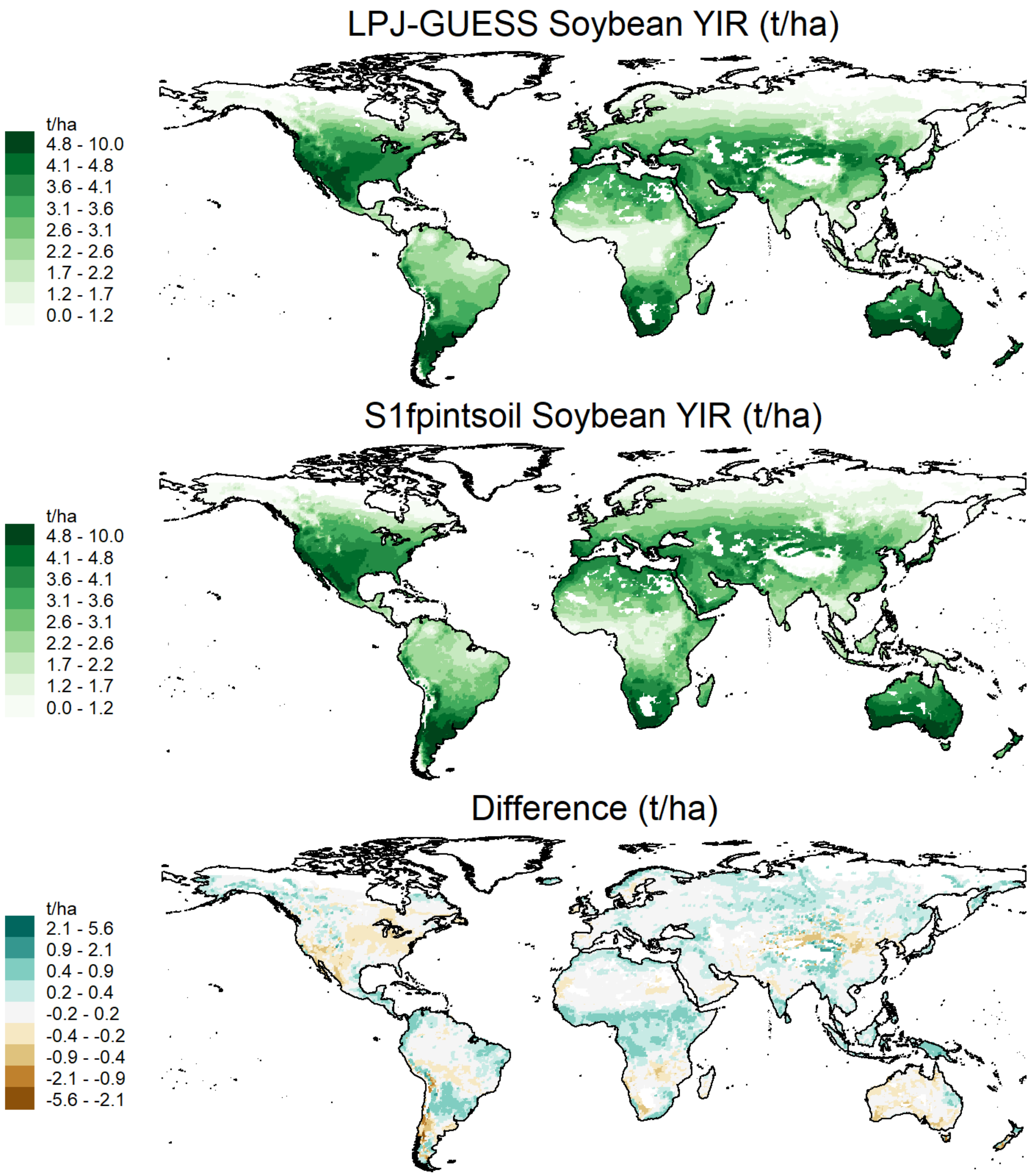

Figure G11. Irrigated soybean yields averaged over 2090–2099 for the LPJmL model and S1fpintsoil specification

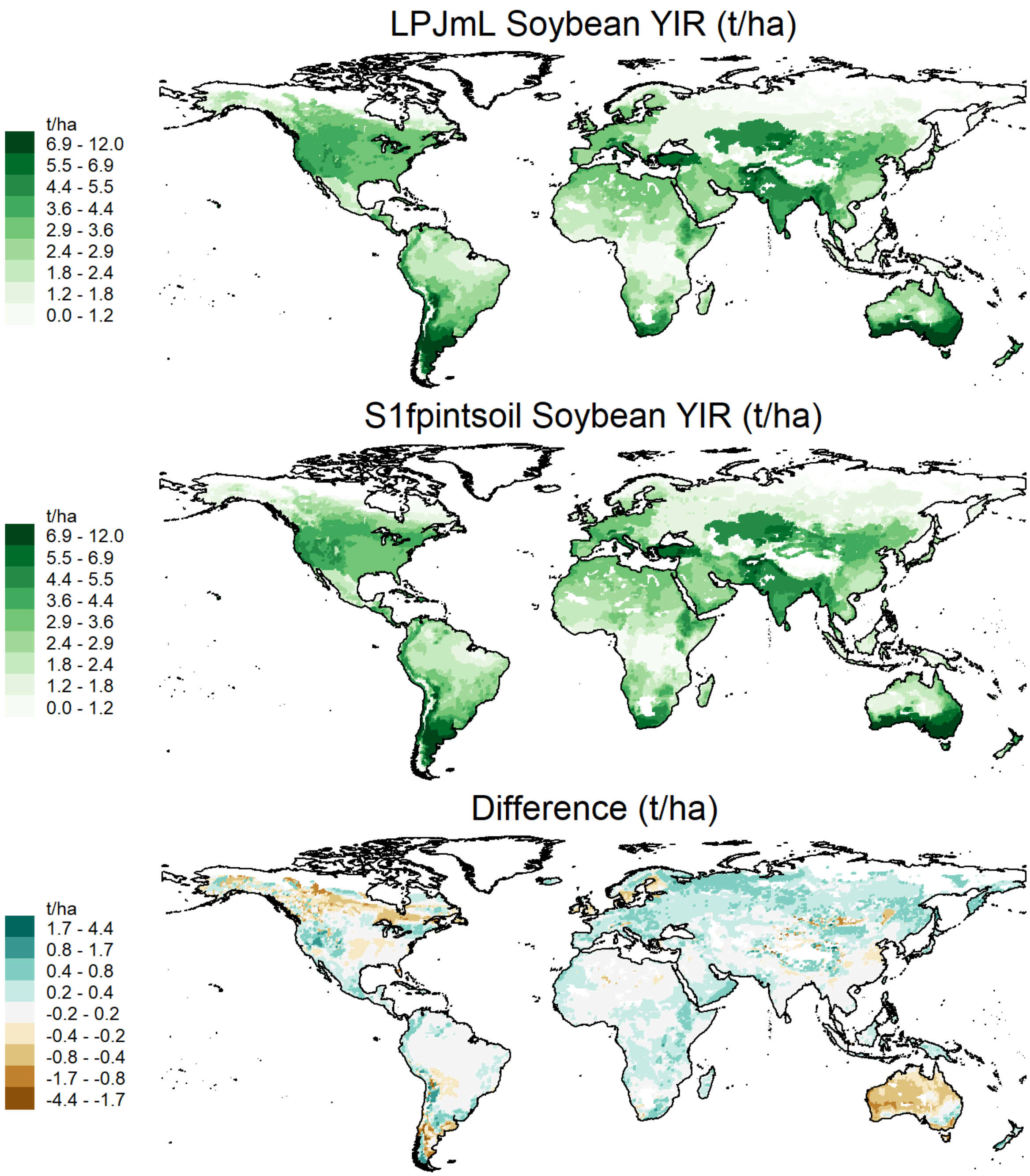

Figure G12. Irrigated soybean yields averaged over 2090–2099 for the PEGASUS model and S1fpintsoil specification

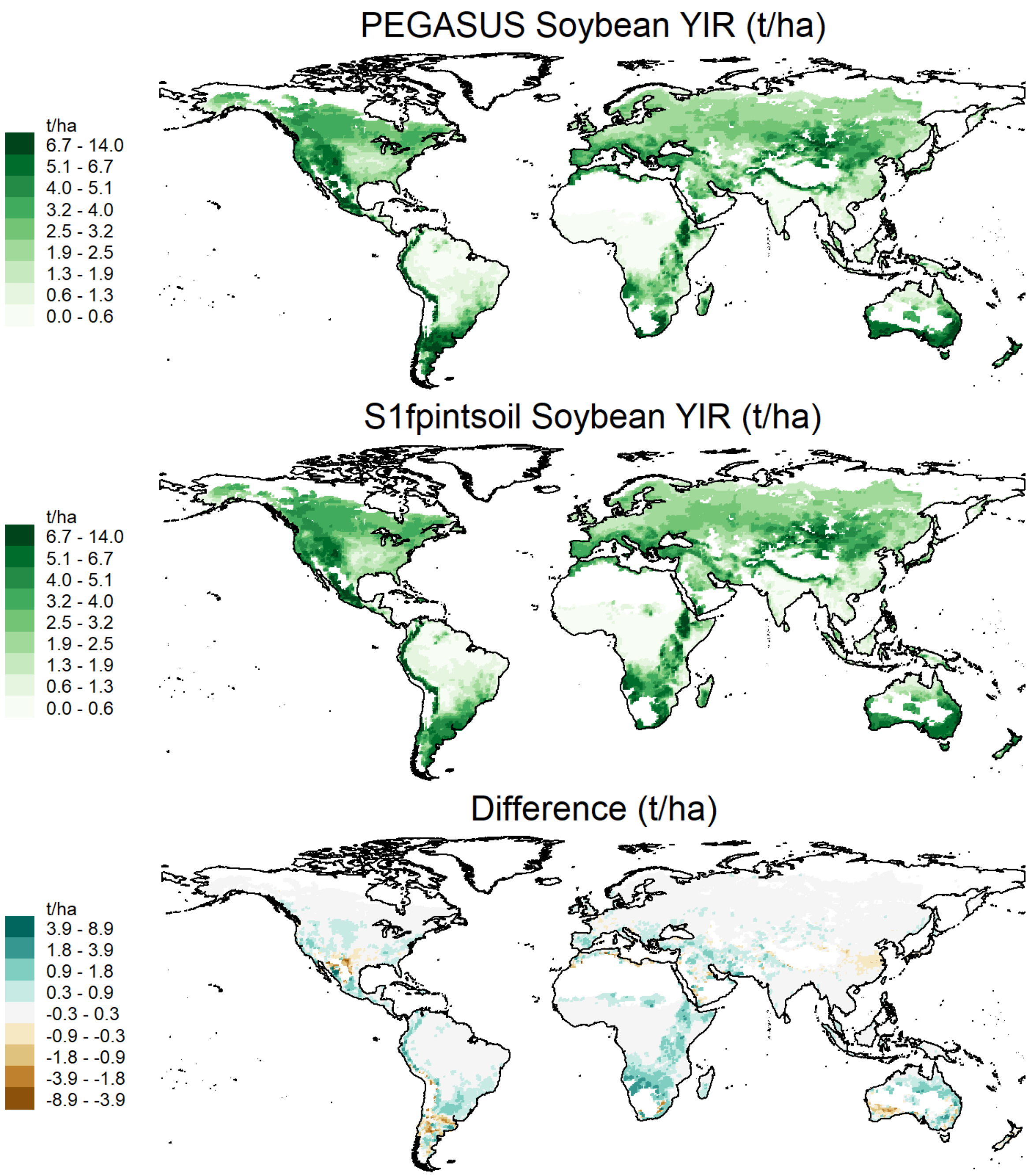

Figure G13. Irrigated wheat yields averaged over 2090–2099 for the GEPIC model and S1fpintsoil specification

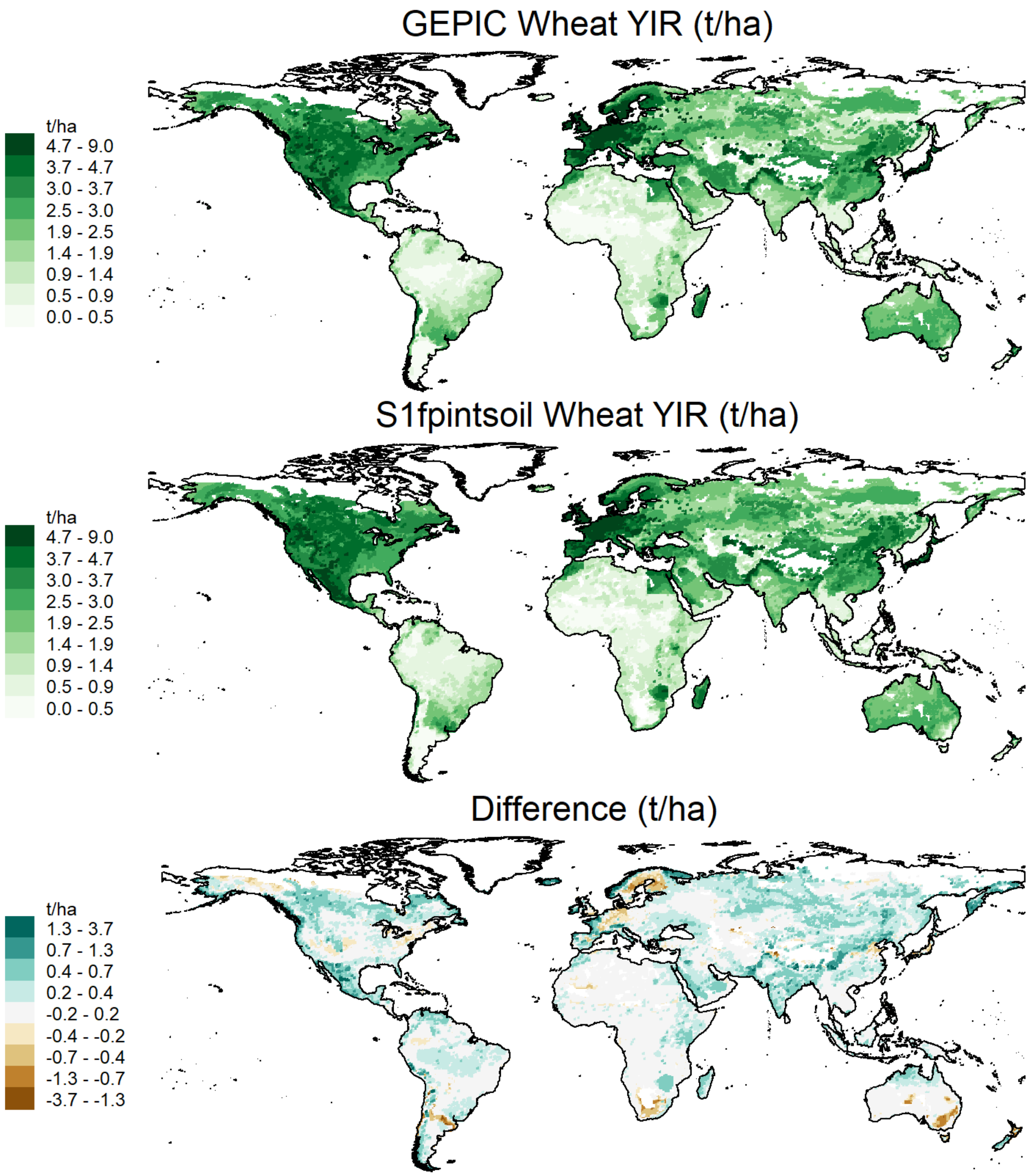

Figure G14. Irrigated wheat yields averaged over 2090–2099 for the LPJ-GUESS model and S1fpintsoil specification

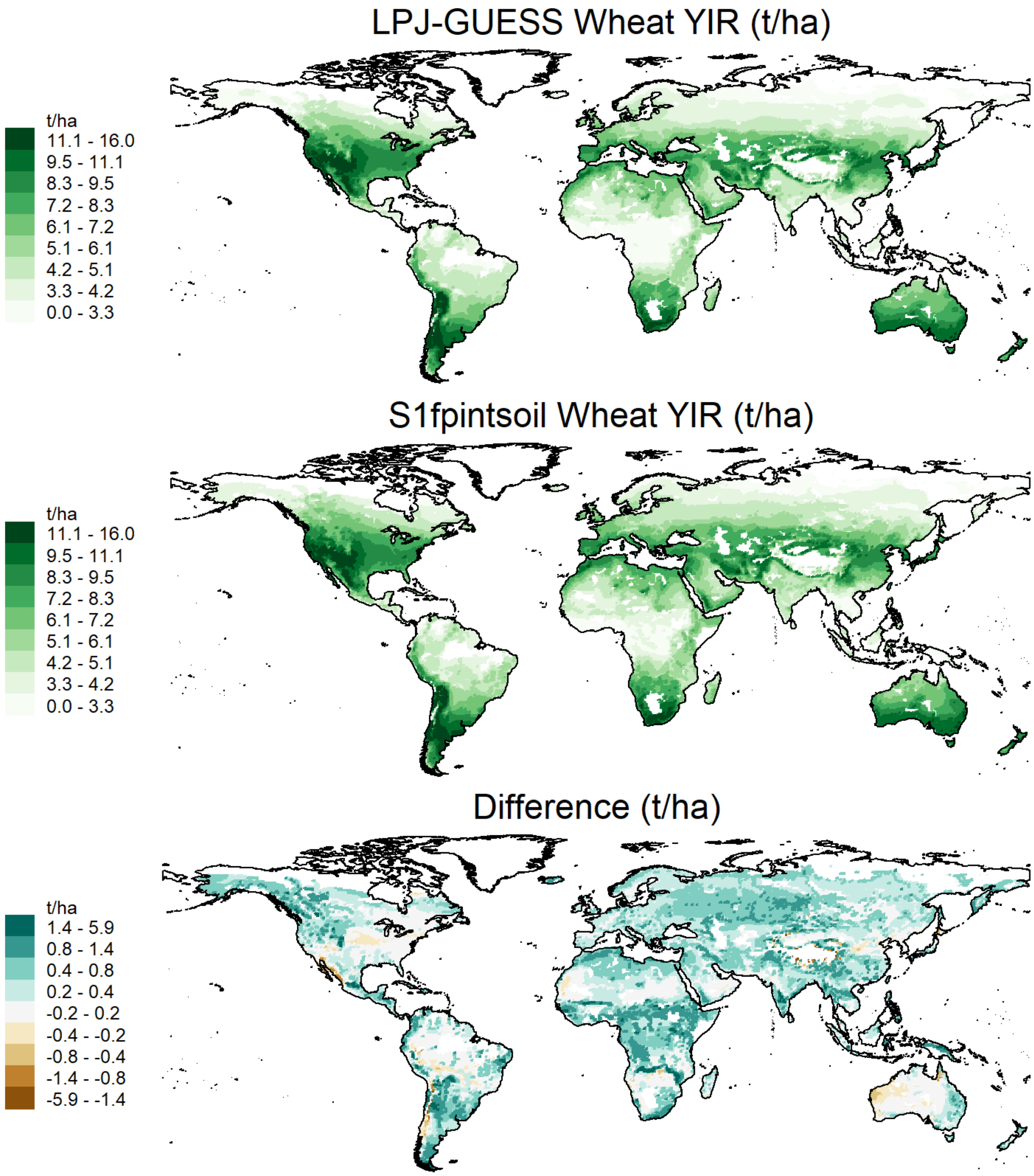

772 **Figure G15. Irrigated wheat yields averaged over 2090–2099 for the LPJmL model and S1fpintsoil specification**

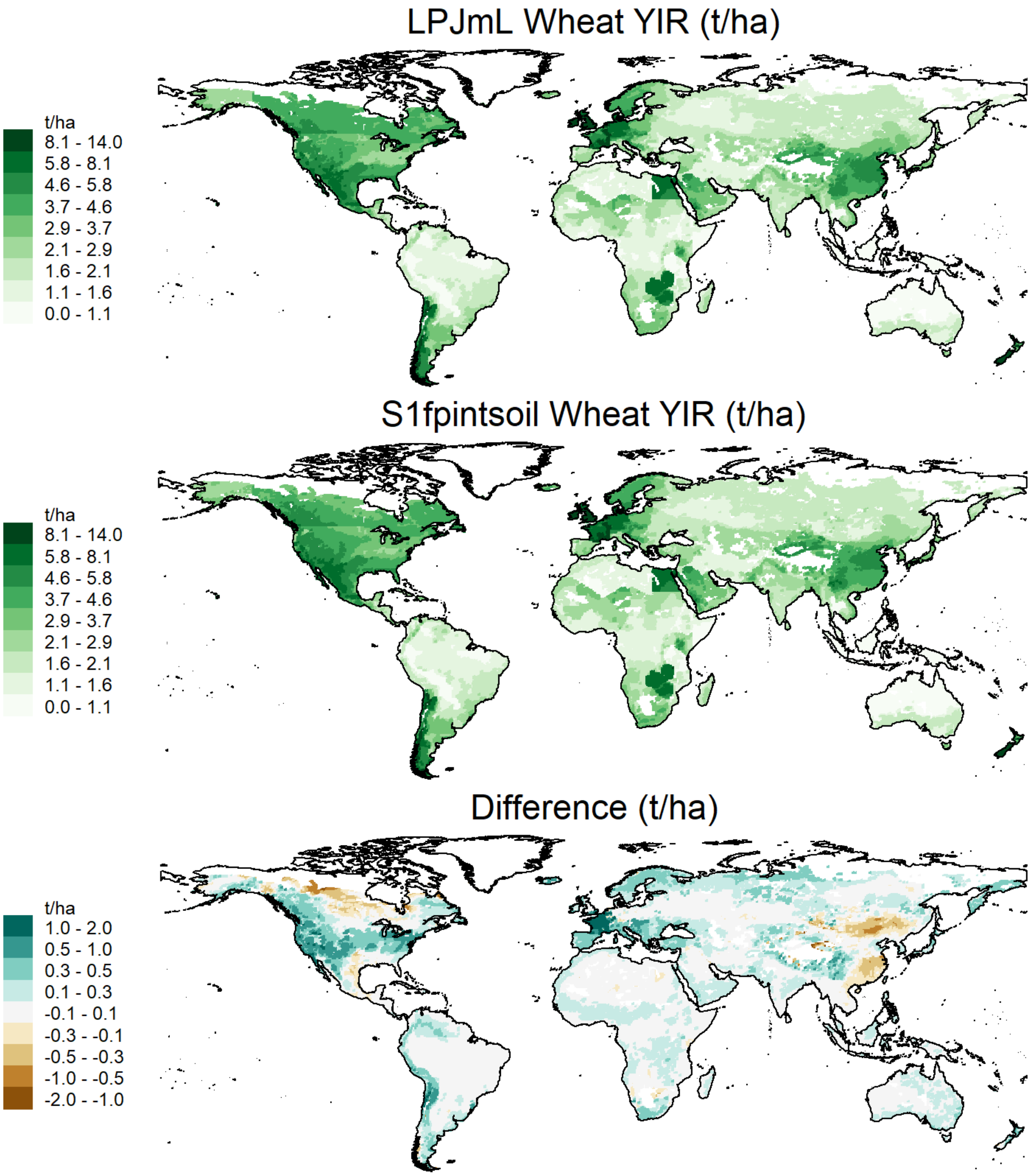

773

Figure G16. Irrigated wheat yields averaged over 2090–2099 for the pDSSAT model and S1fpintsoil specification

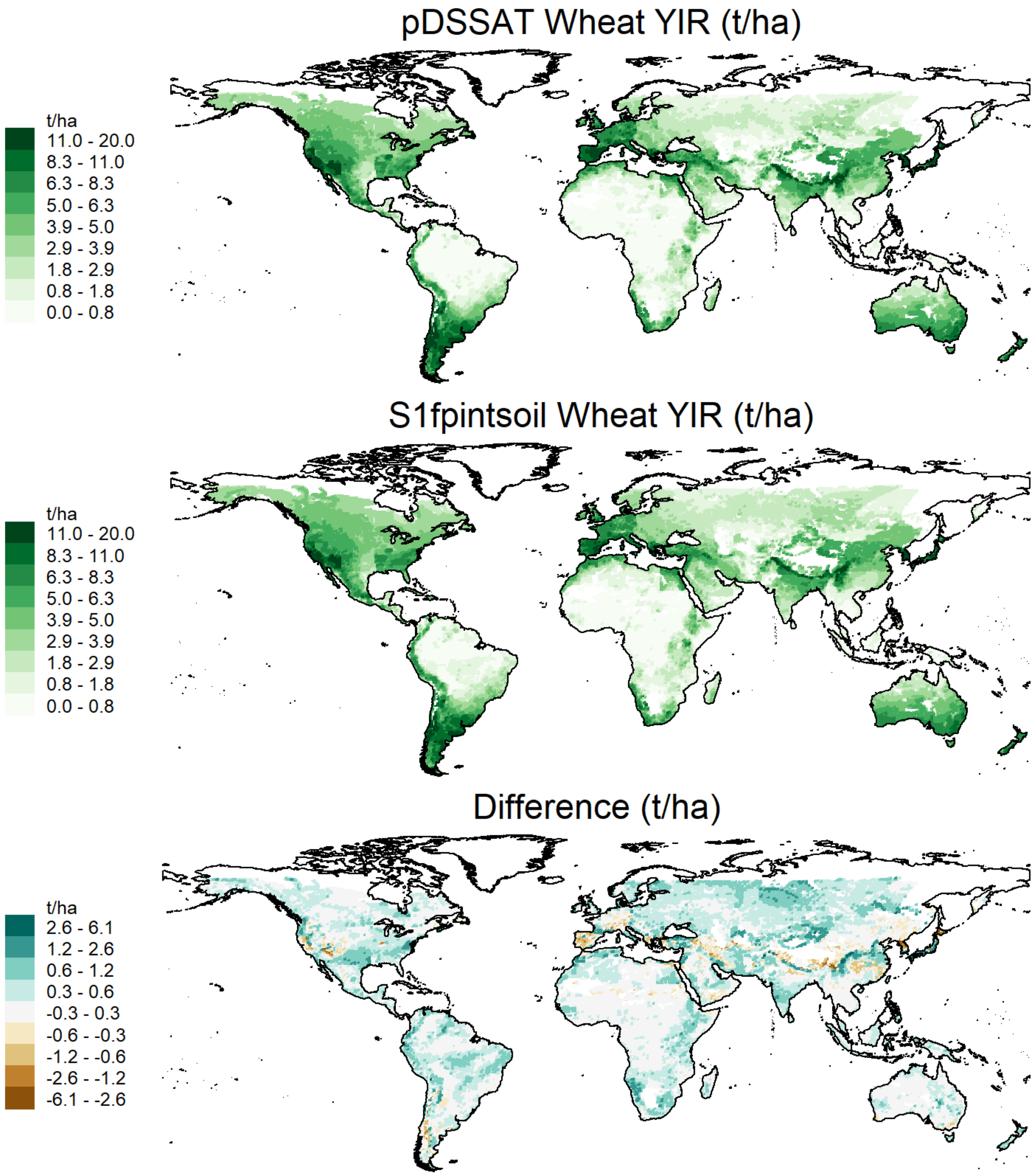

Figure G17. Irrigated wheat yields averaged over 2090–2099 for the PEGASUS model and S1fpintsoil specification

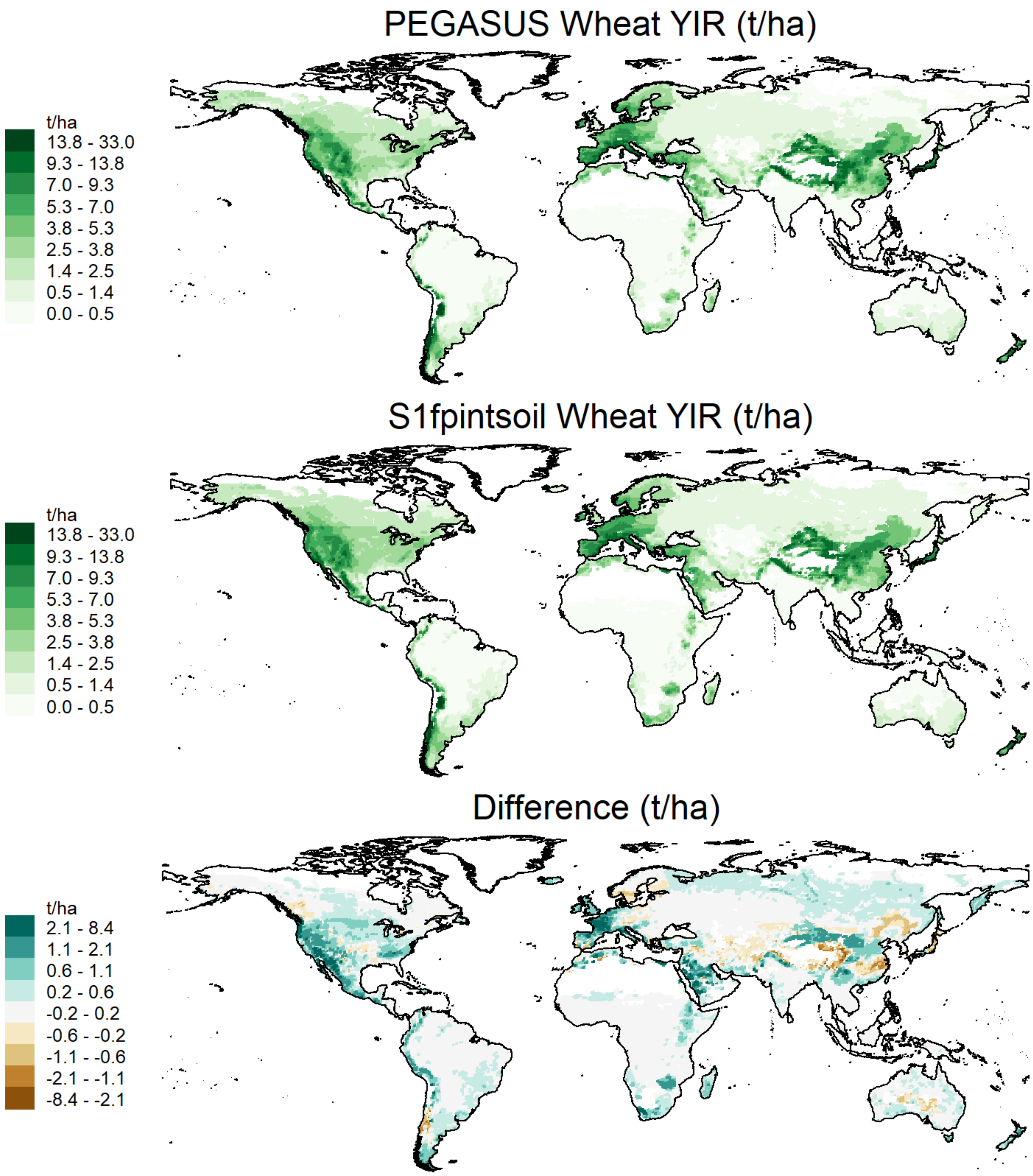

Figure G18. Irrigated crop yields ensemble error averaged over 2090–2099 across GGCMs for the major growing regions

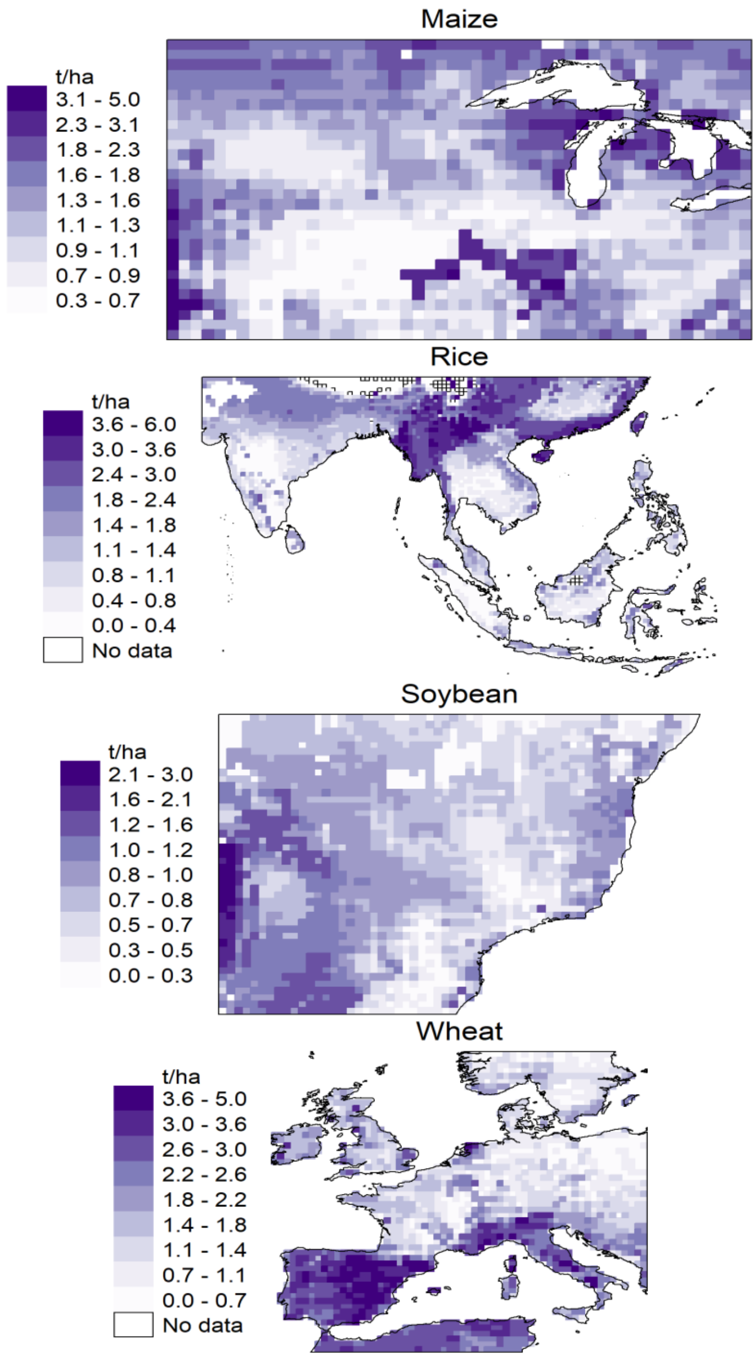

Figure G18. Irrigated crop yields ensemble error averaged over 2090–2099 across GGCMs at the global level

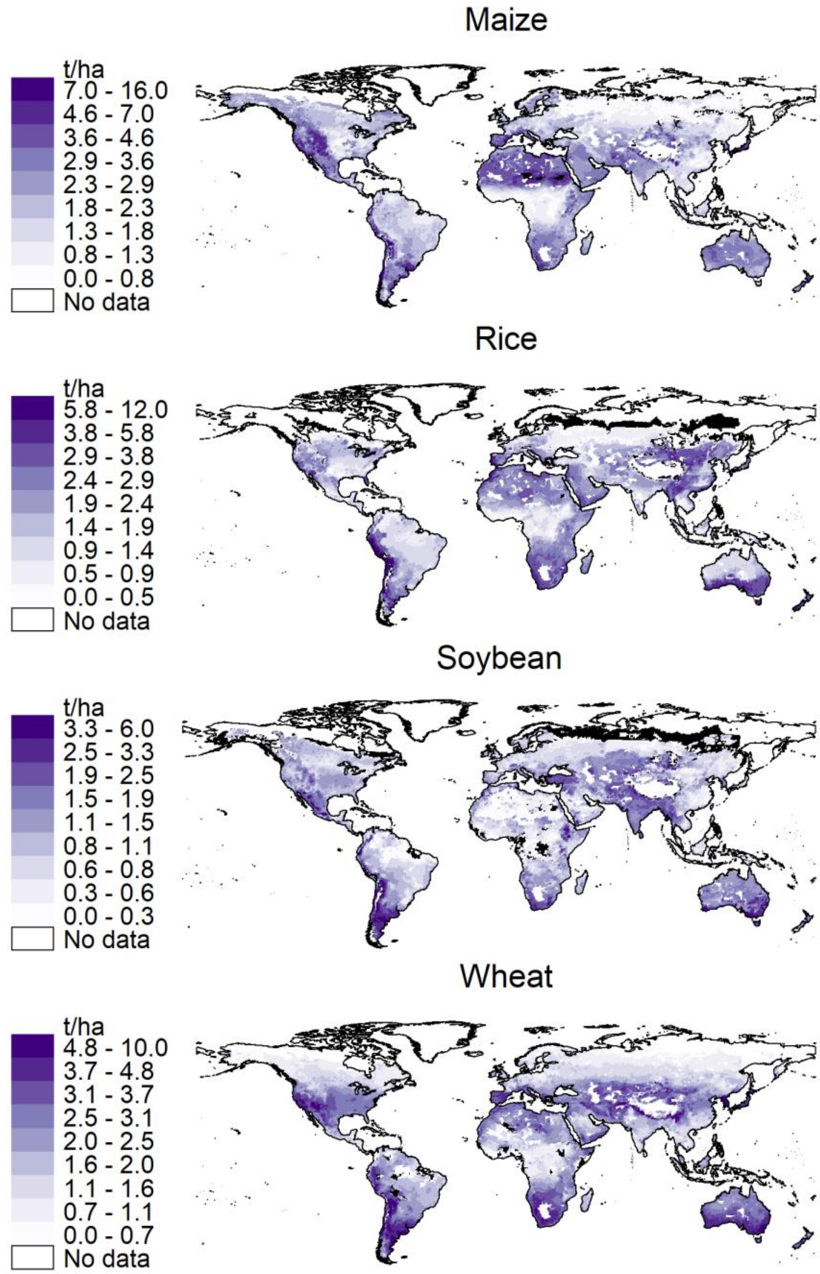

Figure G19. Changes in irrigated maize yields from 2000s to 2090s estimated by the statistical emulators (S1fpintsoil specification) and GGCMs

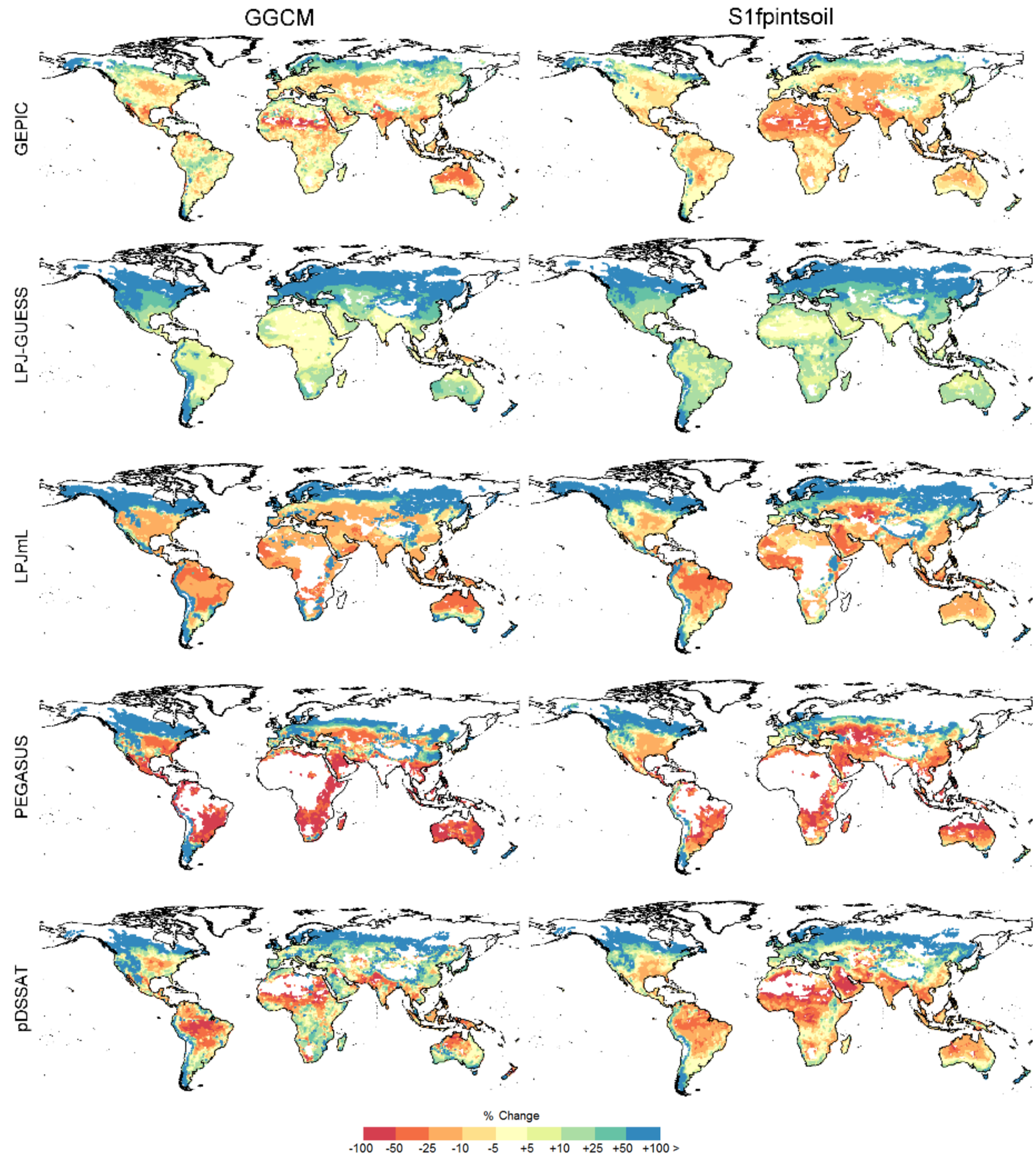

Notes: Grid cells where yields projections from crop models are on average less than 1t/ha over the whole study period are masked in white. Grid cells for which the sign of the impact projected with the emulator is contrary to the sign of the impact projected by the GGCM are masked in black.

Figure G20. Changes in irrigated rice yields from 2000s to 2090s estimated by the statistical emulators (S1fpintsoil specification) and GGCMs

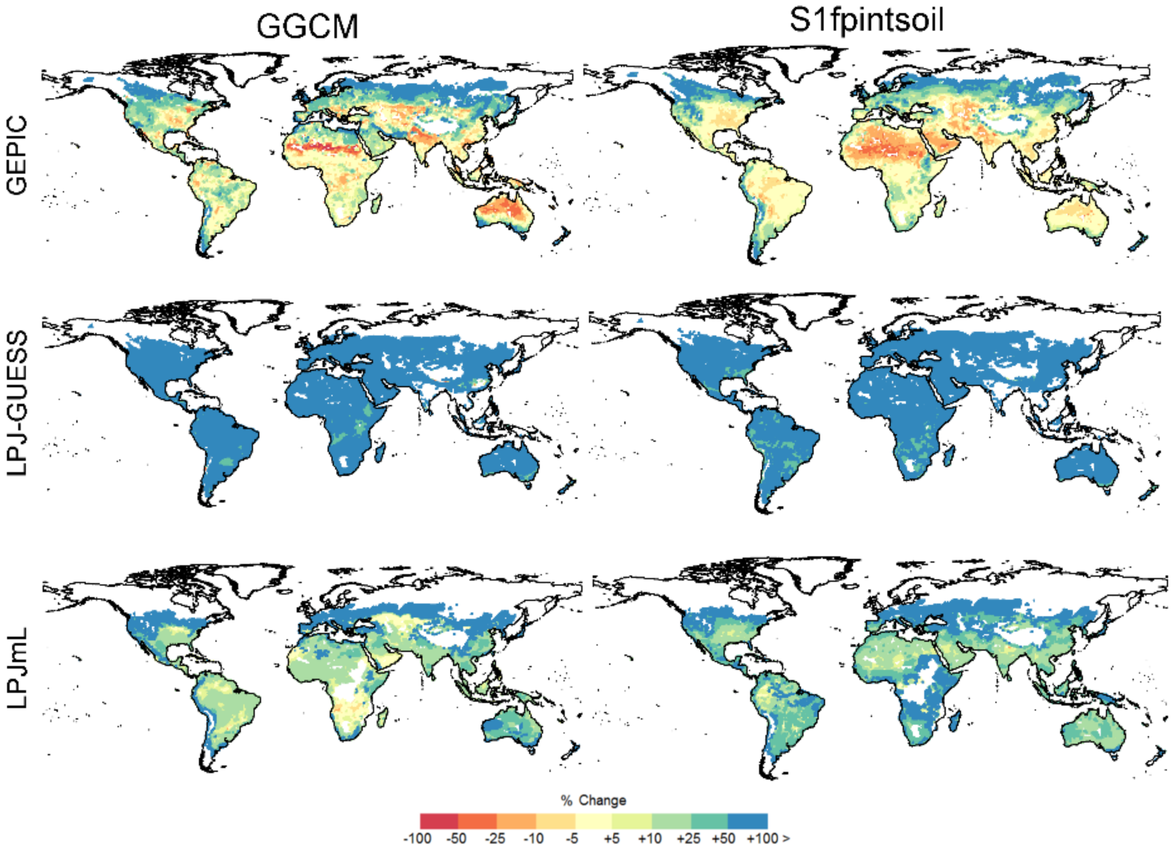

Note: See note of Figure G19.

Figure G21. Changes in irrigated soybean yields from 2000s to 2090s estimated by the statistical emulators (S1fpintsoil specification) and GGCMs

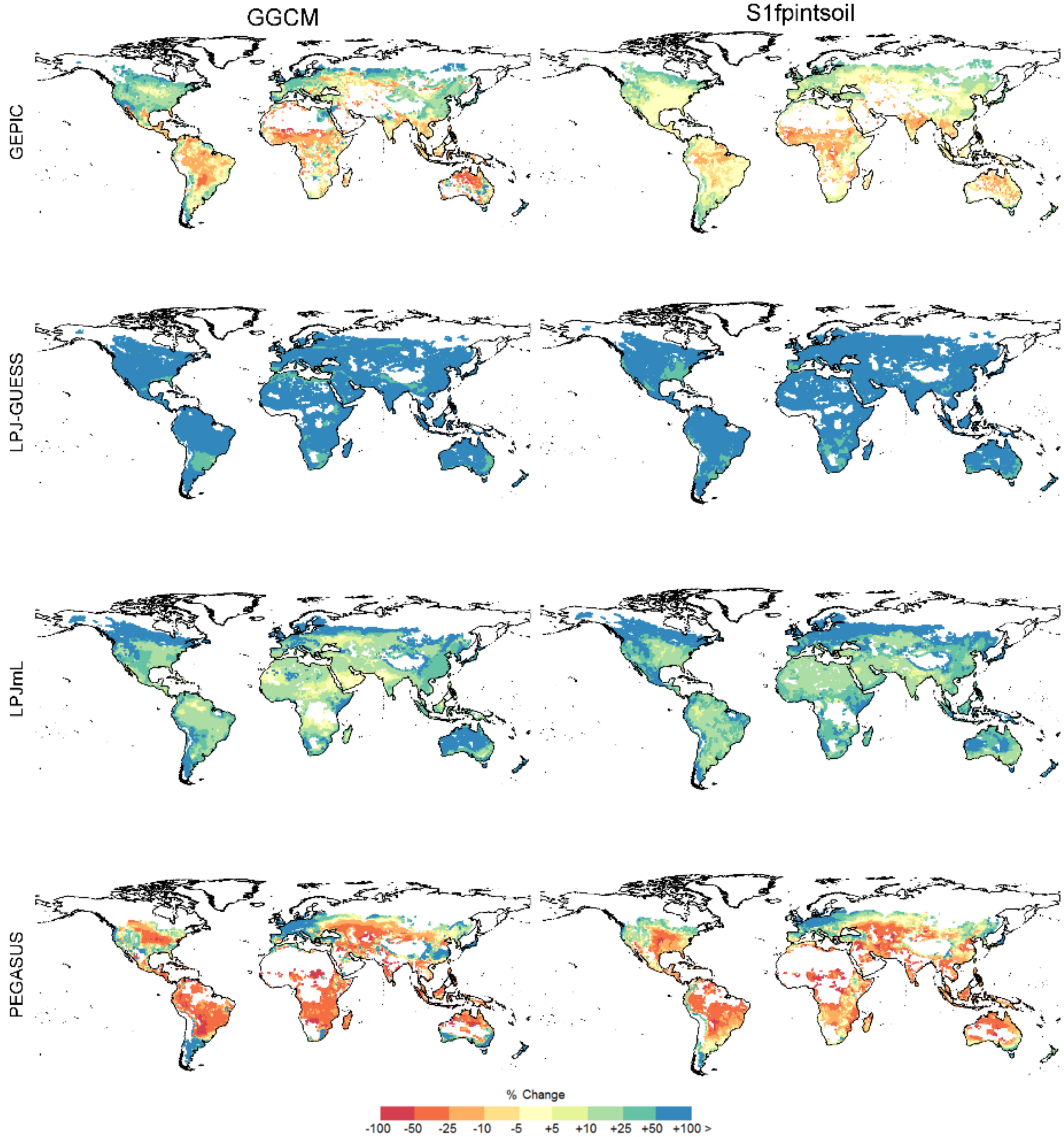

Note: See note of Figure G19.

Figure G22. Changes in irrigated wheat yields from 2000s to 2090s estimated by the statistical emulators (S1fpintsoil specification) and GGCMs

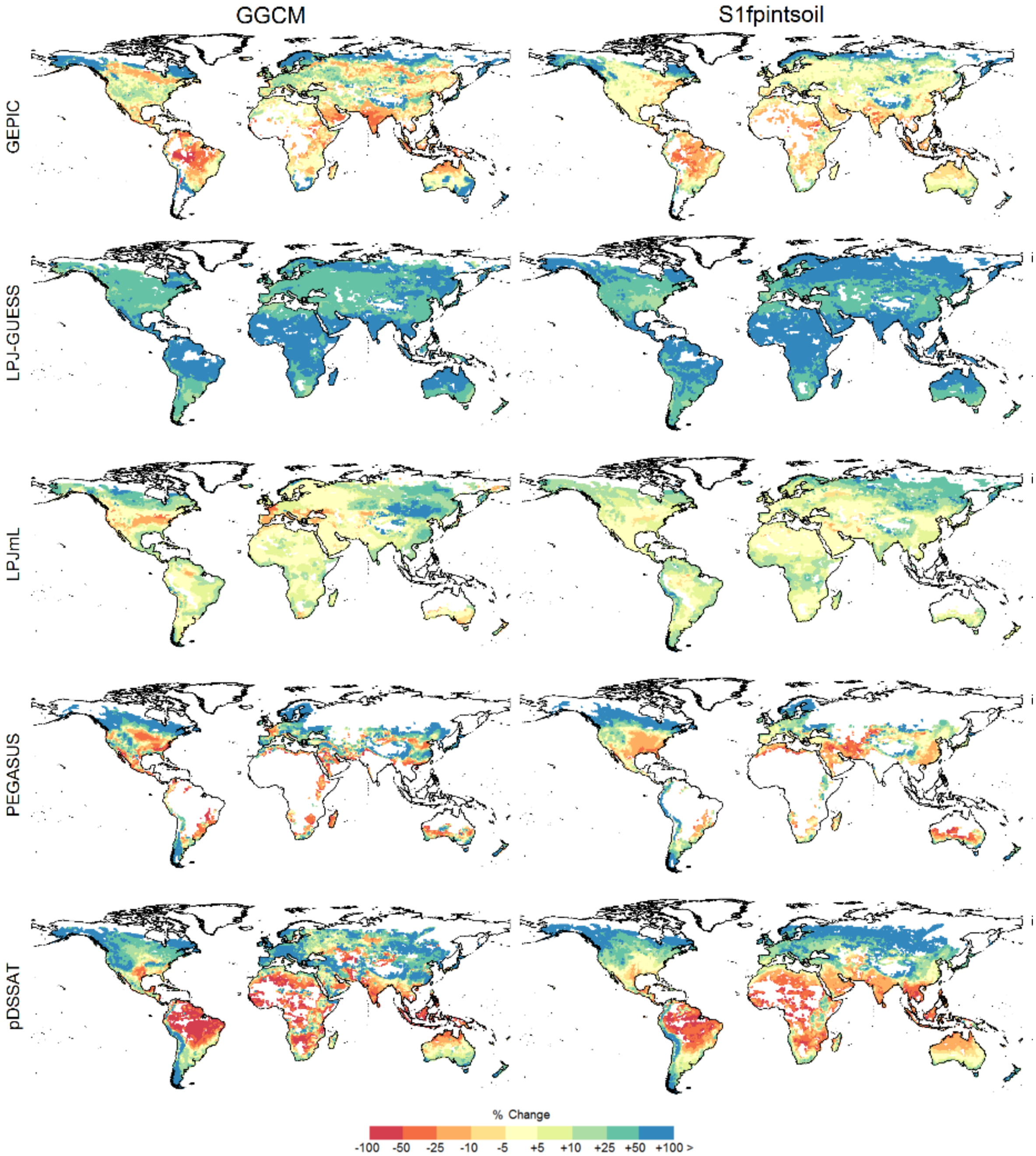

Note: See note of Figure G19.

Appendix H. **IN-SAMPLE VALIDATION FOR *PIRRWW* (S1FPINTSOIL SPECIFICATION)**

Figure H1. Irrigation water withdrawal for maize averaged over 2090–2099 for the GEPIC model and S1fpintsoil specification

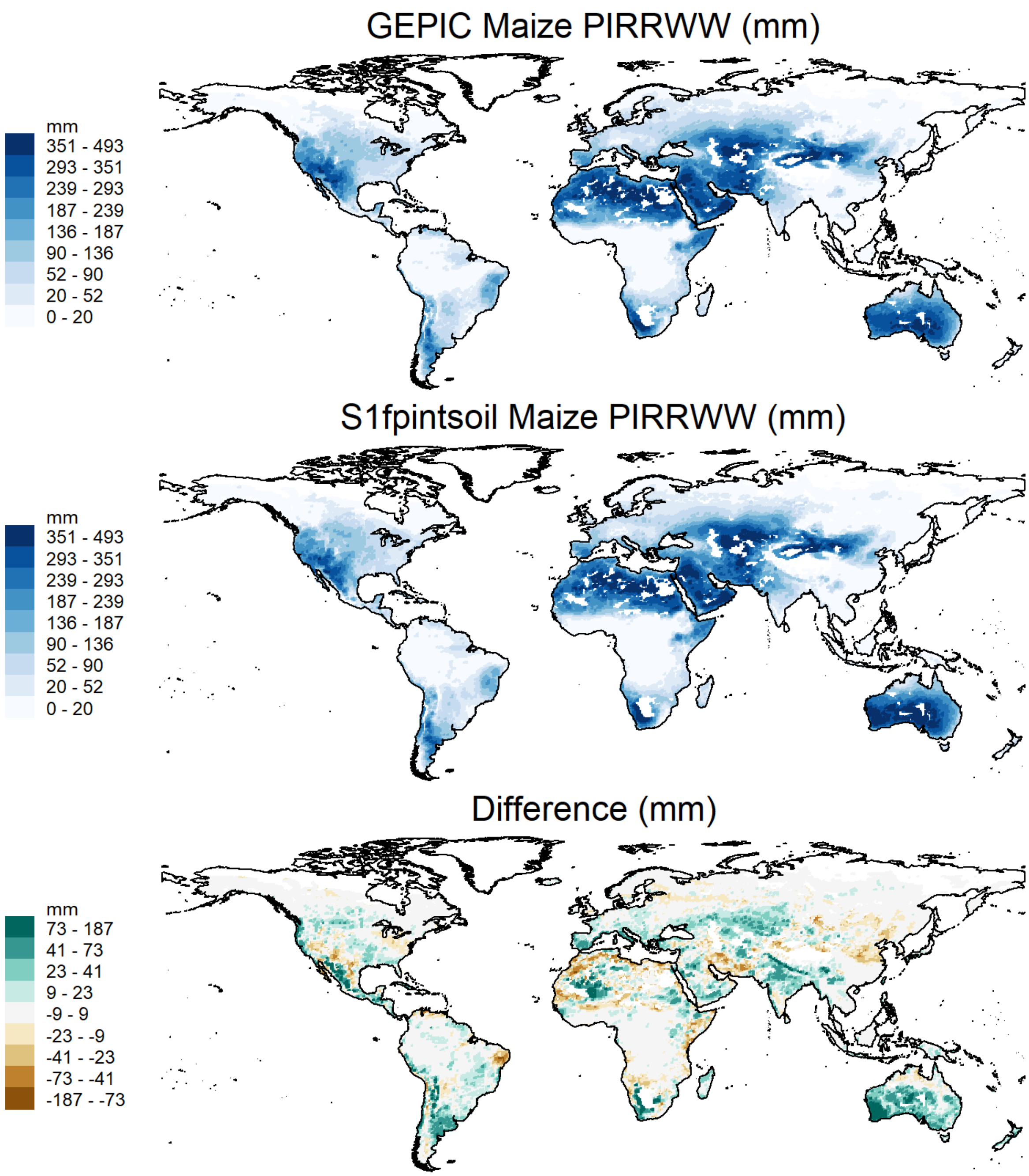

Figure H2. Irrigation water withdrawal for maize averaged over 2090–2099 for the LPJ-GUESS model and S1fpintsoil specification

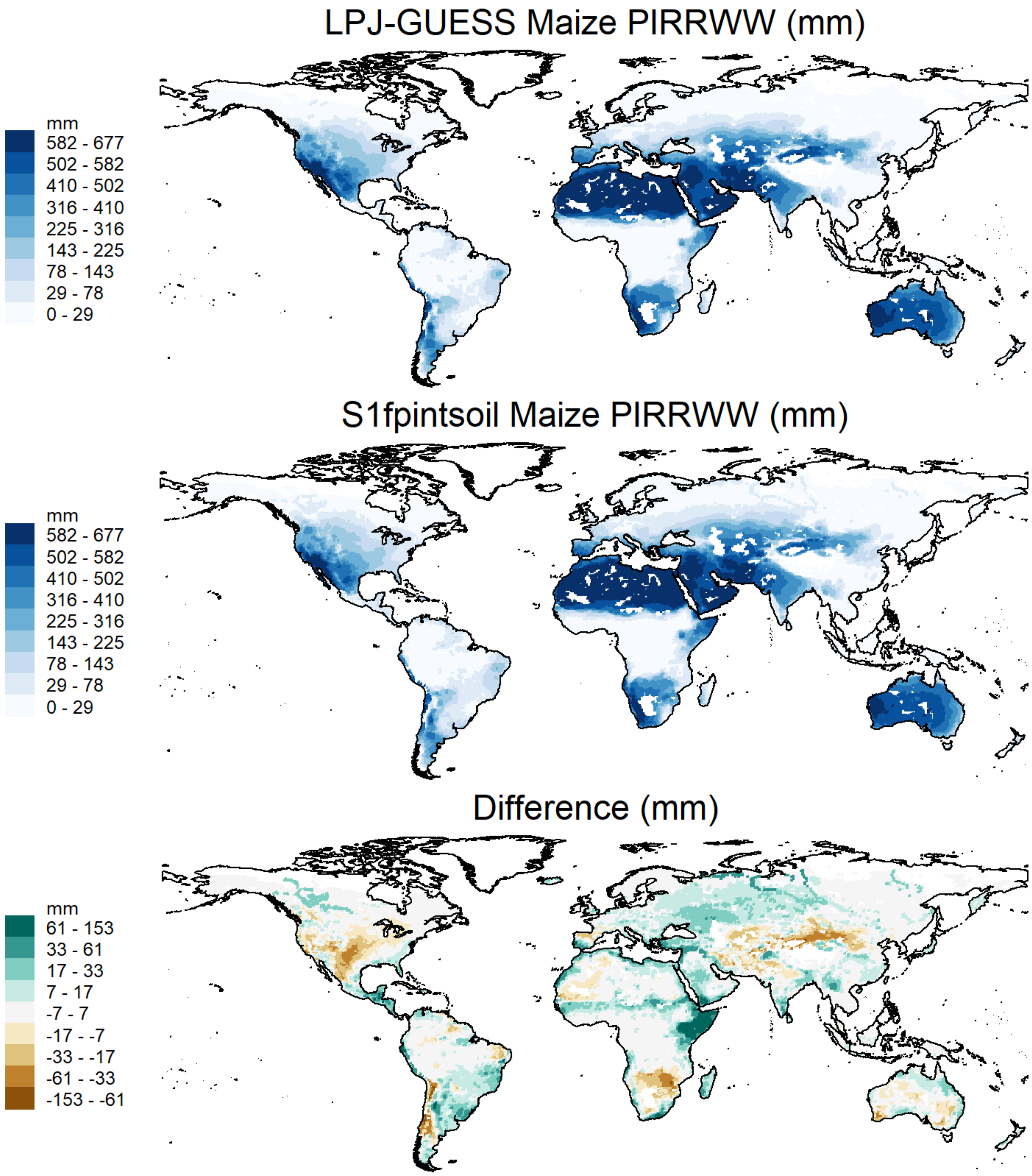

Figure H3. Irrigation water withdrawal for maize averaged over 2090–2099 for the LPJmL model and S1fpintsoil specification

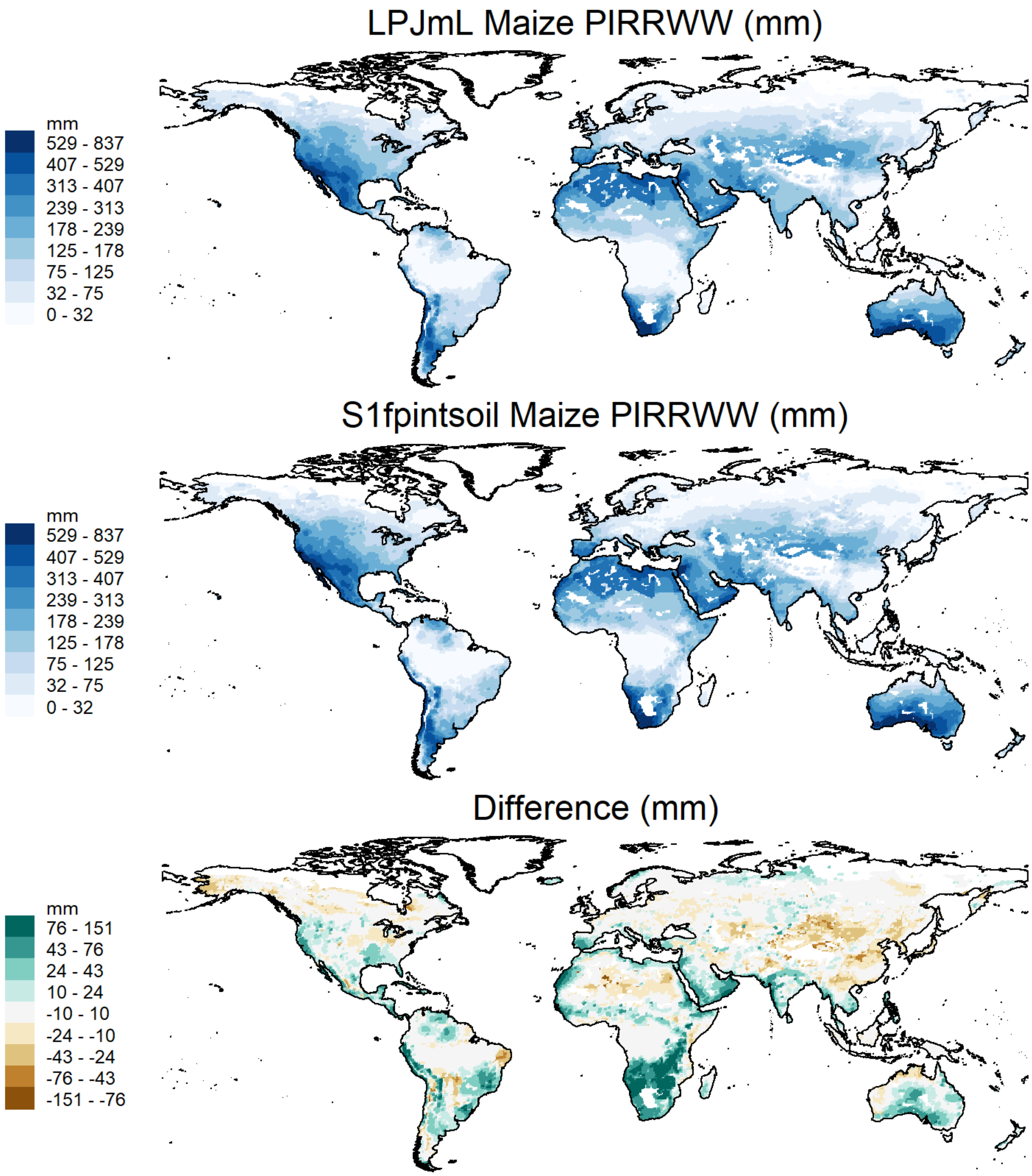

Figure H4. Irrigation water withdrawal for maize averaged over 2090–2099 for the pDSSAT model and S1fpintsoil specification

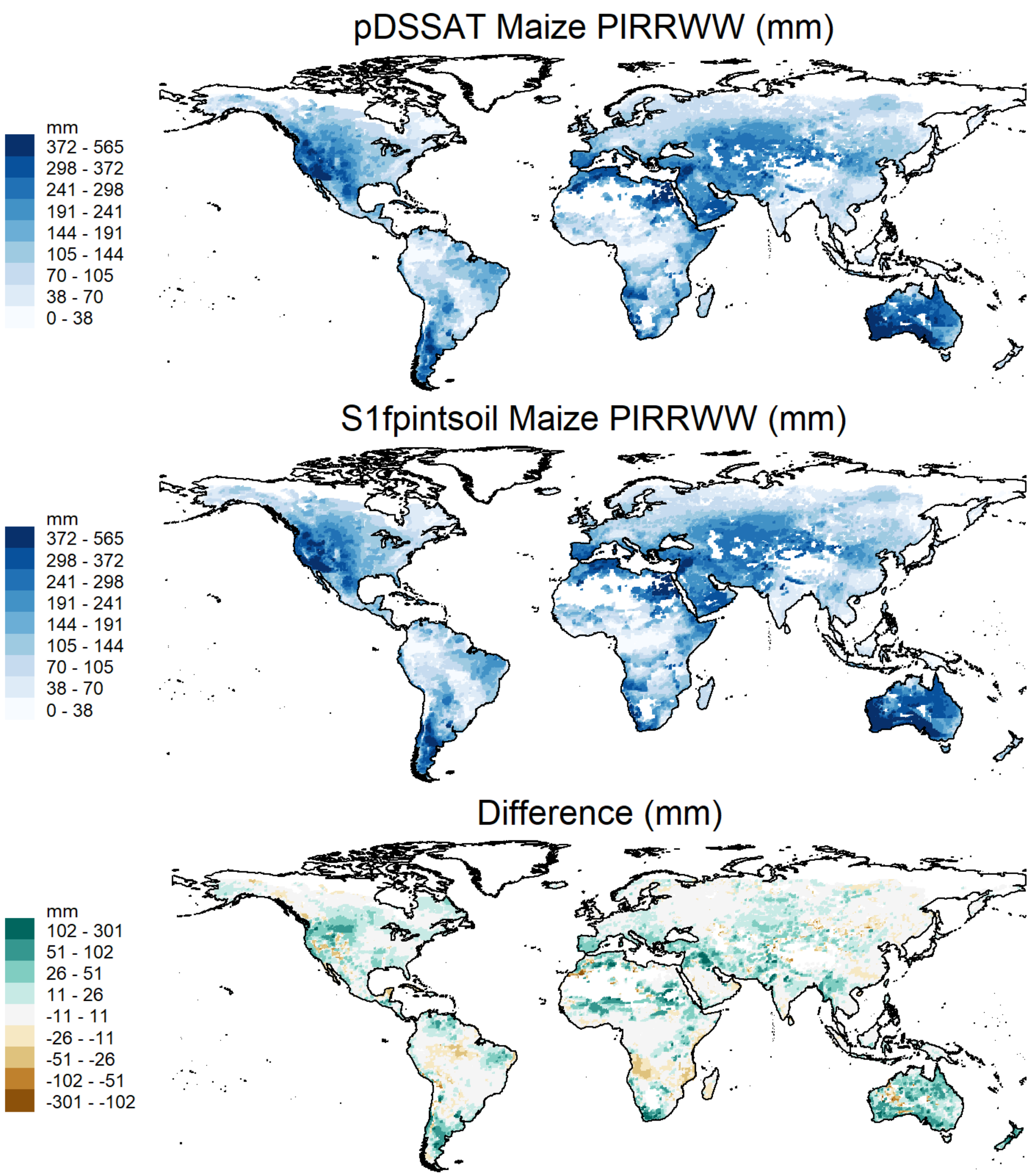

Figure H5. Irrigation water withdrawal for maize averaged over 2090–2099 for the PEGASUS model and S1fpintsoil specification

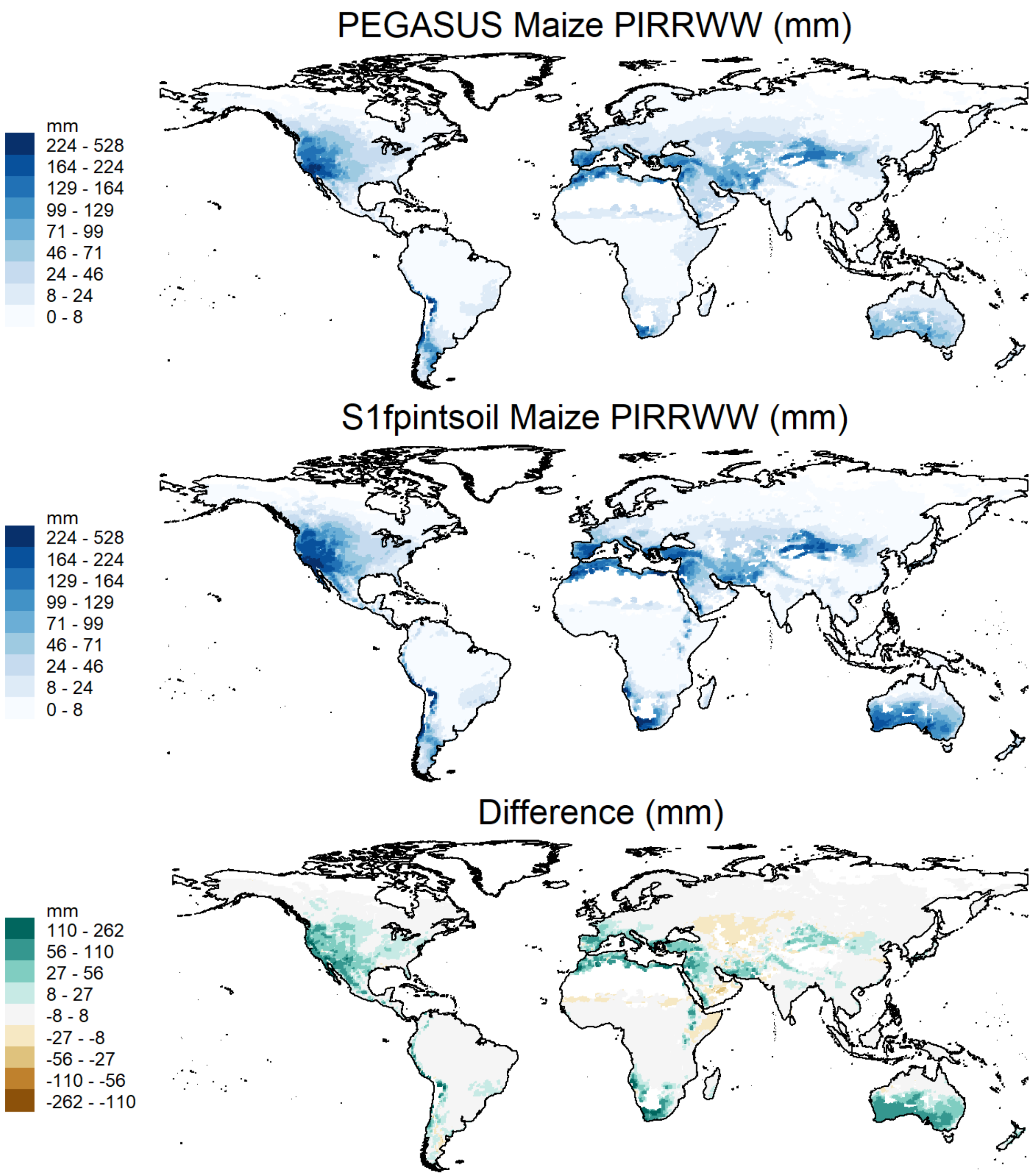

Figure H6. Irrigation water withdrawal for rice averaged over 2090–2099 for the GEPIC model and S1fpintsoil specification

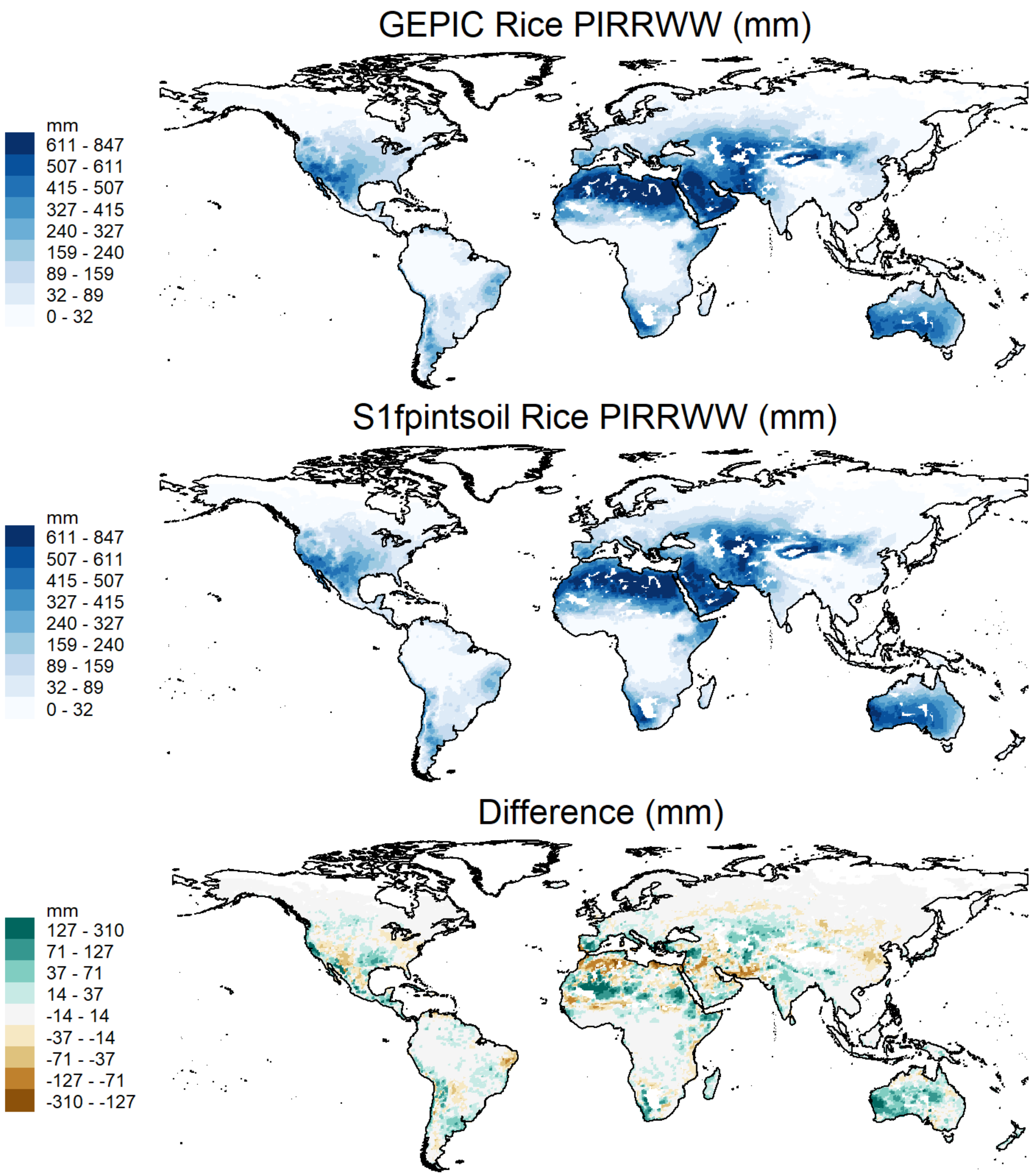

Figure H7. Irrigation water withdrawal for rice averaged over 2090–2099 for the LPJ-GUESS model and S1fpintsoil specification

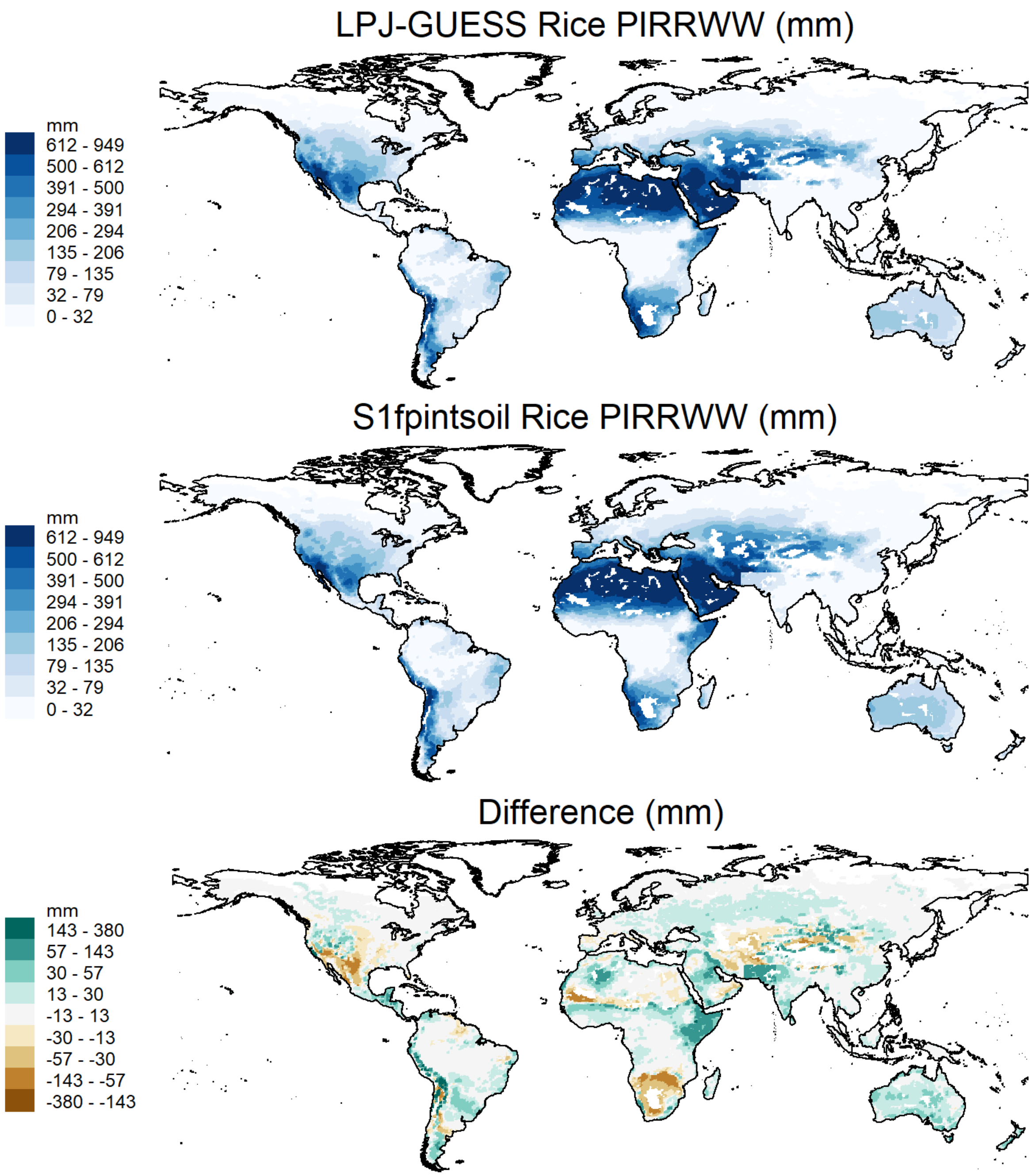

Figure H8. Irrigation water withdrawal for rice averaged over 2090–2099 for the LPJmL model and S1fpintsoil specification

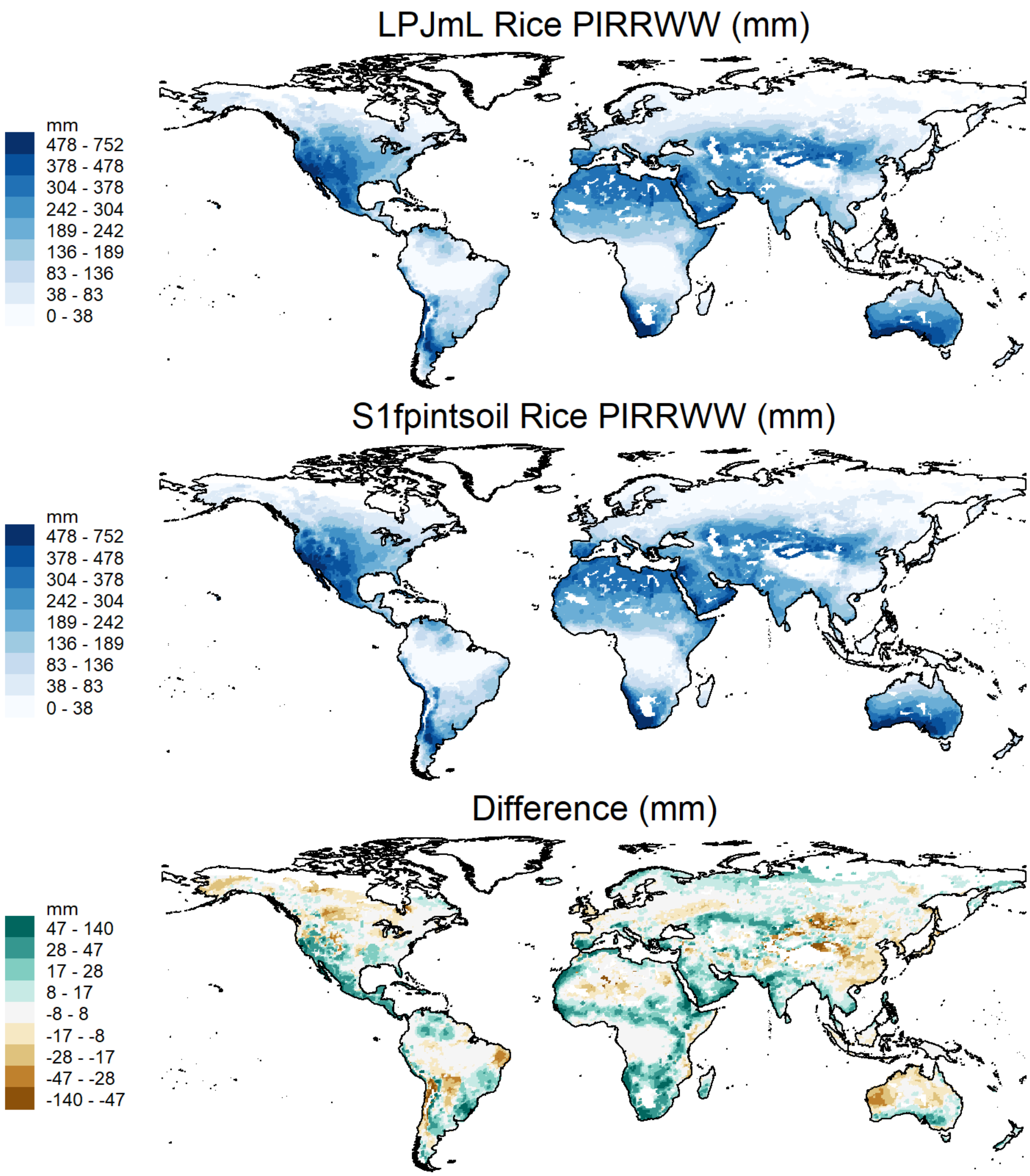

Figure H9. Irrigation water withdrawal for soybean averaged over 2090–2099 for the GEPIC model and S1fpintsoil specification

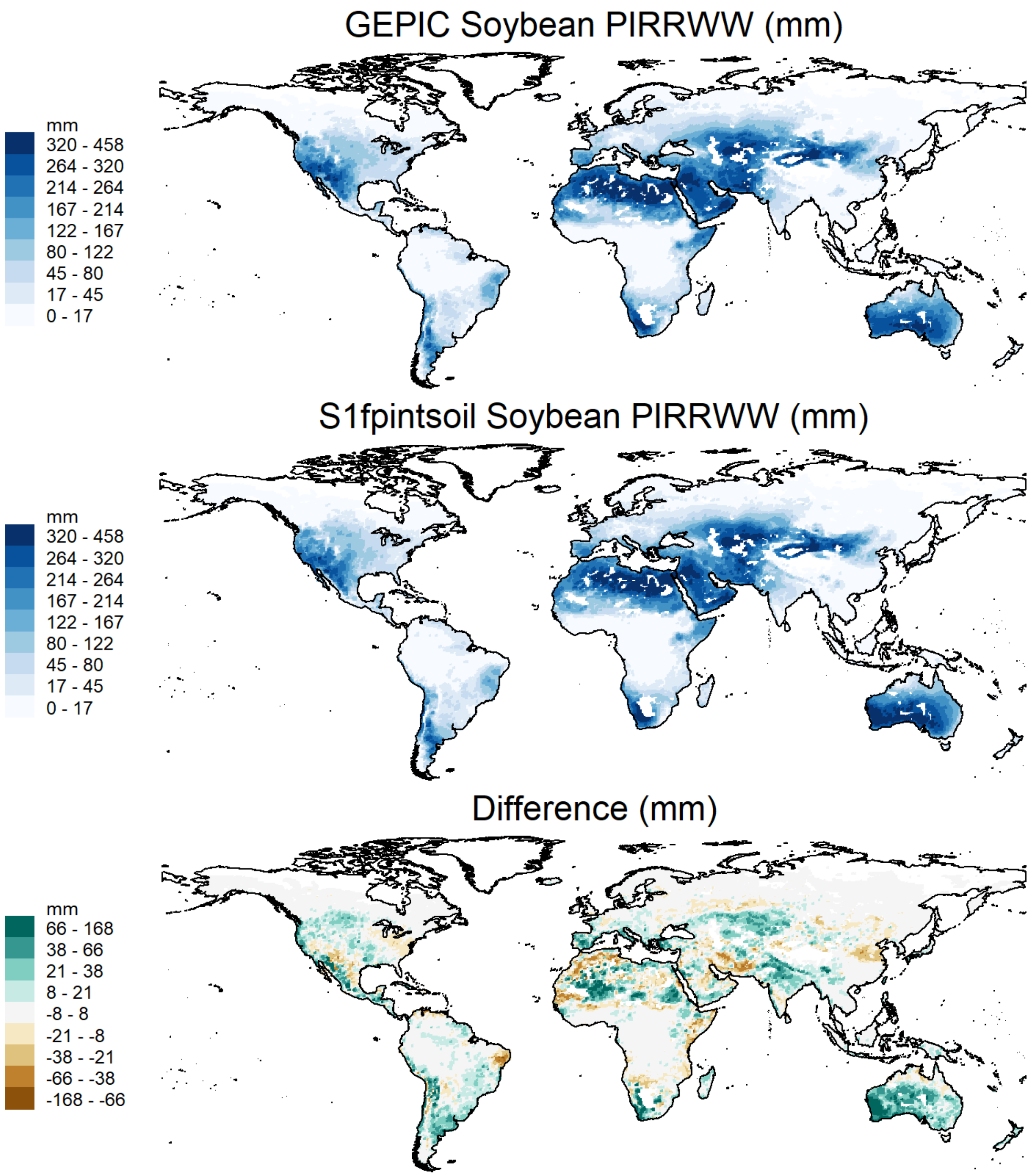

Figure H10. Irrigation water withdrawal for soybean averaged over 2090–2099 for the LPJ-GUESS model and S1fpintsoil specification

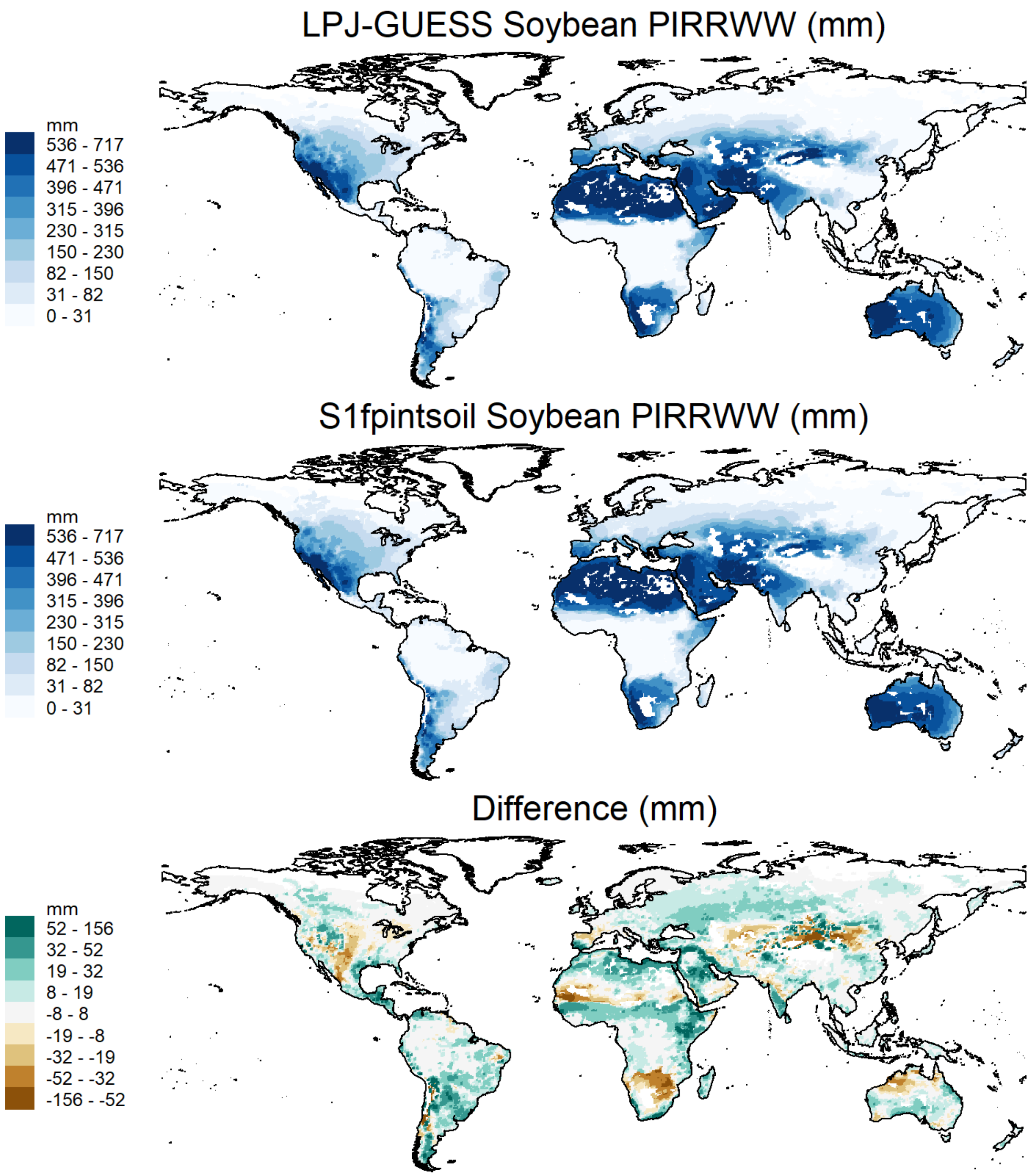

Figure H11. Irrigation water withdrawal for soybean averaged over 2090–2099 for the LPJmL model and S1fpintsoil specification

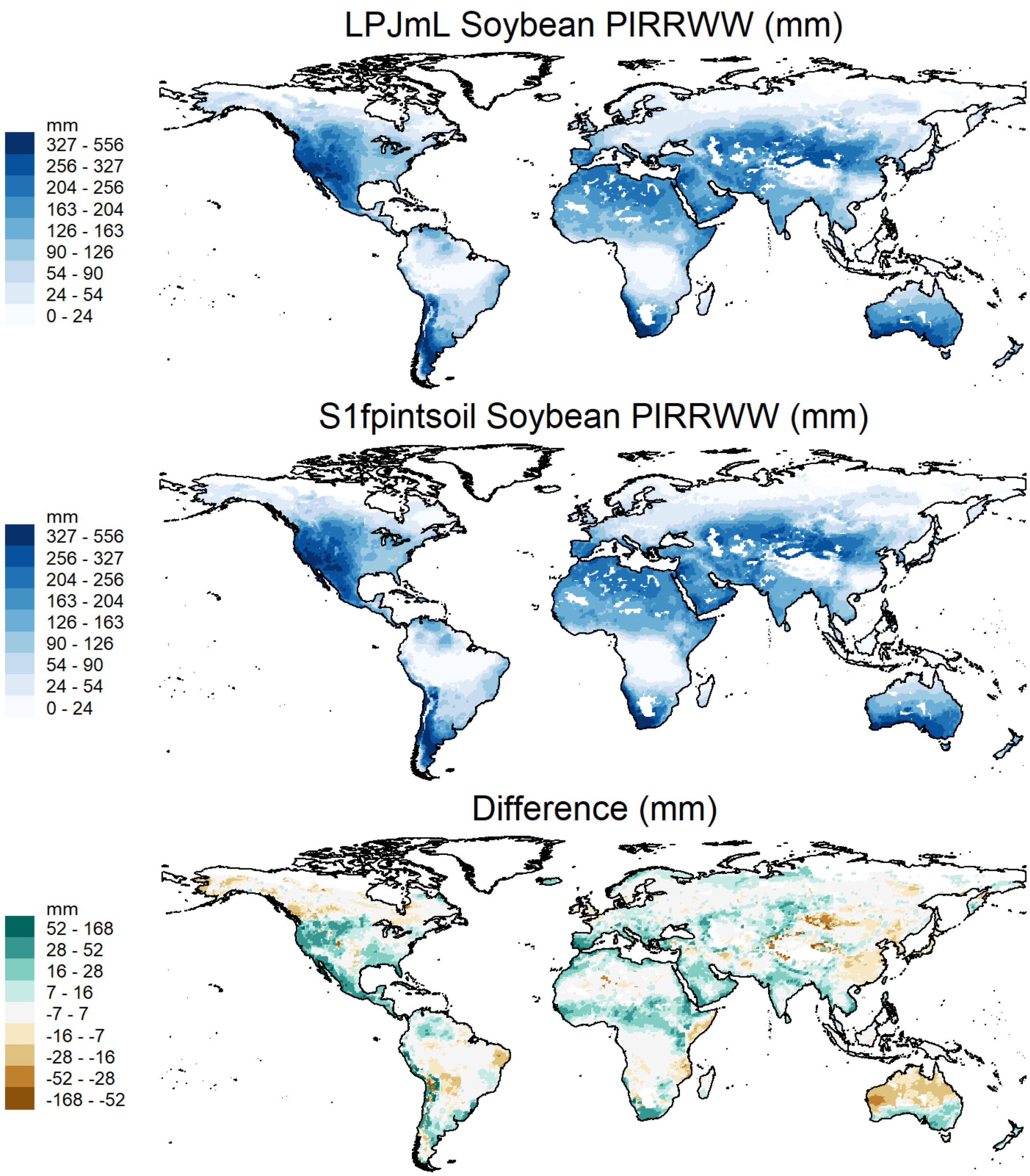

Figure H12. Irrigation water withdrawal for soybean averaged over 2090–2099 for the PEGASUS model and S1fpintsoil specification

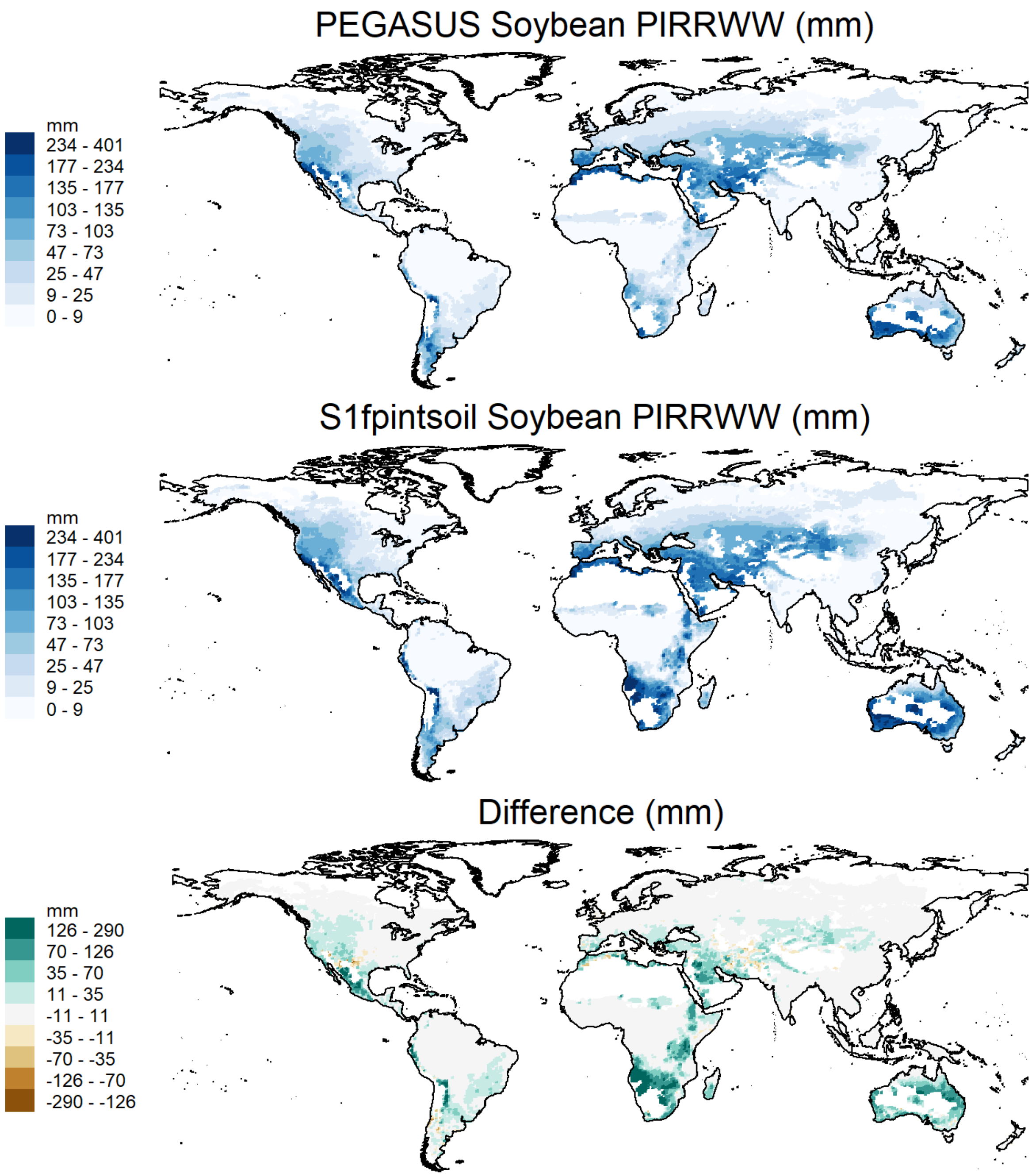

Figure H13. Irrigation water withdrawal for wheat averaged over 2090–2099 for the GEPIC model and S1fpintsoil specification

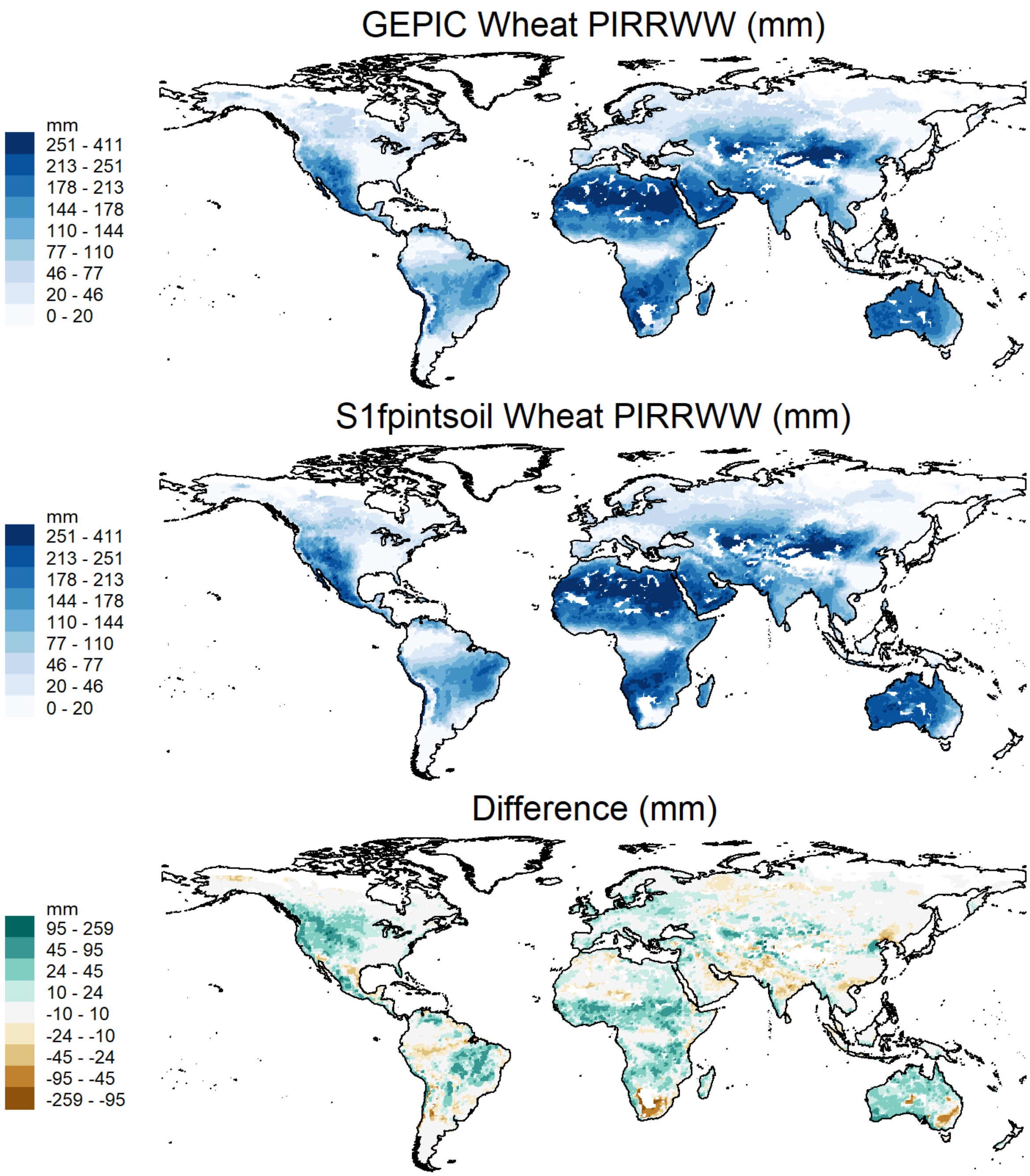

Figure H14. Irrigation water withdrawal for wheat averaged over 2090–2099 for the LPJ-GUESS model and S1fpintsoil specification

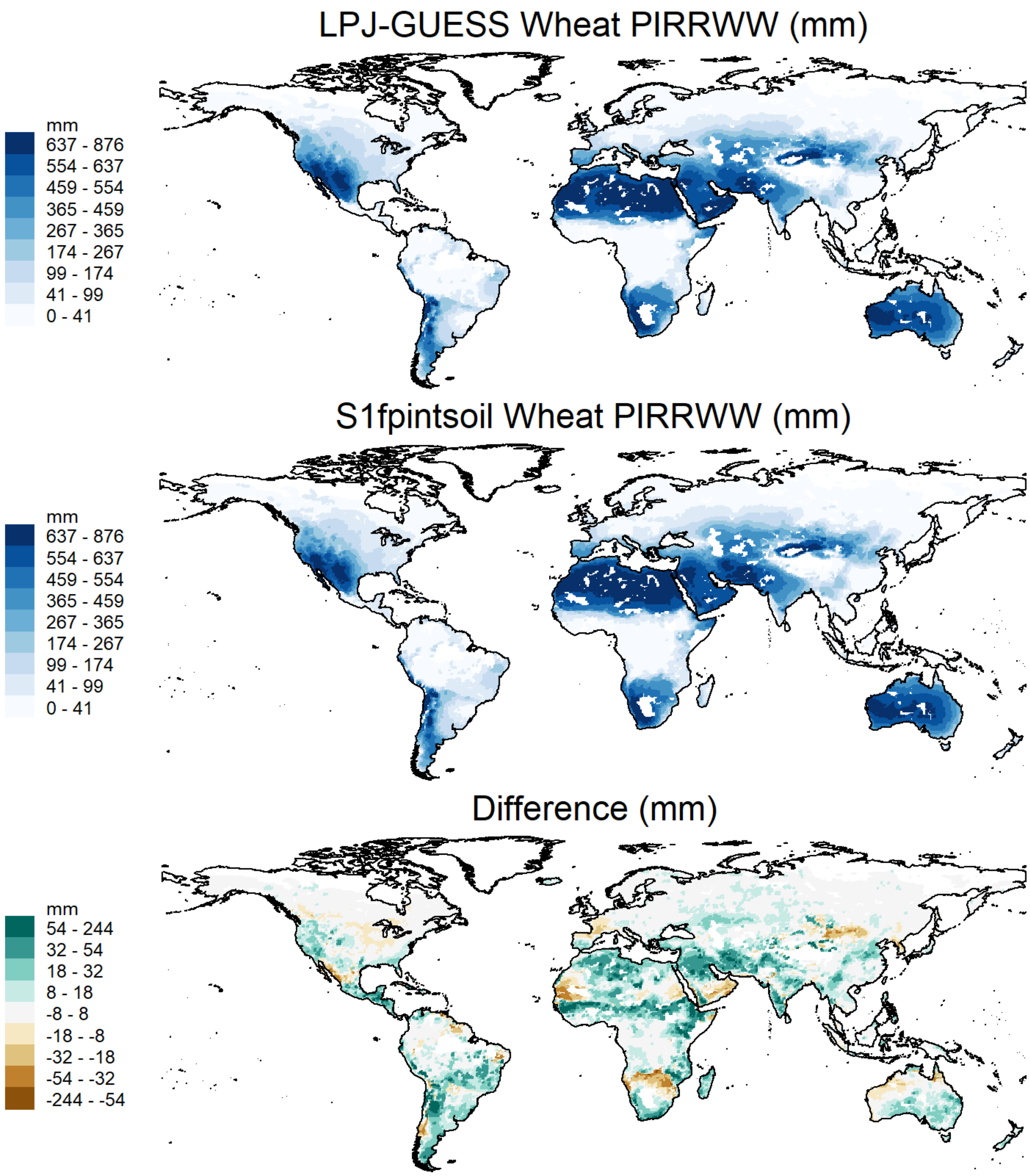

Figure H14. Irrigation water withdrawal for wheat averaged over 2090–2099 for the LPJmL model and S1fpintsoil specification

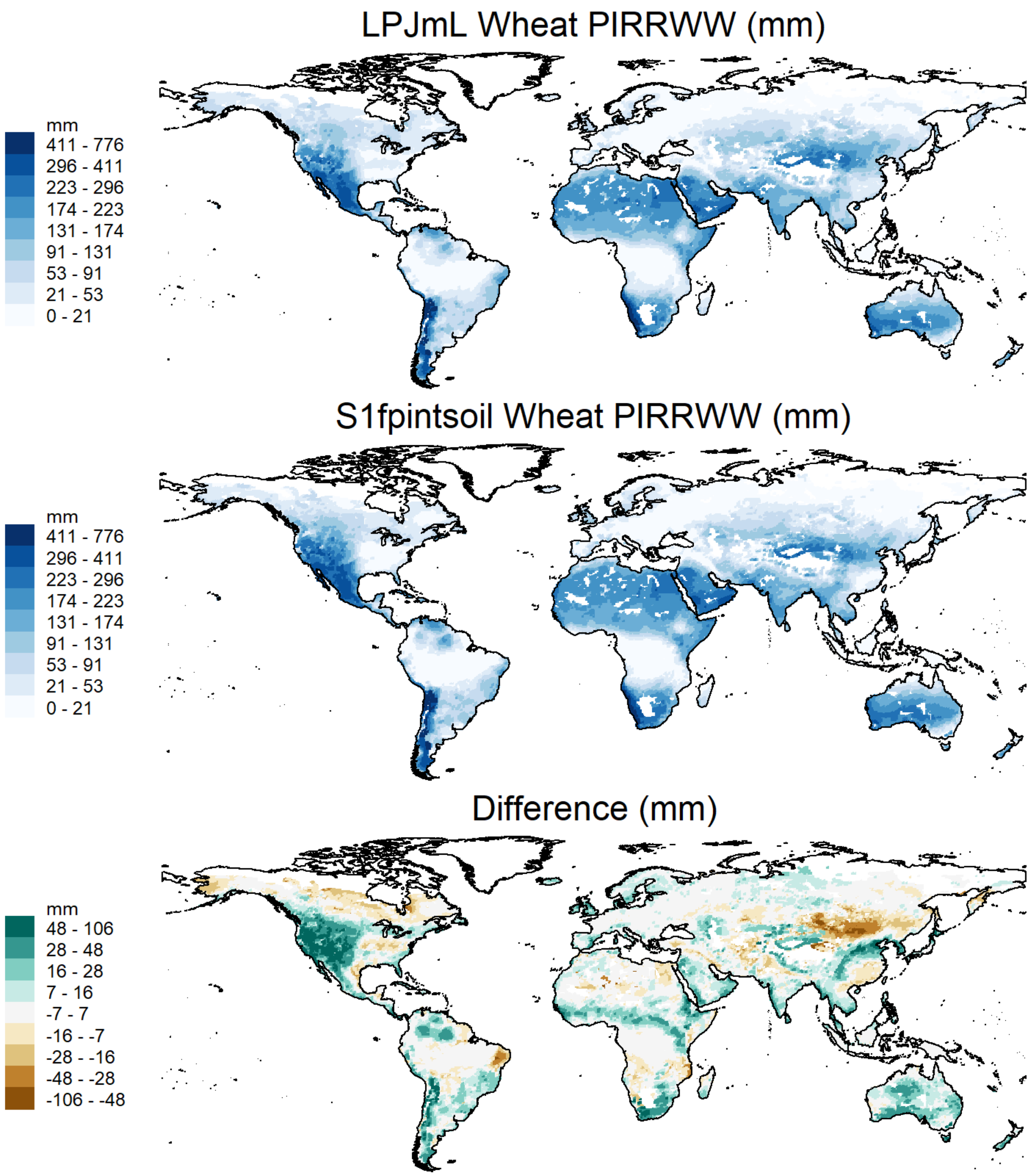

Figure H15. Irrigation water withdrawal for wheat averaged over 2090–2099 for the pDSSAT model and S1fpintsoil specification

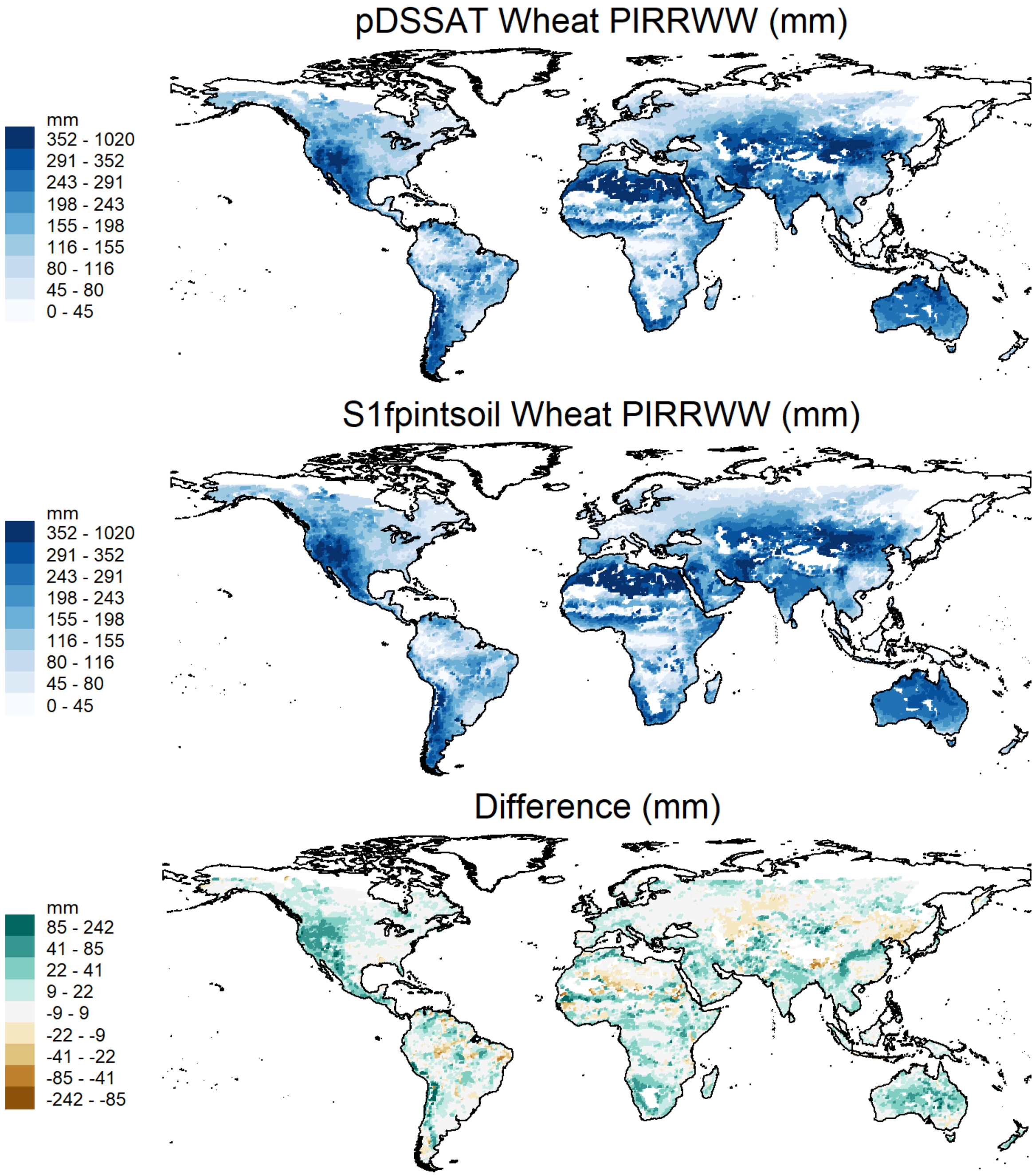

Figure H16. Irrigation water withdrawal for wheat averaged over 2090–2099 for the PEGASUS model and S1fpintsoil specification

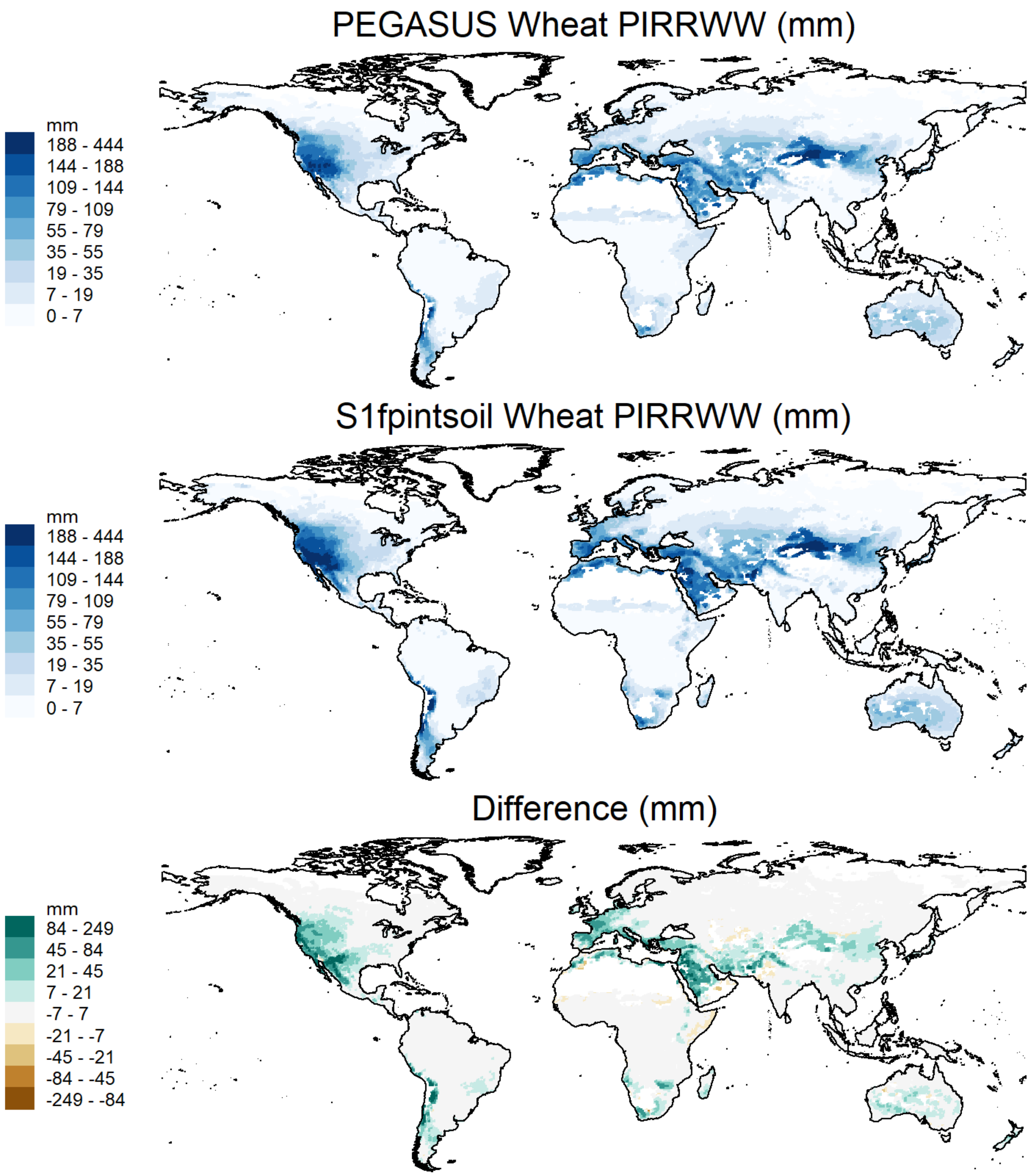

Figure H17. Irrigation water withdrawal ensemble error by crop averaged over 2090–2099 for each major growing region

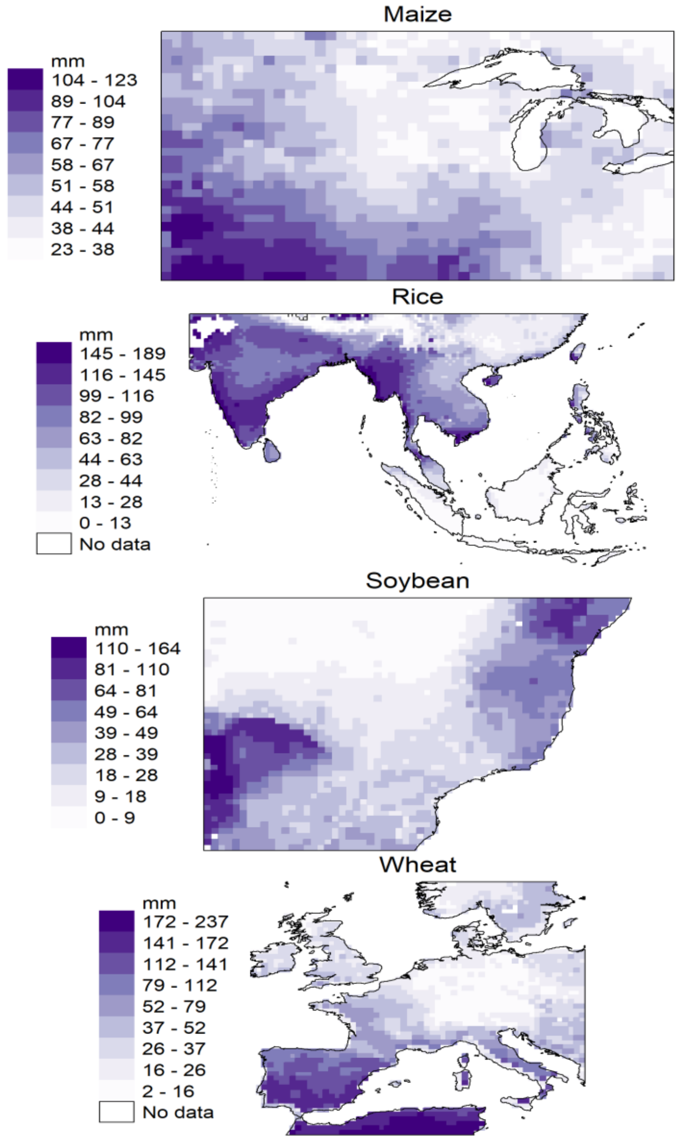

Figure H18. Irrigation water withdrawal ensemble error by crop averaged over 2090–2099 at the global level

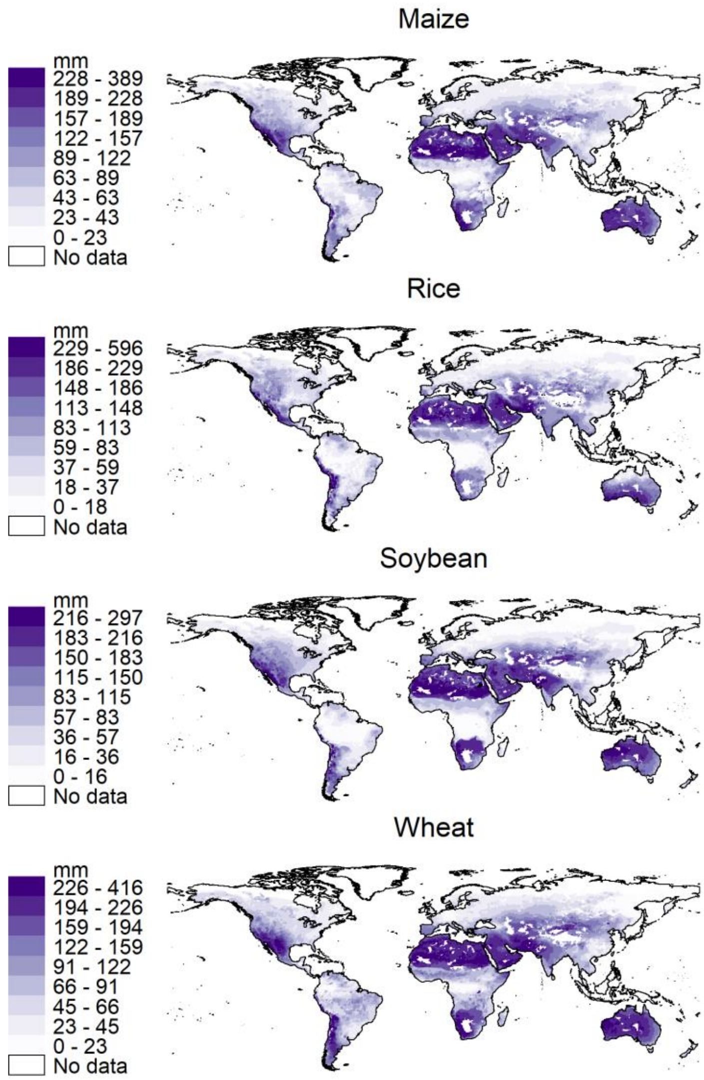

Figure H19. Changes in irrigation water withdrawals for maize from 2000s to 2090s estimated by the statistical emulators (S1fpintsoil specification) and GGCMs

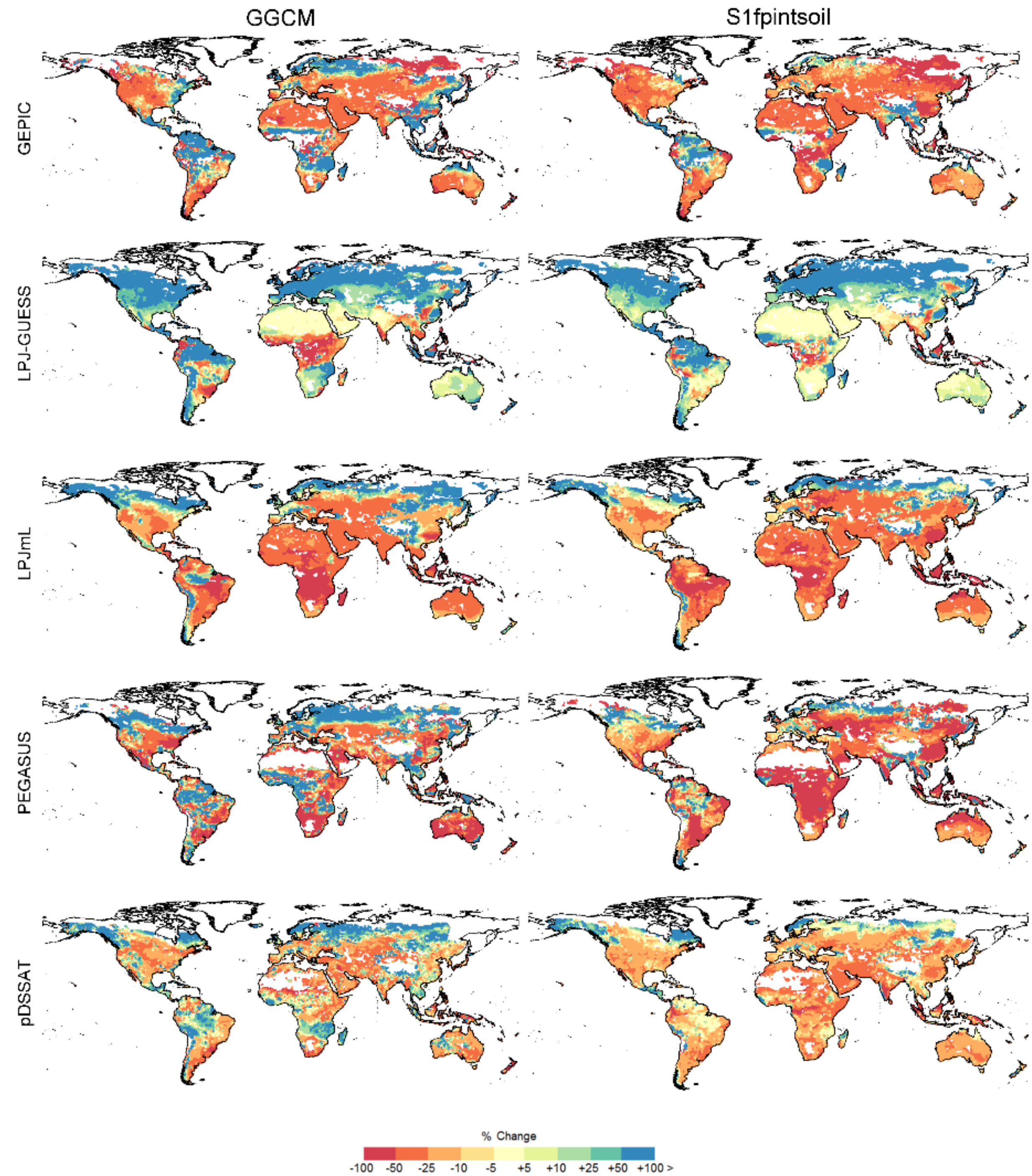

Notes: Grid cells where yields projections from crop models are on average less than 1t/ha over the whole study period are masked in white. Grid cells for which the sign of the impact projected with the emulator is contrary to the sign of the impact projected by the GGCM are masked in black.

Figure H20. Changes in irrigation water withdrawals for rice from 2000s to 2090s estimated by the statistical emulators (S1fpintsoil specification) and GGCMs

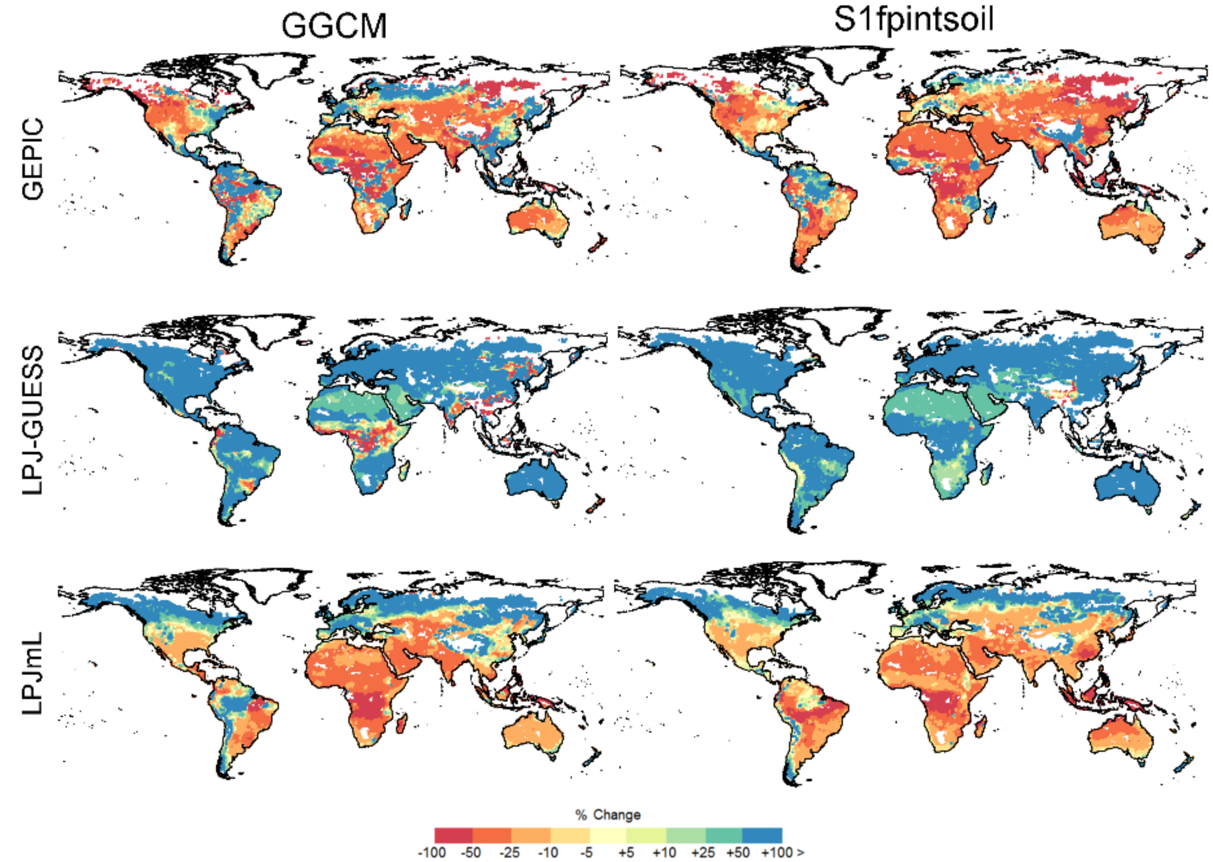

Note: See note of Figure H19.

Figure H21. Changes in irrigation water withdrawals for soybean from 2000s to 2090s estimated by the statistical emulators (S1fpintsoil specification) and GGCMs

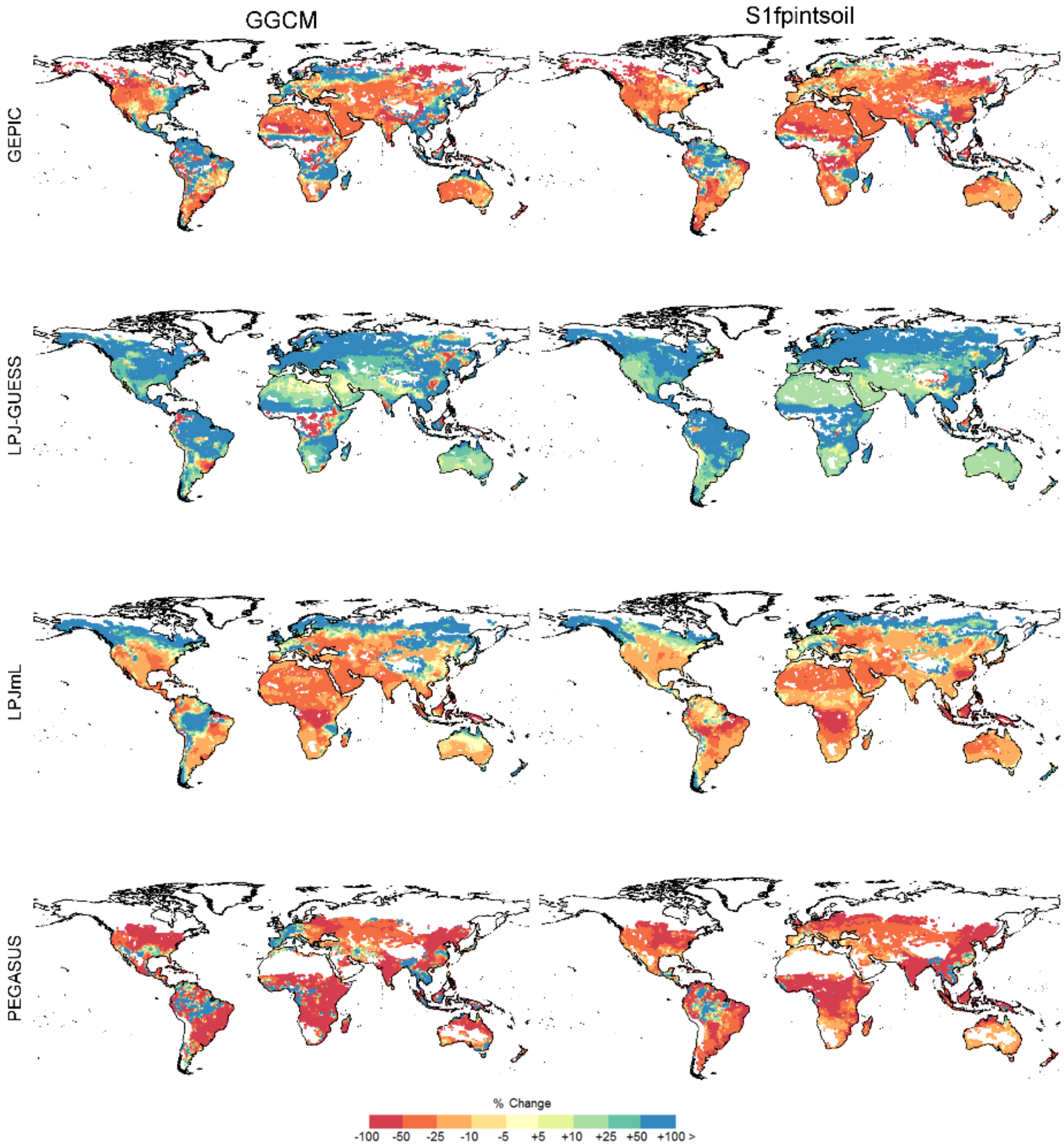

Note: See note of Figure H19.

Figure H22. Changes in irrigation water withdrawals for wheat from 2000s to 2090s estimated by the statistical emulators (S1fpintsoil specification) and GGCMs

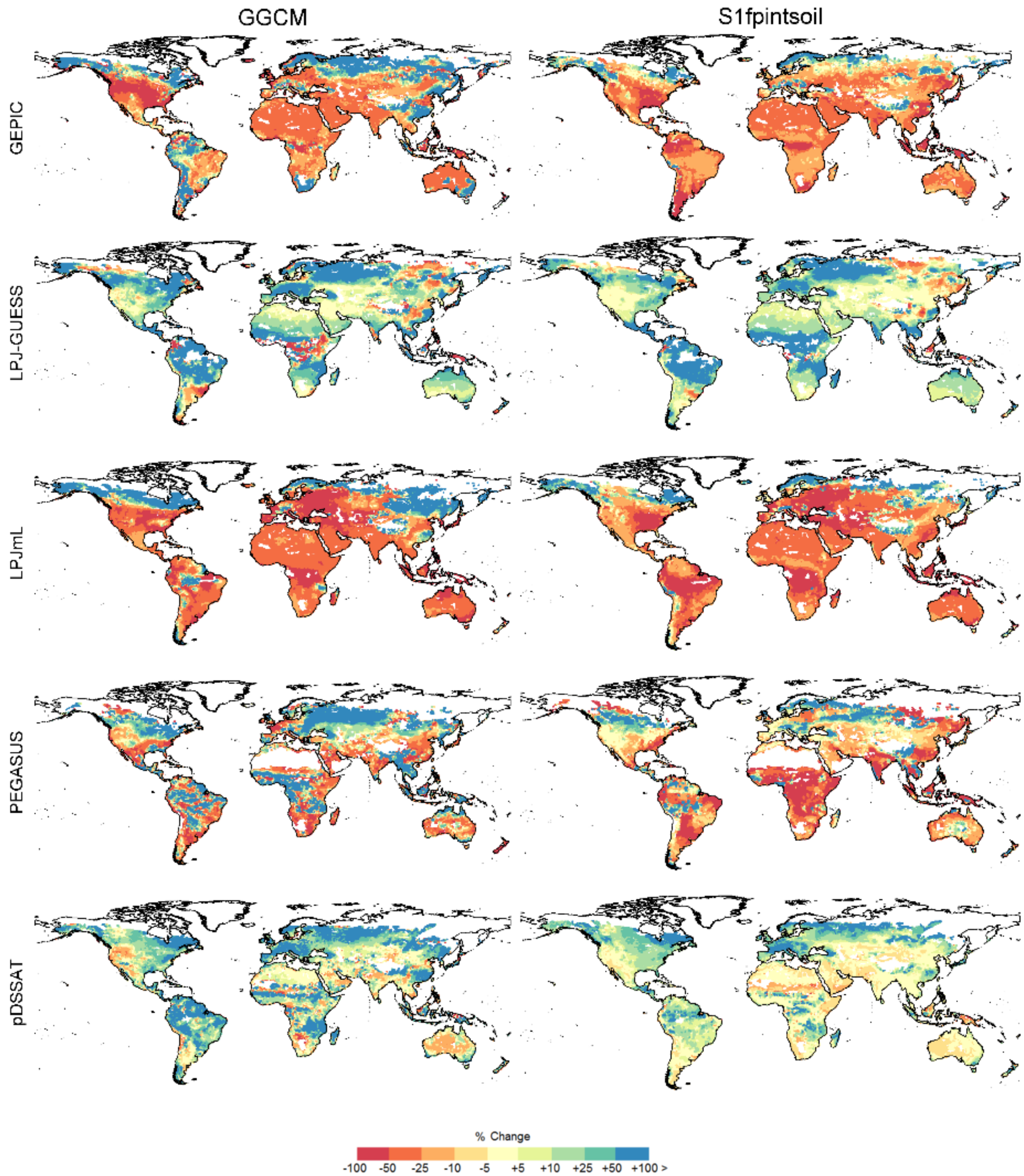

Note: See note of Figure H19.